



Cite this: DOI: 10.1039/d2cs00873d

Emerging electrolytes with fluorinated solvents for rechargeable lithium-based batteries

Yuankun Wang, Zhiming Li, Yunpeng Hou, Zhimeng Hao, Qiu Zhang, Youxuan Ni, Yong Lu, Zhenhua Yan, Kai Zhang, Qing Zhao, Fujun Li and Jun Chen *

Electrolytes that can ensure the movement of ions and regulate interfacial chemistries for fast mass and charge transfer are essential in many types of electrochemical energy storage devices. However, in the emerging energy-dense lithium-based batteries, the uncontrollable side-reactions and consumption of the electrolyte result in poor electrochemical performances and severe safety concerns. In this case, fluorination has been demonstrated to be one of the most effective strategies to overcome the above-mentioned issues without significantly contributing to engineering and technical difficulties. Herein, we present a comprehensive overview of the fluorinated solvents that can be employed in lithium-based batteries. Firstly, the basic parameters that dictate the properties of solvents/electrolytes are elaborated, including physical properties, solvation structure, interface chemistry, and safety. Specifically, we focus on the advances and scientific challenges associated with different solvents and the enhancement in their performance after fluorination. Secondly, we discuss the synthetic methods for new fluorinated solvents and their reaction mechanisms in depth. Thirdly, the progress, structure–performance relationship, and applications of fluorinated solvents are reviewed. Subsequently, we provide suggestions on the solvent selection for different battery chemistries. Finally, the existing challenges and further efforts on fluorinated solvents are summarized. The combination of advanced synthesis and characterization approaches with the assistance of machine learning will enable the design of new fluorinated solvents for advanced lithium-based batteries.

Received 29th November 2022

DOI: 10.1039/d2cs00873d

rsc.li/chem-soc-rev

Renewable Energy Conversion and Storage Center (RECAST), Haihe Laboratory of Sustainable Chemical Transformations, Key Laboratory of Advanced Energy Materials Chemistry (Ministry of Education), College of Chemistry, Nankai University, Tianjin, 300071, China. E-mail: chenabc@nankai.edu.cn



Yuankun Wang

Yuankun Wang received his Bachelor's, Master's, and PhD degrees from the Henan University of Urban Construction, China University of Petroleum, and Xi'an Jiaotong University, respectively. Currently, he is a Postdoctoral Research Fellow at the Key Laboratory of Advanced Energy Materials Chemistry (Ministry of Education) in Nankai University under the supervision of Prof. Jun Chen. His research interests cover battery-related materials, including novel electrolyte and electrode materials.



Jun Chen

Jun Chen obtained his BS and MS degrees from Nankai University in 1989 and 1992, respectively. He received his PhD from the University of Wollongong (Australia) in 1999. Currently, he is an Academician of the Chinese Academy of Sciences, Fellow of The World Academy of Sciences (TWAS), Director of the Key Laboratory of Advanced Energy Materials Chemistry (Ministry of Education), Vice President of Nankai University, and founding Editor-in-Chief of eScience. His research focuses on the synthetic chemistry of inorganic and organic functional materials and the development of batteries.

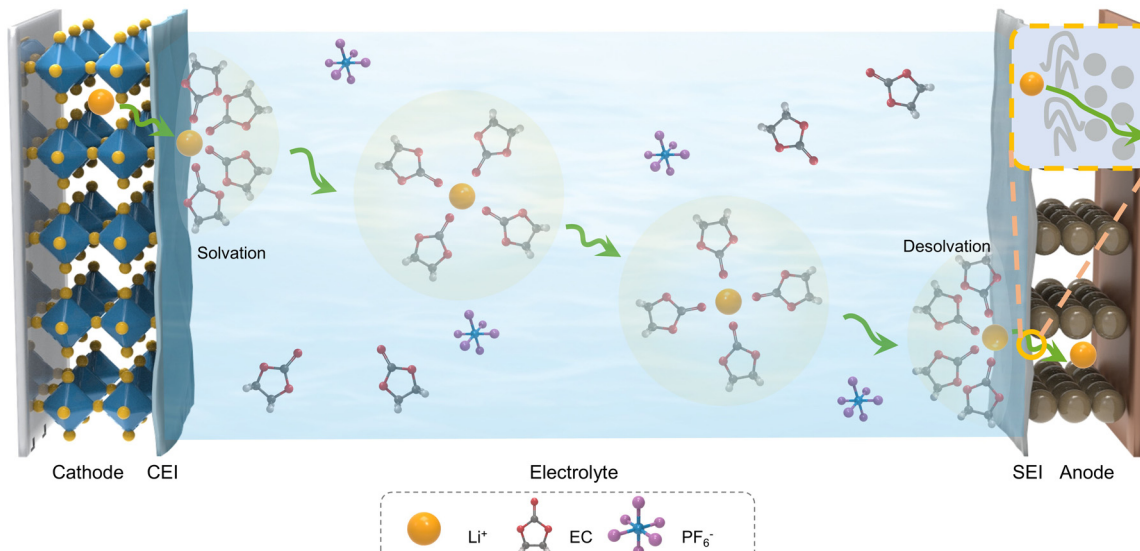


Fig. 1 Schematic of the main components and ion transport in a battery (vehicular motion mechanism). The red circle refers to the solvation structure. The arrows represent the route of ion transport during the charging process.

batteries (LIBs) have achieved great success in the field of electrochemical energy storage since their first commercialization by Sony in 1991.⁵ Currently, LIBs are composed of a graphite anode, lithiated transition metal oxide/polyanion cathode (such as LiCoO_2 (LCO) and LiFePO_4 (LFP)), and non-aqueous Li-ion conducting electrolyte (Fig. 1).^{6,7} The energy density of a battery is calculated by multiplying its output voltage and specific capacity. To achieve a high energy density of 600 W h kg^{-1} , a target proposed by many countries, the specific capacity and voltage difference between two electrodes should be as high as possible. In this case, cathode materials with higher voltage and capacity, such as Li-rich Mn-based materials ($x\text{Li}_2\text{MnO}_3(1 - x)\text{LiTMO}_2$ (TM = Ni, Mn, Co, etc.; $0 < x < 1$)⁸ and Ni-rich $\text{LiNi}_x\text{Mn}_y\text{Co}_{1-x-y}\text{O}_2$ (NMC, $x \geq 0.5$, $x + y < 1$)^{9,10} are gaining increasing attention. Alternatively, several burgeoning anodes (such as lithium metal^{11–14} and silicon/carbon anode^{15–17}) with much higher specific capacities than that of graphite have been widely investigated. Consequently, emerging cathode and anode materials pose stringent demands on the properties of electrolytes. However, unlike the rapid and continuous breakthroughs in electrode materials, the state-of-the-art electrolytes are still based on carbonate-based electrolytes. The regular composition of electrolytes, for example, 1 M LiPF_6 in a solution of ethylene carbonate (EC) and linear carbonate esters, suffers from inferior performance when coupled with novel electrodes, including poor anodic stability at high voltages of $> 4.3 \text{ V}$, incompatibility with lithium metal, poor temperature tolerance, and severe safety concerns.¹⁸

Presently, significant efforts have been devoted to exploring new electrolytes to adapt to high-energy-density Li-based batteries, such as molecular structure engineering of solvents,^{19,20} designing ionic liquids,^{21–23} and synthesizing solid electrolytes.^{24–28} Due to their compatibility with the current industrial manufacturing process and expertise,

developing novel liquid solvents seems to be promising for fast commercialization.²⁹ It is widely accepted that slight molecule-structural reconstruction can have significant impacts on the physical or chemical properties of materials; therefore, introducing functional groups or unique components in electrolyte molecules is feasible to obtain advanced electrolyte solvents.³⁰ In particular, electrolytes containing fluorinated solvents can overcome many issues associated with traditional electrolytes, such as unstable interface, rapid capacity attenuation at extreme temperatures, and high flammability.^{31–33} Herein, the term “fluorinated solvent” refers to aprotic solvents containing fluorine. The incorporation of fluorine in solvent molecules has been pursued due to its highest electronegativity in the periodic table, low polarizability, and high ionization enthalpy. For example, as one of the most successful case, fluoroethylene carbonate (FEC) shows noticeable improvements in melting point, anodic stability, and film-forming ability on the anode surface compared with EC.⁶ Even in all-solid-state electrolytes, FEC can satisfy the requirement of improving the interface stability.³⁴ Inspired by the advances and limitations of FEC, different fluorinated solvents have been developed to date.

In this case, the rapid development of fluorinated solvents makes it necessary to provide a comprehensive review on this topic. Indeed, only a few previous works summarized the application of fluorinated solvents in Li batteries, focusing on their physicochemical properties and battery applications.^{30,35–38} However, to date, there are still two key issues that need to be summarized and discussed. Firstly, the relationship between structure and property, which is a rule directly related to the design principles of fluorinated solvents for LIBs, is undefined. For example, what influence does the amount and position of fluorine atoms have on the physicochemical properties of electrolytes? What are the differentiations in the

effects of fluorine on different type of solvents? What are the changes in solvation structure and interface compatibility of electrolytes after introducing fluorinated solvents? Secondly, a detailed discussion on the methodologies for synthesizing fluorinated solvents is still lacking. Therefore, a review deciphering the design principles, classifying the synthesis methods, and revealing the relationship between structure and electrochemical performance is significant to guide the further development of fluorinated electrolytes.

Herein, firstly, we highlight the indicators used to reflect the properties of electrolytes and how they are affected by the structures of molecules. Next, we summarize the general design principles for fluorinated solvents, together with the advances and issues associated with various solvents before and after fluorination, and discuss the approaches for the synthesis of fluorinated solvents. Subsequently, we provide a detailed review on the various types of fluorinated solvents and analyze the strategies for the selection of solvents for specific applications by comparing the most relevant properties. Finally, we present a general conclusion and perspective on the challenges and future directions of fluorinated solvents.

2. Basic parameters and design principles for fluorinated solvents

In this chapter, initially we briefly describe the electrochemical process that the electrolyte participates in, followed by a discussion on the basic parameters of solvents or electrolytes. Then, the design principles of advanced fluorinated solvents are summarized by highlighting the advances and issues associated with different types of solvents.

2.1 Electrochemical processes that electrolytes participate in

As shown in Fig. 1, the cathode, anode, and electrolyte are basic components of batteries, where all electrochemical reactions ideally occur at the interface between the electrode and electrolyte, and the electrolyte usually only serves as an ionic conductor (excluding dual-ion batteries). In this context, Li^+ ions are shuttled back and forth between the cathode and anode, depending on the direction of the internal electric field. Actually, Li^+ ions are usually surrounded by a certain number of solvent molecules. In this case, interphases are inevitably formed on the anode (named solid electrolyte interphase, SEI) and cathode (named cathode electrolyte interphase, CEI) due to the uncontrollable side reactions between the electrolyte and electrode, which play a vital role in regulating the ionic transport. Therefore, in Li-based cells, the ion transport associated with the electrolyte during discharge usually involves five steps (the charging process is reversible) including Li^+ diffusion through the SEI, Li^+ solvation in the electrolyte, Li^+ migration with solvent molecules around them, Li^+ desolvation from the electrolyte, and Li^+ diffusion through the CEI.³⁹ These processes can be divided into bulk transport and interface transport. The former is related to the ionic conductivity of the

electrolyte, while the latter involves the solvation/de-solvation process and ion migration through the interphase.

2.2 Basic parameters

Fig. 2a summarizes the main solvent-related parameters and their influencing factors in electrolyte chemistry, including melting point, boiling point, viscosity, and dielectric constant. Here, the parameters related to solid-state polymers, such as glass-transition temperature (T_g), will not be covered. After the introduction of Li salts, the above-mentioned parameters can change significantly. Fig. 2b shows the relationship and factors influencing different electrolyte properties. An elaborate discussion is presented as follows.

2.2.1 Melting and boiling points. The melting point (mp) and boiling point (bp) are the most common parameters that describe the physical properties of electrolytes and play an important role in determining the service temperature and safety of batteries. For a given molecular substance, its melting and boiling points strongly depend on the strength of its crystal lattice, which are primarily governed by non-covalent interactions and molecular structure.^{40,41} Given that most organic molecules only possess paired electrons, the magnitude of their magnetic forces is negligible.⁴² In many cases, the electrically related forces, including van der Waals interactions and dispersion (London) forces, determine the non-covalent interactions in organic molecules. In general, greater non-covalent interactions lead to higher melting and boiling points.⁴³ From a molecular structure point of view, a molecule with a greater surface area contributes a more effective contact area for interaction, and thus its boiling point is higher.⁴⁴ For example, the boiling point of cyclic solvents is higher than that of both linear and branched isomers. Alternatively, there is a simple and counter-intuitive empirical rule (Carnelley's rule) in describing the melting point, where high molecular symmetry is related to a high melting point, which is rationalized as a higher molecular symmetry means a higher packing coefficient of molecules, leading to a higher ratio of occupied space to free space in the crystal.⁴⁵ For example, the high melting of EC is considered to be related to its high molecular symmetry.⁶ Furthermore, the conformational freedom also influences the melting point of solvents, namely, a molecule with a higher degree of conformational freedom with possess a lower melting point.⁴⁶ For example, ethyl butyrate ($-85.8\text{ }^\circ\text{C}$) possesses a lower melting than methyl butyrate ($-93\text{ }^\circ\text{C}$).⁴⁷

2.2.2 Viscosity. The viscosity (η) of a fluid is defined as the measured internal resistance (frictional property) or drag force that hinders the liquid flow. It is mainly associated with two parameters, as follows: (1) van der Waals interactions and (2) the ability of molecules to arrange and fit themselves in the flow process.³⁰ The former is mainly affected by the dipole moment of molecules, while the latter is related to their shape and rigidity. Apparently, a larger dipole moment and rigidity result in higher viscosity. For example, partially fluorinated solvents, both linear and cyclic ones, exhibit higher viscosity than their non-fluorinated counterparts due to the presence of the highly electronegative fluorine atom.^{35,37,48} Furthermore,

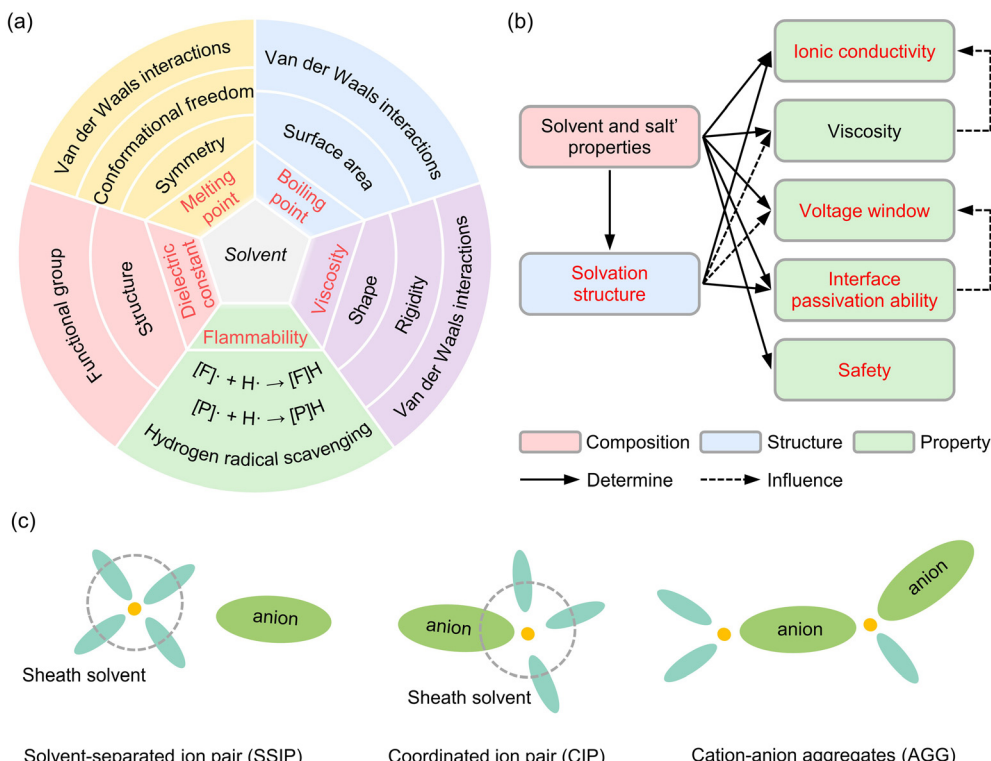


Fig. 2 (a) Representative parameters of electrolyte solvents and factors influencing them from a molecular scale view. (b) Relationship and factors influencing different electrolyte properties. Fonts in red refer to the parameters highlighted in this section. (c) Schematic illustration of three solvation structures, *i.e.*, solvent-separated ion pair (SSIP), coordinated ion pair (CIP), and cation–anion aggregates (AGG).

increasing the temperature can reduce the viscosity due to the weakened polar–polar interactions between the solvent molecules. Alternatively, linear solvents usually show lower viscosity than cyclic ones due to the presence of linear alkyl chains, which endow higher flexibility in molecule arrangement and fitting. The viscosity of EC (1.76 mPa s at 40 °C) is higher than that of dimethyl carbonate (DMC, 0.59 mPa s at 25 °C). In addition, cyclic structures and unsaturated groups (carbon–carbon double/triple bonds) also exhibit more rigid structures, contributing to higher viscosity.⁴⁹

2.2.3 Dielectric constant. The dielectric constant (ϵ), also known as permittivity, is related to the electronic polarizability (α) of a material based on the Clausius–Mossotti relation, reflecting the interatomic and intermolecular attractions.⁵⁰ This is an important physical property describing the capability of solvent molecules to solvate salts.⁶ Generally, in a solvent with a higher dielectric constant, salts tend to exhibit a higher dissociation degree (lower ion pairing) at a given concentration. Dielectric constant has a significant effect on the behavior of electrolytes, including their ionic conductivity, solvation structure, and electrolyte-derived interface chemistry at both electrodes.⁵¹ For example, Kim *et al.* suggested that the high dielectric constant of EC can decrease the electric field intensity, which favors the formation of mechanically and electrochemically stable SEI layers to suppress the growth of lithium dendrites.⁵¹ The dielectric constant of electrolytes is determined by the temperature and electrolyte composition.⁵² As

mentioned above, high temperature can enhance the molecular thermal motion to overcome the dipole–dipole interactions; thus, the dielectric constant decreases with an increase in temperature. Recently, Zhang *et al.* demonstrated that the change rule of the dielectric constant of binary mixtures is related to the strength of their intermolecular interactions.⁵² For solvents with weak intermolecular interactions (such as ether-based mixtures), the dielectric constant of binary solvent mixtures complies with the linear superposition rule. On the contrary, solvents with strong intermolecular interactions follow a polynomial function (eqn (1) and (2)).

$$\epsilon = e^F \quad (1)$$

$$F = p \ln \epsilon_1 + q \ln \epsilon_2 + pq \sum_{i=0}^2 m_i (p-q)^i \quad (2)$$

where ϵ refers to the dielectric constant of the mixture. ϵ_1 and ϵ_2 are the dielectric constants of solvents 1 and 2, respectively. p and q are the proportion of solvents 1 and 2, respectively. $p + q = 1$. m_i ($i = 0, 1, 2$) is the model parameter.

The dielectric constant of electrolytes shows a volcano trend as the salt concentration increase. The rationale behind this phenomenon can be ascribed to the compromise between the enhanced dielectric constant from the cation–anion coordination and decreased dielectric constant from the solvent in the solvation shell. However, from a molecular structure point of view, providing a general trend for the change in the dielectric

constant with the molecular structure or the functional group is challenging. For example, cyclic carbonates have much higher dielectric constants than that of linear and branched carbonates, whereas cyclic and linear ether exhibit similar dielectric constants. Furthermore, introducing fluorine into PC (64.9) causes a significantly elevated dielectric constant (190 for mono-fluorinated propylene carbonate (FPC), 2-2), but the case is opposite in EC (90.5) and its fluorinated counterpart, fluorooethylene carbonate (FEC, $\epsilon = 79.7$).⁵³ Notably, the dielectric constant is not sensitive to the density and steric hindrance of the solvent, which also affects the lithium solvating ability.^{54,55}

2.2.4 Solvation structure. The solvation structure has a profound and complex influence on the properties of the electrolyte, including ionic conductivity, voltage window, desolvation barrier, and interfacial chemistry. In this case, different spectroscopic techniques and computations have been employed to characterize the solvation structure of electrolytes, but this is still challenging to describe it accurately.^{56,57} To date, some vital information have been obtained, as follows: (1) Li⁺ is energetically favorably coordinated with the dipoles (nucleophilic sites) of the solvent, such as carbonyl (C=O) in carbonates, where the Coulombic attraction of Li⁺ ions is neutralized;^{58,59} (2) the Li⁺ coordination number in the electrolyte is determined by the type and concentration of salt and the nature of the solvent molecules;^{60,61} (3) the solvation structures in bulk electrolytes and electrode/electrolyte interface are different, even without the presence of an electric field; and (4) it is still under debate whether Li⁺ prefers to interact with the solvent with a higher dielectric constant or donor number in a mixed solution. Therefore, more advanced characterization methods need to be developed to reveal the formation and evolution of the solvation structure during the electrochemical process. The three most accepted solvation configurations are described in Fig. 2c, including solvent-separated ion pair (SSIP), coordinated ion pair (CIP), and cation–anion aggregates (AGG). In traditional commercial electrolytes, SSIP dominates in the solvation structure. Specifically, many free solvent molecules and anions can be observed in these electrolytes. Increasing the salt concentration will reduce the free solvent molecules and enhance the cation–anion interaction. At the high-concentration, which is an inaccurate term widely used to describe the region where the salt concentration exceeds the maximum ionic conductivity requirements, the deficiency of solvent molecules will result in the emergence of the unique CIP and AGG. This unusual solvation structure increases the electrolyte volatility, accelerating the formation of LiF-rich interfacial layers, and thus stabilizing the cathode and anode simultaneously.

2.2.5 Ionic conductivity. Ionic conductivity is one of the most important parameters for electrolytes given that it describes the movement of ions for ongoing electrochemical reactions. It determines the power densities of the batteries employed to some extent. A semiempirical value is that the ionic conductivity of electrolytes must be more than 0.1 mS cm⁻¹ to ensure a sufficient ion concentration at the electrode surface.⁴⁷ Given that the Li⁺ ions in the bulk electrolyte

permanently move with the coordinated solvent molecules, both the solvent and salt dictate the ionic conductivity. According to eqn (3), the ionic conductivity is directly related to the salt concentration and electrolyte viscosity.

$$k = \sum_i \frac{(Z_i)^2 F C_i}{6\pi\eta r_i} \quad (3)$$

where Z_i is the charge number in the charging process, C_i is the molar concentration of salt, and F and η are the faradaic constant and viscosity, respectively. r_i is the radius of the solvation ions.

Generally, it is considered that low viscosity favors ion diffusion in the electrolyte, while a high dielectric constant is required to promote ion dissociation.⁶² However, it should be noted that for traditional Li batteries, where only Li⁺ ions are involved in the redox reaction, the Li-ion transference number (t_{Li^+}) must be considered to evaluate the ion transport properties in the bulk electrolyte.

2.2.6 Interface passivation ability. Presently, no solvent can simultaneously meet the stability requirement towards both the anode and cathode, especially in cells with a highly reductive lithium metal anode and aggressive spinel-type cathode, and thus an electron-insulating passivation layer is needed at the electrode/electrolyte interface.^{53,64} Based on the solvation structure, the passivation layer on the electrode surface can be derived from the solvent or salt.⁶⁵ This layer plays a crucial role in dictating the electrolyte stability by isolating the electrolyte components from the electrode surface, suppressing the transition-metal dissolution at the cathode and mitigating the volume changes and active material loss at the anode.^{66–68} Accordingly, an interface layer with mechanically, electrochemically, thermally, and kinetically stable features are desirable. Specifically, high mechanical stability can help suppress the formation and growth of dendrites, providing a stable interface environment for ion transport. Furthermore, high electrochemical/chemical stability can decrease the side reactions between the electrolyte and electrode, avoiding electrolyte drying. Additionally, high thermal stability is vital to allow the cells to operate at high temperature. High kinetic stability means the interface layer shows high ionic conductivity. However, it is difficult to achieve these requirements simultaneously. Thus, as a compromise, a “stable interface” should contain high mechanical stability, high electrochemical/chemical stability, and suitable kinetic stability. For example, the SEI layer formed from the decomposition of EC is beneficial for the operation of graphite anodes, where ion transport through the interface is vital for the kinetics and stability of the electrochemical process. However, EC-derived SEIs generally show poor ion transport at low temperature.

2.2.7 Voltage window. The voltage window of an electrolyte depends on the nature of the solvent and interphase chemistry. The highest occupied molecular orbital (HOMO) and the lowest unoccupied molecular orbital (LUMO) of the electrolyte components are common indicators in determining the voltage window of an electrolyte. Generally, electrolytes are

thermodynamically stable when the electrochemical potentials of the electrodes are located in the LUMO–HOMO range.^{69–71} An ideal electrolyte should possess a sufficiently high LUMO and low HOMO to avoid side reactions between the electrolyte and electrodes. It should be noted that a higher LUMO or lower HOMO does not necessarily ensure a broader voltage window. For example, the HOMO level of EC is lower than that of DMC, whereas the oxidation potential of EC (4.8 V) is a slightly lower than that of DMC (5.0 V) on a Pt electrode.^{72,73} According to the simplified computational model, and discrepant reaction kinetics and interfacial chemistry of different solvents are the reasons for these anomalies. Another important factor affecting the voltage window of electrolytes is the properties of the interface layer. A compact and effective SEI/CEI layer can suppress the side reactions between the electrode and electrolyte. For example, an LiF-rich SEI in localized high-concentration LiFSI-DME electrolyte enabled stable cycling of the LiCoO₂ cathode under a high charge voltage of 4.5 V.⁷⁴ A boron-containing CEI layer derived from allylboronic acid pinacol ester (ABAPE) was responsible for the improved anodic stability of electrolytes towards the Ni-rich cathode.⁷⁵

2.2.8 Safety. Toxicity, combustion, and explosion are the main safety risks for battery manufacturing and application. Here, we focus on the latter two, where the term “safety” mainly refers to the flammability of electrolytes. The flash point (FP), the temperature at which the vapor pressure of a flammable (or combustible) liquid reaches the lowest flammable limit, is an essential indicator for estimating the thermal runaway (smoke, fire, and explosion) of electrolytes.⁷⁶ A solvent with a lower FP is usually more hazardous than one with a higher FP. The FP of a solvent is associated with its vapor pressure, *i.e.*, a lower vapor pressure or higher boiling point indicates a higher FP.⁷⁷ In the case of solvent mixtures, the most common form for electrolytes, their FP is determined by the component with the highest volatility.³⁰ In the case of commercial carbonate-based electrolytes, the low FP of linear carbonates, such as DMC (17 °C) and DEC (31 °C), poses serious security risks in practical applications. Hess *et al.* reported that the FP of 1 M LiPF₆ EC/DMC (1:1 in weight) electrolyte is as low as 25.5 °C.⁷⁸ Therefore, it is urgent to improve the safety of electrolytes. Regarding high-safety electrolytes, another critical indicator, the self-extinguishing time (SET), which describes the combustion time of an electrolyte after it is ignited, is widely applied. According to the proposal by Xu *et al.*, electrolytes can be classified into three types, *i.e.*, nonflammable (SET < 6 s g⁻¹), flame retardant (20 s g⁻¹ < SET < 6 s g⁻¹), and flammable (SET > 20 s g⁻¹).⁷⁹ Here, the introduction of fluorine or phosphine in the molecular structure of solvents is an effective strategy to reduce their flammability. Many novel non-flammable solvents have been developed to date, which will be discussed in detail in the following sections.

2.3 Design principles of fluorinated solvents

2.3.1 Ideal electrolyte solvents. The properties of ideal electrolyte solvents can be mainly described as follows: (1) low viscosity and high solvation ability (high dielectric constant

or large donate number), which ensure fast ion transport, (2) wide liquidus range and high flash point (or low self-extinguishing times), which enable operation under different conditions without compromise in performance or safety, (3) wide electrochemical window or good interface compatibility (capable of forming a stable interfacial layer), which satisfies the requirement of high-energy-density batteries with Li metal anode and high voltage/capacity cathode, (4) low weight and good wettability, which minimize the mass and provide good interfacial contact with all components of the batteries, and (5) low cost and environmentally friendly. Most of the available solvents do not satisfy all the requirements of an ideal electrolyte, and hence new solvent molecules with as many of the above-required characteristics as possible need to be developed.

2.3.2 Advances and issues of different solvents. Table 1 summarizes the most common solvent molecules used in electrolyte chemistry for Li-based batteries and their corresponding benefits and drawbacks. To date, almost all types of functional groups have been evaluated in different cell chemistry, but obviously, none of them can meet the requirement of an ideal electrolyte solvent. In this case, electrode materials play an essential role in screening suitable solvents. Ether-based solvents were first used in Li-based batteries when Whittingham invented the titanium disulfide cathode in 1976.⁸⁰

Due to the failure of lithium metal anode in practical application and the development of carbonaceous anode, the mainstream electrolyte solvent gradually changed from ether to ether/ester mixtures and mixed ester solvents. When paired with graphite anodes or high-voltage cathodes (more than 4 V), ether undergoes co-intercalation into graphite or continuous oxidative degradation. In addition to ether and ester-based electrolytes, other solvents have also been investigated. Sulfone and nitrile have high anodic stability but cannot form a stable SEI on the anode surface. Phosphate solvents are flame-retarding or non-flammable, which are suggested to resolve safety concerns. However, their poor anode compatibility leads to obvious performance compromises in cycle life and cell capacity. Carboxylates can improve the low-temperature performance of batteries but are unable to form a protective SEI. Therefore, the further rational design of novel solvents is desirable to address these issues.

2.3.3 Characteristics of C–F systems. Table 2 lists the electronic properties of H and F.⁸¹ Obviously, the significantly different properties of H and F imply that fluorination can dramatically change the physical and chemical properties of molecules. Firstly, the high electronegativity of fluorine results in the formation of strongly polarized C–F bonds ($\delta^+C \rightarrow F\delta^-$), causing a change in the polar character of fluorinated molecules.⁸² Partially fluorinated molecules show more significant polarity than non-fluorinated ones, while perfluorinated solvents exhibit non-polar character and low polarizabilities. Secondly, the higher ionization energy and lower polarizability of F than H result in weaker intermolecular interaction in perfluorinated molecules. Thirdly, the considerable bond

Table 1 Common electrolyte solvents and their basic features

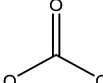
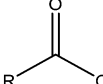
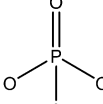
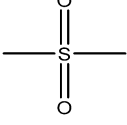
Name	Functional group	Remarks
Ether		High compatibility with Li metal anode; High ionic conductivity; Low viscosity; Low oxidation potential; Low dielectric constants
Carbonate		High oxidation potential; Moderate dielectric constants; Poor anodic stability on Li anode
Carboxylate		Wider service temperature ranges; Faster interfacial kinetics High resistive SEI
Phosphate		Nonflammability; Miscible with carbonates; High viscosity; Anodically unstable
Nitrile		High oxidation potential; High dielectric constants; anode unstable
Sulfone		High oxidation potential; Poor wettability toward separator; High viscosity; Improves thermal stability; Poor SEI stability
Fluorinate-linkage		Improves interfaces on the cathode and/or anode; Lower combustibility, If all-fluorinated, nonflammability; Low ion conductivity

Table 2 Atomic physical properties of H and F

	H	F
Electronic configuration	$1s^2$	$1s^2 2s^2 2p^5$
Electronegativity (Pauling)	2.20	3.98
Ionization energy (kJ mol^{-1})	1312	1681
Polarizability (Å^3)	0.667	0.557
Electron affinity (kJ mol^{-1})	74.0	332.6
Bond energies of C-X in CX_4 (kJ mol^{-1})	446.4	546.0
Bond lengths of C-X (\AA)	1.091	1.319
van der Waals radius (\AA)	1.20	1.47

energy of the C-F bond generally ensures high chemical and thermal stability of fluorinated solvents. For example, alkyl fluorides show $10^2\text{--}10^6$ higher resistance toward nucleophilic substitution than the corresponding alkyl chlorides.⁸² The shielding and inductive effect of fluorine on the carbon it is bonded to is responsible for the lower reactivity of fluorinated solvents. Fourthly, fluorinated molecules undergo defluorination in the presence of a reducing agent to form the corresponding fluorides.

2.3.4 Overview of fluorinated solvents and their corresponding electrolytes. As mentioned above, in comparison with non-fluorinated solvents, fluorination can greatly perturb the physicochemical properties of fluorinated solvents.⁸³ Specifically, formulated electrolytes containing fluorinated solvent enhance the electrochemical properties of batteries (Fig. 3).

Physical properties. The influence of fluorination on the physical properties varies with different fluorinated solvents. In the case of fluorinated cyclic solvents, their melting point and permittivity decrease with an increase in the fluorine content, while fluorinated linear esters show the opposite trend. The type of fluorinated functional groups also affects the properties of fluorinated solvents. For example, fluorinated linear ethers with C-F termination show higher viscosities and comparable solvating power than their non-fluorinated counterparts. However, in the case of polyfluorinated and perfluorinated solvents, the individual dipole moments of the C-F bonds are canceled, leading to extremely low polarity, and thus lower viscosity and capacity to dissolve lithium salts.⁸⁴ Therefore, polyfluorinated and perfluorinated solvents are capable of acting as unique media to regulate the viscosity, wettability, combustibility, and interfacial compatibility of electrolytes.^{85–87}

Solvation structure. The strong electron-withdrawing nature of fluorine can affect the solvating power of solvents. Su *et al.* examined a series of electrolyte solvents, among which the fluorinated solvents exhibited lower capability to solvate Li^+ than their non-fluorinated counterparts.⁵⁵ The weak solvating power of fluorinated solvents can increase the content of anions in the solvation sheath, enhancing the Li^+ -anion interaction strength. Therefore, even in “dilute” salt concentrations (1 M), CIP and AGG species could be observed in some electrolytes with fluorinated solvents.^{88,89} Recently, Cui *et al.* reported

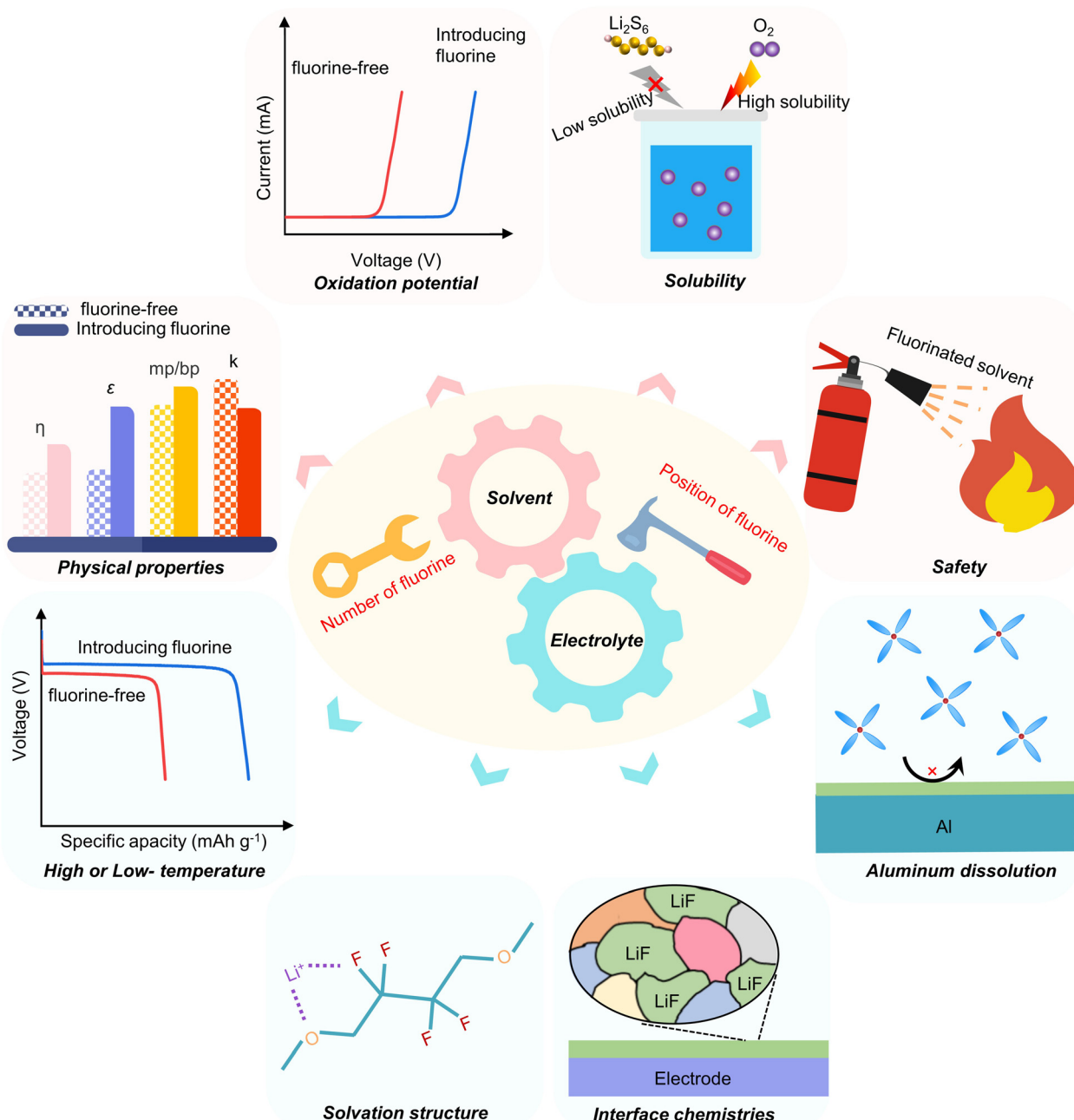


Fig. 3 Advanced functions related to fluorinated solvents and their corresponding electrolytes, where η , ϵ , mp/bp, and k represent viscosity, dielectric constant, melting point/boiling point, and ionic conductivity, respectively.

that in some cases, the fluorine in the solvent molecules also coordinates with Li ions to form unique Li–F interactions in the solvation structures.^{90,91} It should be noted that these unusual solvation structures favor the interface stability but lower the ionic conductivity. Alternatively, highly fluorinated diluents (polyfluorinated and perfluorinated solvents) show poor solvating power, exerting a minimal change in the solvation structure of electrolytes.⁹² However, we emphasize that even this tiny change in solvation structure can significantly affect the properties of the electrolyte. For example, a diluent with a certain solvating power can deteriorate the recyclability of the lithium

metal, whereas a weak-coordinated diluent is beneficial for the formation of a homogeneously distributed, ultra-high Li₂O content in SEI, enabling a high CE of Li.^{93,94}

Interface chemistries. Fluorinated solvents also enhance the properties of the interface layer. Firstly, the degradation of fluorinated solvents inevitably results in the formation of an interface layer (SEI or CEI) with rich LiF or F-containing composites, thus offering high chemical and mechanical stability.³⁵ For example, FEC and EC display different decomposition mechanisms. The reduction products of FEC contain

poly(VC) and LiF; however, organic species-rich ($\text{CH}_2\text{OCO}_2\text{Li}$)₂ and ($\text{CH}_2\text{CH}_2\text{OCO}_2\text{Li}$)₂ with the minority of Li_2CO_3 could be detected in EC.^{6,95}

In comparison to ethyl methyl carbonate (EMC), the oxidation decomposition of (2,2,2-trifluoroethyl)methyl carbonate (FEMC) can produce extra CH_2CF_3^- , which can react with metal cations on the cathode surface to generate the corresponding metal fluorides.⁹⁶ Secondly, the unique Li^+ -anion solvation structures in fluorinated solvents with low solvating power also favor the formation of LiF, *i.e.*, an anion-derived interface layer. In lithium metal battery systems, LiF contributes to the formation of a dense and well-passivated interface layer, permitting uniform ion flux and reducing the interfacial resistance.^{2,20} It is worth noting that the poor ionic conductivity of LiF may deteriorate the interfacial ion transport in battery systems with a carbon-based anode.⁹⁷

Balancing the bulk and interface transport. Given that fluorination can decrease the ionic conductivity of the electrolyte, balancing the bulk and interface transport is one of the most important concerns in designing advanced fluorinated solvents. As shown in Fig. 4a, the distance of the position of fluorine from the characteristic functional groups of molecules is highly related to the properties of solvents and their formulated electrolytes. In the case of fluorinated linear molecules, the strong electron-withdrawing $-\text{CF}_3$ group in the α site can reduce the molecular polarity drastically, lowering the solvating power of the fluorinated solvent, and thereby decreasing the bulk transport in the electrolyte.⁹⁸ Besides, α -fluorinated molecules show higher activity for the generation of LiF on the lithium surface than their β -fluorinated analogs.⁹⁹ However, this does not mean that α -fluorinated molecules exhibit high interface stability toward the lithium anode. Alternatively, the $-\text{CF}_3$ group at the γ site imposes a weak withdrawing effect on fluorinated molecules. Therefore, β -fluorinated molecules may represent an optimal balance to tune the properties of fluorinated solvents. For example, Su *et al.* demonstrated that a β -fluorinated sulfone, 1,1,1-trifluoro-2-(methylsulfonyl)ethane (TFEMS), displays middle-ground properties among its analogs, delivering “enough” anodic stability and conductivity.⁹⁸ Recently, Xie *et al.* further highlighted the “magic” function of fluorine at the β site.¹⁰⁰ They found that the C-F bond on the fluoroalkyl ($-\text{CF}_2\text{CF}_2-$) chain shows high reactivity to construct a fluorinated SEI when an active end group is attached to the β site. This fluorinated SEI features well-distributed LiF, benefitting the fast and uniform transport of Li^+ , and thus rendering highly reversible Li plating/stripping. Alternatively, reducing the degree of fluorination from the $-\text{CF}_3$ group to the asymmetric $-\text{CHF}_2$ group can induce the formation of local dipole, which enables increased intermolecular interactions (Fig. 4b).⁹⁰ These partially fluorinated molecules can reduce the ion cluster, increasing the ion motion, while maintaining high interface stability.

Oxidation potential. In general, fluorine on either cyclic or linear solvents can significantly increase the oxidation

potential. Firstly, the introduction of fluorine can lower the energy of the molecular HOMO and LUMO, which may induce both a higher oxidation and reduction potential.^{101–103} This leads to higher oxidation voltages in most fluorinated solvents compared to their non-fluorinated counterparts. Secondly, the improved interface chemistries derived from the decomposition of fluorinated solvents or anions enable the expulsion of the solvent molecules away from the aggressive cathode surface and isolation of electrons. In many cases, it is not easy to intentionally decouple the single effect of the two reasons described above due to their synergistic effect in many electrolyte systems. Notwithstanding, the incorporation of fluorine in the solvent molecule does not always lead to higher抗氧化, given that the fluorination position and molecular configuration also play an important role.^{101,104} For example, the oxidation peak of γ -butyrolactone (γ GBL, 6.1 V) is 0.2 V higher than that of β -fluoro- γ -butyrolactone (β -F- γ -BL, 5.9 V).¹⁰⁵ Similarly, the oxidation resistance of fluorinated sulfolane (TMS) is different when fluorine is substituted at different positions.¹⁰⁴

High temperature. At high temperatures ($> 50^\circ\text{C}$), the side reactions between the electrolyte and electrodes increase due to the altered chemical potential of the electrode (higher cathode potential (μ_c) and lower anode potential (μ_a)) and accelerated reaction kinetics, according to Nernst and Gibbs–Helmholtz equations.⁷⁰ The CEI and SEI formed at high temperatures are typically thicker than that formed at room temperature, resulting in the loss of active Li.¹⁰⁶ Besides the thicker interface layers, high temperatures also lead to the generation of more HF, transition metal (TM) dissolution, and gas release.⁶ Alternatively, the introduction of fluorinated solvents can alleviate these issues due to their intrinsic high thermal stability and/or capability of producing more stable interface layers with a high LiF content.³³

Low temperature. The low-temperature performance of electrolytes is not only associated with the physical properties of their solvents but also related to the ion transport and desolvation barriers in the bulk electrolyte and interface layers.^{107–110} For example, the introduction of fluorine near O atom-containing functional groups can be a double-edged sword, where on the one hand, fluorination can lower the electron density around the oxygen atom, favoring the desolvation process during the electrochemical reaction; on the other hand, fluorination can decrease the surface tension of solvent molecules and improve the wettability of the electrolyte, thus decreasing the contact resistance. More importantly, the improved interfacial chemistries in the electrolyte with fluorinated solvents favor rapid interfacial ion transport at low temperature. However, the high viscosity of partially fluorinated solvents can decrease the ion conductivity of the electrolyte. Meanwhile, the solvating power of fluorinated solvents is reduced, increasing the possibility of salt precipitation at low temperatures. Therefore, the fluorinated solvents for

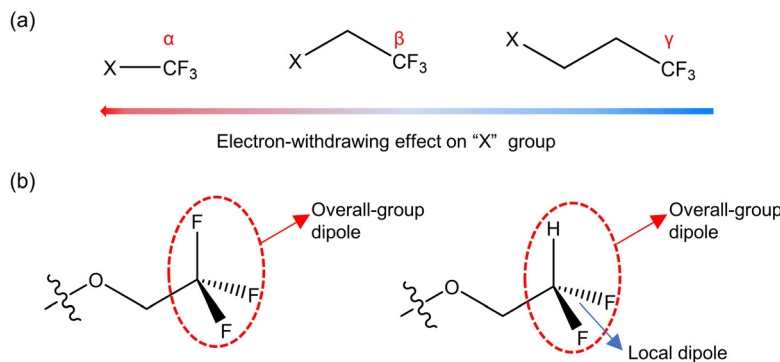
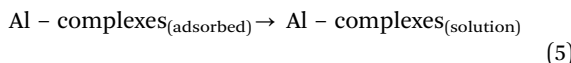
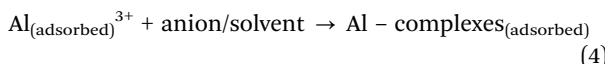


Fig. 4 Proposed strategies to balance the bulk and interface transport of fluorinated solvents. (a) Schematic illustration of electron withdrawing effect of fluorine at different positions on "X" group. (b) Spatial configuration and dipole direction of $-CF_3$ and $-CF_2$. Fig. 4a is redrawn based on ref. 98. Fig. 4b is redrawn based on ref. 90.

low-temperature electrolytes need to achieve a balance between ion transport and salt dissolution.

Aluminum dissolution. Aluminum (Al) in batteries will be subjected to electrochemical corrosion by the electrolyte components in the absence of a dense passivation layer.^{111,112} For example, in an electrolyte with lithium imide salts, the generated $[Al(N(SO_2CF_3)_2)]^{3+x-}$ complex ion is the main reason for the dissolution of aluminum.¹¹³ Alternatively, the dissolution of Al^{3+} from Al can be promoted by the protons generated from the oxidation of the electrolyte solvent (such as EC) at high voltage.¹¹⁴ These processes can be described as eqn (4) and (5).¹¹⁵



In a conventional electrolytic system, *i.e.*, LiPF₆-mixed carbonate system, the formation of insoluble AlF₃/LiF through the reaction between F[−] and Al³⁺/Li⁺ plays a critical role in suppressing the further dissolution of Al.¹¹⁶ However, in some high-energy-density batteries, LiPF₆ is often excluded. Although the actual mechanism is controversial, utilizing fluorinated solvents represents another strategy for alleviating or completely inhibiting the dissolution of aluminum. Shkrob *et al.* reported that the limited solubility of AlF₃ coordination polymers in fluorinated carbonate can promote the formation of AlF₃ to protect the Al surface, isolating Al from the electrolyte.¹¹⁷ Another possible mechanism for suppressing Al dissolution is derived from the decomposition of fluorinated solvents.¹¹⁸ Besides, the unique Li-anion solvation structure in electrolytes with fluorinated solvents also favors the formation of robust passivation layers on the Al surface.⁹¹

Safety. The highly volatile and flammable electrolyte solvents pose many safety risks and create engineering challenges in battery manufacturing.^{32,119} In the case of the traditional phosphate flame-retardant, a trade-off exists between flame-

retardant efficiency and battery performance, which means that a low content of flame-retardant is not enough to make the electrolyte non-flammable and a high flame-retardant dosage does not afford good interface compatibility, resulting in a poor electrochemical performance.^{120,121} Fortunately, fluorination is supposed to resolve this trade-off issue given that it can improve the SEI-forming ability of phosphates.⁷⁹ Furthermore, inducing fluorine can help to further reduce the flammability. As demonstrated by Mönnighoff *et al.*, the SET of phosphates decreases with an increase in fluorine content, although this effect is not linear.¹²² Besides, perfluoroether co-solvents can also lower the flammability of solvents by scavenging H[•] radicals through F[•] radicals.¹²³ However, the runaway pathway is still observed in perfluoroether-based electrolytes, although they show different thermal runaways compared with conventional non-fluorinated solvent-containing electrolytes, as demonstrated by Hou *et al.*¹²⁴

Solubility for specific applications. In the case of Li–O₂ batteries, the dissolution and diffusion of oxygen in non-aqueous electrolytes are indispensable for the electrochemical reaction to proceed.¹²⁵ Generally, partially fluorinated and perfluoro solvents exhibit high oxygen solubility and fast dissolution kinetics due to their high porosity.^{126,127} Consequently, a higher active oxygen utilization was achieved in electrolytes containing fluorinated solvents, leading to the improved discharge performance of Li–O₂ batteries.¹²⁸ Alternatively, the high chemical stability of fluorinated solvents shows high resistance against the nucleophilic attack of oxygen species.^{129,130} These features are of great interest in applying fluorinated solvents in Li–O₂ batteries.

The “shuttle effect” of polysulfides (PS) is responsible for deteriorating the cycling stability of Li–S batteries.^{131,132} Due to the higher electronegativity and larger van der Waals radius of fluorine atoms, fluorinated solvents, especially perfluoro solvents, show higher steric hindrance and weaker interaction with PS than their fluorine-free counterparts.^{133,134} Therefore, electrolytes that utilize fluorinated solvents as co-solvents have limited PS solubility.^{135,136} Košir *et al.* demonstrated that a fluorinated electrolyte with 1,2-(1,1,2,2-tetrafluoroethoxy)ethane

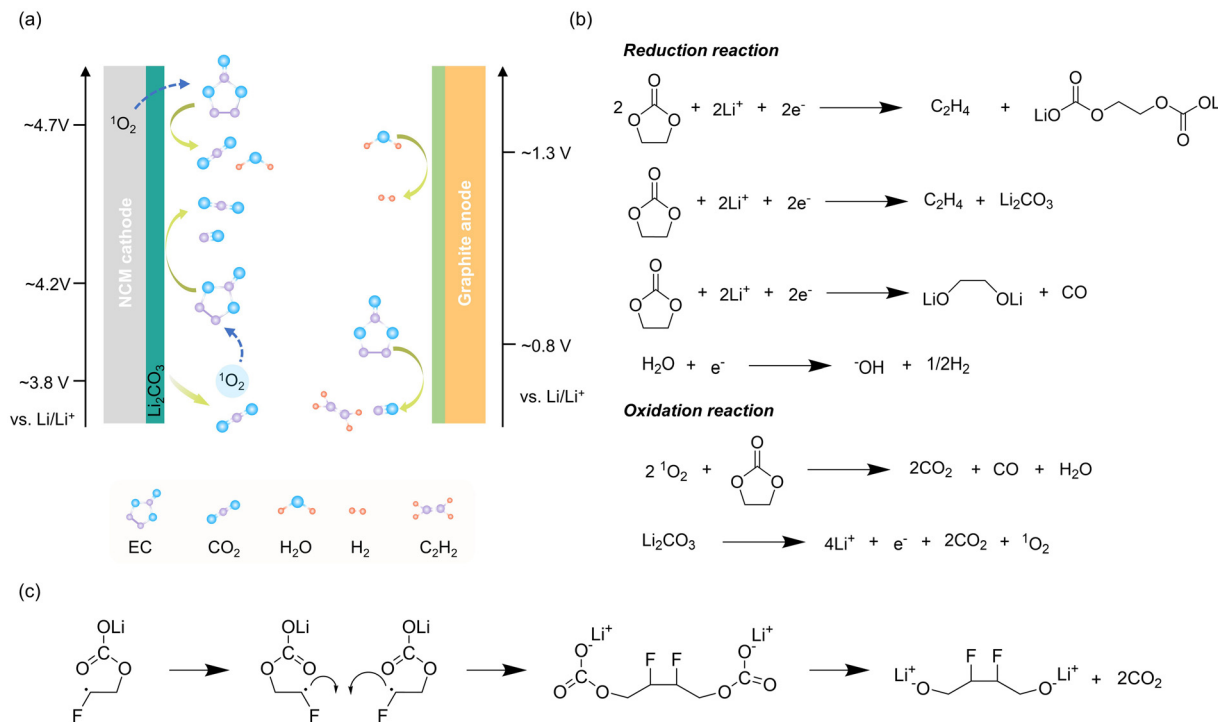


Fig. 5 (a) Schematic illustration (not exhaustive) of the gas generation mechanism in NCM||graphite cells using carbonate-based electrolytes. (b) Reduction and oxidation of EC-based electrolyte in NCM||graphite cells. (c) Proposed CO₂ generation mechanism from FEC. Fig. 5c is redrawn based on ref. 152.

enabled about 25× lower concentration of PS in the separator than that of conventional ether-based electrolyte.¹³⁷ Furthermore, with the aid of additives (LiNO₃ or LiFSI), fluorinated solvents also favor the suppression of the self-discharge of Li–S batteries due to the formation of a robust SEI layer.^{138,139}

Gas generation and evolution. The gas generation (C₂H₄, H₂, CO, CO₂, etc.) from electrolyte decomposition at both electrodes can induce serious safety issues (such as thermal runaway) and performance degradation in batteries.^{140–143} Fig. 5a displays the gas evolution of NCM||graphite cells in conventional carbonate-based electrolytes. C₂H₄ and CO gases are generated from the decomposition of the electrolyte, while H₂ is evolved from the reduction of the R–H species/trace amounts of H₂O in the electrode and electrolyte (Fig. 5b).^{144,145} In particular, CO₂ originates either from surface contaminants from the cathode (such as Li₂CO₃) or the reaction of EC with singlet oxygen released from the cathode at high voltages.^{146,147} Unlike the magic changes mentioned above, the function of fluorinated electrolytes in mitigating gas generation is unsatisfactory. Fluorinated ether can reduce, but not eliminate, gas generation.^{148,149} On the contrary, in cells with fluorinated carbonate ester, more gas products (especially CO₂) are detected compared with that containing EC, which can be ascribed to the fluorine-containing SEI formed on the graphite surface, limiting the consumption of CO₂.^{150,151} Although the detailed paths differ, the initial ring-opening and electron

transfer occur similarly for the decomposition of EC and FEC to produce CO₂ (Fig. 5c).¹⁵²

2.3.5 Comparison of various fluorinated solvents. To better understand the specific advantages and disadvantages of various fluorinated solvents, seven key parameters are summarized and compared in Fig. 6. Fluorinated esters show the best balance for cells with a graphite anode. Furthermore, fluorinated esters show excellent anodic stability, enabling the operation of a highly reversible 5 V battery.^{85,153} Similarly, fluorinated ethers undoubtedly attracted the main research attention in lithium metal batteries due to their high compatibility with lithium metal and middle anodic stability, which can satisfy a 4 V class cathode. In particular, fluorinated linear esters and ethers exhibit good wettability toward the separator and electrode, which is extremely important for reducing the electrolyte usage. However, as mentioned above, the safety issues related to gas generation (especially in the case of Li-rich Mn-based cathodes) and flammability are still problematic in fluorinated esters and ethers. Moreover, unlike fluorinated esters with sufficient solvating power, fluorinated ethers may suffer from salt precipitation at low temperatures, hindering the low-temperature operation of batteries. Fluorinated sulfones and nitriles inherit the high oxidation potential of their non-fluorinated counterparts. However, the introduction of fluorine into sulfones and nitriles results in an unsatisfactory performance improvement toward graphite anode in terms of cathodic stability. Furthermore, fluorination significantly increases the viscosity of nitriles, resulting in an order of

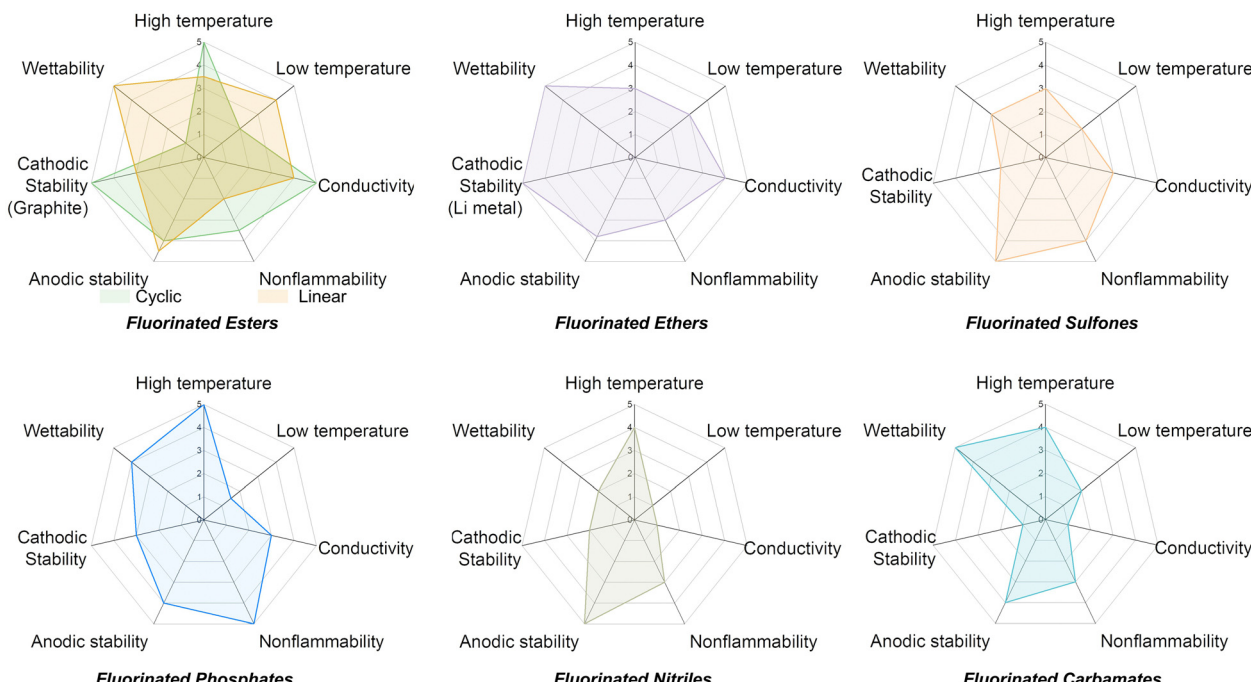


Fig. 6 Comparison of the key parameters of various non-fluorinated and fluorinated solvents. The rating of 1–5 represents poor, inferior, middle, reasonable, and excellent, respectively.

magnitude lower ionic conductivity of fluorinated nitriles than non-fluorinated ones.¹⁵⁴ Fluorinated phosphates show the best flame retardance among fluorinated solvents; however, their large molecular structure may hinder the ion transport at low temperature. Alternatively, the introduction of fluorine in carbamates can sharply deteriorate the ionic conductivities.¹⁵⁵

Overall, the introduction of fluorine exerts many favorable benefits for developing advanced electrolytes that can reach the boundary of electrolytes towards an ideal territory. It is not surprising that fluorinated solvents have garnered significant attention in the past two decades. However, fluorination cannot solve all the issues to achieve ideal electrolytes for lithium-based batteries (see the deteriorated physical properties of fluorinated carbamates). Accordingly, as a compromise, the mixed solvent strategy will continue to prevail for a long time. This further requires the accurate revelation, tuning, and prediction of the physicochemical properties, solvation structures, and interface compatibilities of electrolytes with fluorinated solvents. The emerging highly powerful supercomputing capabilities have great potential to enable the design of new fluorinated solvents with well-balanced properties. Thus, efforts to create a database of the currently reported results, and then rapid screening and predicting all-balanced fluorinated solvents by emerging artificial intelligence and machine learning methods are urgent.

3. Synthesis of fluorinated solvents

Over the past 20 years, nearly all newly developed fluorinated solvents in the field of batteries involve two key reactions, *i.e.*,

nucleophilic and electrophilic reactions. Although the reaction paths and mechanisms for the synthesis of these solvents are known, they remain unfamiliar to the researchers entering this field for the first time. Thus, it is necessary to discuss and analyze different synthetic methods and their reaction mechanisms. In this section, the two common strategies for synthesizing fluorine-contain solvents will be summarized, namely, the selective formation of new C–F bonds and functionally modified fluorinated molecules.

3.1 Selective formation of new C–F bond

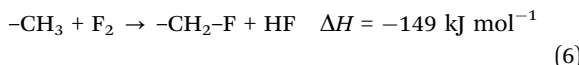
Although there are many different strategies to synthesize organofluorine solvents for LIBs, the selective incorporation of fluorine in organic compounds is still challenging, especially in terms of regio- and stereoselectivity.¹⁵⁶ The main challenges related to the formation of new C–F bonds arise from the intrinsic characteristics of fluorine. From a kinetic point of view, the high electronegativity and small ionic radius of fluorine make it easy to form strong hydrogen bonds, reducing its nucleophilicity.¹⁵⁷ The formation of C–F bonds is kinetically constrained in hydrogen-bond donor solvents.¹⁵⁸ Alternatively, fluorine exhibits strong nucleophilicity in aprotic solvents, exacerbating the uncontrolled side reactions. In this section, we discuss the methods for fluorination and corresponding mechanisms for exploiting new solvents for LIBs. Table 3 summarizes the advantages and disadvantages of different fluorination methods employed in electrolyte engineering.

3.1.1 Direct fluorination. Direct fluorination is conducted by attacking the target reactant with electrophilic fluorinating agents.^{159,160} The most common fluorination agent for direct

Table 3 Comparison of different fluorination methods

	Advantages	Disadvantages
Direct fluorination	Convenient and fast	Special equipment or techniques requirement
Halogen exchange	Easy to control, low cost	Low yield
Deoxofluorination	Abundant fluorine reagent and flexible reaction routes	Low yield, difficult to purification
Electrochemical fluorination	Easy scale-up	Relatively poor selectivity

fluorination is fluorine gas.¹⁶¹ Although this reaction is vigorously exothermal, it is easily controlled in a strong acid medium, resulting in an acceptable selectivity and yield (eqn (6)).¹⁶⁰



For example, fluorinated-EC (FEC, F₂EC, and F₃EC) can be obtained *via* the direct fluorination of EC in a mixture gases of fluorine (F₂) and nitrogen (N₂) at high temperature (Fig. 7a).¹⁶² Also, other fluorinated esters, such as fluorinated γ -butyrolactone (γ -GBL), dimethyl carbonate (DMC), and propylene carbonate (PC), can be obtained by utilizing the same protocol.^{163,164} However, this strategy is associated with some drawbacks, such as the high toxicity of F₂, special equipment or technique requirement, and poor selectivity.

3.1.2 Halogen exchange. Halogen exchange is another fluorination method that has been employed in industrial processes, especially for the synthesis of FEC. The mechanism of this reaction involves a nucleophilic substitution process (S_N1 or S_N2), where the nucleophilic reagents attack the carbon atom linked with the leaving group (Fig. 7b). For example, FEC can be obtained from chloroethylene carbonate by halogen exchange with KF. However, despite its potential utility, this protocol requires further optimization of the reaction paths and conditions to improve the yield to about 50%.

3.1.3 Deoxofluorination. Deoxofluorination is a critical method to transform alcohols into aliphatic fluorides.^{165–167} Various deoxofluorination reagents, including Et₂NSF₃ (DAST), FluoLead, XtalFluor, and (MeOCH₂CH₂)₂NSF₃ (Deoxofluor), have been exploited to date.¹⁶⁸ The mechanism of deoxofluorination is also a typical nucleophilic substitution, in which the reagents are susceptible to nucleophilic attack by activated hydroxy and accompanied by Walden inversion of substrates during the reaction process (Fig. 7c). The fluorination reagent and base have a significant effect on the fluorination efficiency and side reactions (mainly fluorine elimination).¹⁶⁹ For example, the combination of perfluorobutylsulfonyl fluoride (PBSF) and 7-methyl-1,5,7-triazabicyclo[4.4.0]dec-5-ene (MTBD) produced 92% fluorinated γ -GBL.¹⁷⁰ However, the yield decreased to 74% when 1,8-diazabicyclo[5.4.0]undec-7-ene (DBU) was employed.

3.1.4 Electrochemical fluorination. Electrochemical fluorination (anodic fluorination) has been employed to obtain fluorinated solvents due to its relatively mild and safe operating conditions as well as ease to scale-up.¹⁷¹ In the traditional anodic fluorination process, a metal electrode and nucleophilic agents are employed, where the reactants undergo

electrochemical oxidation, and then react with F[−] to obtain fluorinated molecules (Fig. 7d).^{162,172} Fig. 7e depicts the general reaction mechanism of this process. During the electrochemical synthesis process, the electrolytic solvents, fluorinated agents, and work electrodes significantly affect the selectivity and efficiency of fluorination. For example, about 67% FEC could be harvested during the anodic fluorination process in a system composed of 4-phenylthio-1,3-dioxolan-2-one as the reactant, Et₃N·5HF as the nucleophilic agent, and CH₂Cl₂ as the solvent (Fig. 7f).¹⁷³ However, no FEC could be obtained when the solvent was changed to DME. Besides, solvent-free anodic fluorination strategies have also been exploited recently. Fuchigami *et al.* synthesized a series of highly regioselective fluorinated cyclic ethers, such as fluorinated 1,4-dioxane, fluorinated 1,2-dioxolane, and FEC, in solvent-free conditions with satisfactory yields.¹⁷⁴ Although the selectivity and yield of anodic fluorination have been remarkably improved over 30 years, the cost of this technique needs to be further verified for large-scale electrolyte production.

3.2 Functional modification of fluorinated molecules

The modification of fluorinated molecules with specific functional groups is a promising approach to access fluorinated compounds that are difficult to synthesize by direct fluorination. The difficulties in C–F bond formation at specific position sites and reductive elimination of C–F bond can be circumvented through this strategy.¹⁵⁷ By modifying fluorinated solvents with function groups, a variety of esters, carbamates, ethers, phosphates, sulfones, and nitriles have been rationally designed and synthesized.

3.2.1 Synthesis of fluorinated esters and carbamates. Fluorinated PC derivatives play a crucial role in electrolyte engineering due to their better anodic stability or SEI forming ability than their PC counterparts.^{175,176} Similar to EC, these solvents can be obtained by the cycloaddition and esterification reaction of the corresponding fluorinated epoxides and carbon dioxide (CO₂ gas) in the presence of a particular catalyst (Fig. 8a).^{177,178} Besides, the substitution reaction of an acyl chloride is another prevalent approach in developing new solvents, especially in fluorinated solvents. The intrinsic electron-deficient carbonyl of acyl chloride makes it highly reactivity with active hydrogen (such as hydroxy, amino, and carboxyl) to generate the corresponding acyl compounds. Sasaki *et al.* synthesized a series of fluorinated methyl propyl carbonate (MPC) with reactants of fluoropropanol and methyl chlorocarbonate (Fig. 8b).¹⁷⁹ Bolloil *et al.* utilized different carbamic chlorides and fluorinated alcohol as the starting reactants to prepare three fluorinated N,N-carbamates (Fig. 8c).⁴⁰

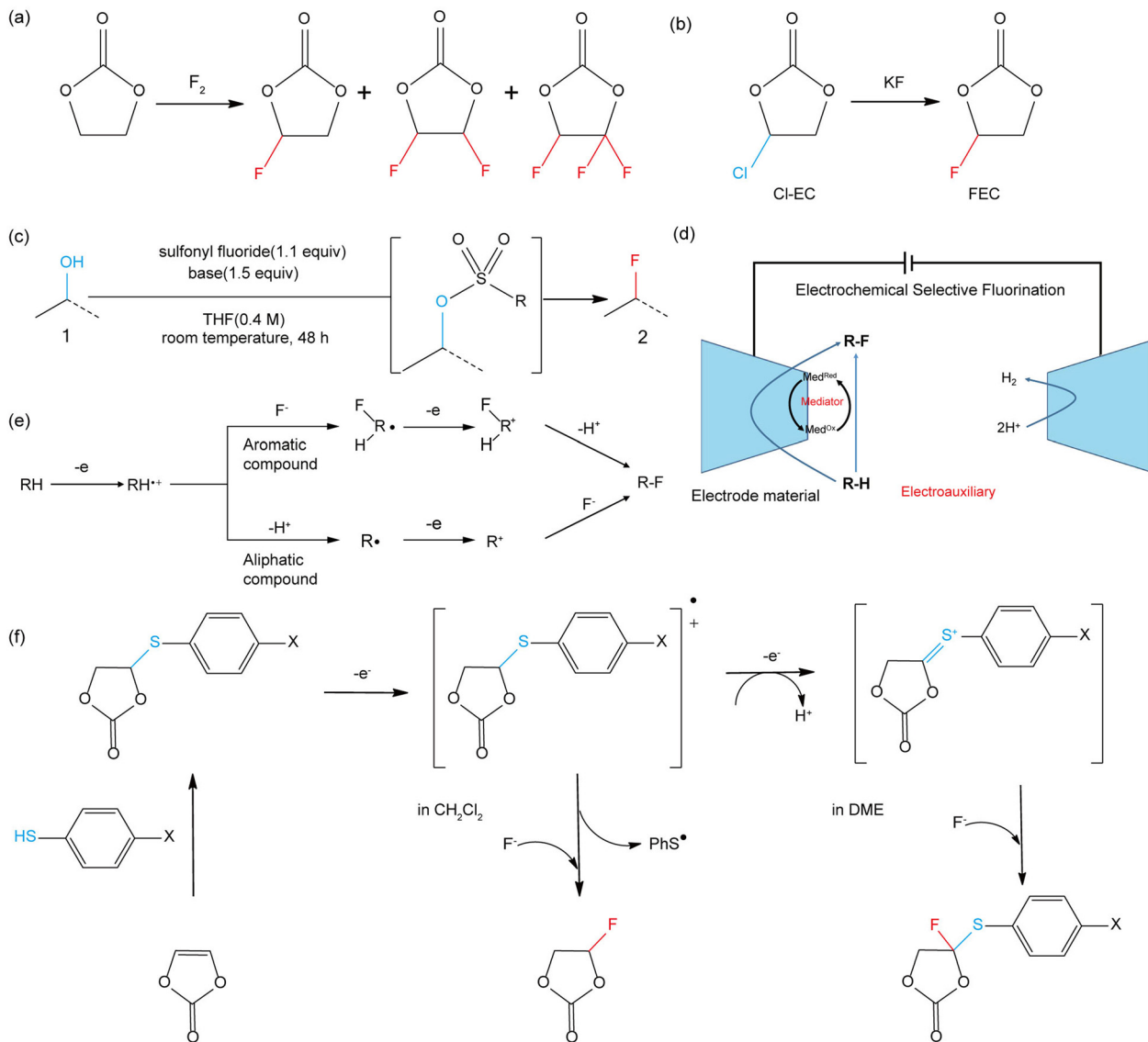


Fig. 7 Schematic illustration of the formation of a new C-F bond. (a) Synthesis of fluorinated-EC through direct fluorination of EC. (b) Synthesis of FEC via a halogen exchange process. (c) Reaction mechanism of deoxofluorination. (d) Electrochemical anodic fluorination. (e) General reaction mechanism for electrochemical fluorination. (f) Anodic fluorination of 4-arylthio-1,3-dioxolan-2-ones in different solvents. Fig. 7d and e are redrawn based on ref. 172. Fig. 7f is compiled based on ref. 173.

3.2.2 Synthesis of fluorinated ethers. Williamson ether synthesis, first developed in 1544 by V. Cordus and proposed in 1851 by W. Williamson, is one of the most important approaches to synthesize alkyl ethers due to its simplicity and general applicability in both laboratory and industrial synthesis.¹⁸⁰ As shown in Fig. 9a, this reaction proceeds *via* nucleophilic substitution of a halide ion in an alkyl halide by an alkoxide anion (such as sodium alkoxide), producing symmetrical and asymmetrical ethers.¹⁸¹ The activity of alkyl halides and leaving groups follow the order of methyl > allyl, benzyl > primary carbon > secondary carbon, and OTs ~ I > OMs > Br > Cl, respectively. Utilizing sulfonyl chloride (including *p*-toluenesulfonyl chloride (TsCl) and methylsulfonyl chloride) as examples, the S center in sulfonyl chloride is susceptible to

nucleophilic attack by the hydroxyl group, producing a compound with an easy-to-leave group. To date, abundant ethers have been developed using this strategy, including fluorinated or partially fluorinated 1-ethoxy-2-methoxyethane (EME),¹⁰¹ 1,4-dimethoxybutane (FDMB)⁹¹ and 2-ethoxy-4-(trifluoromethyl)-1,3-dioxolane (cFTOF)⁸⁹ (Fig. 9b-d). Their properties will be discussed in detail in Section 4.2. It should be noted that some issues, such as low yield and difficulties in purification caused by the multistep reaction path and good miscibility of products in solvents, need to be solved in the future.

3.2.3 Synthesis of fluorinated phosphates and sulfones. Phosphonic chlorides, such as phosphorus oxychloride, represent an essential substrate for developing new organic phosphates. The reaction between phosphonic chloride and alcohol

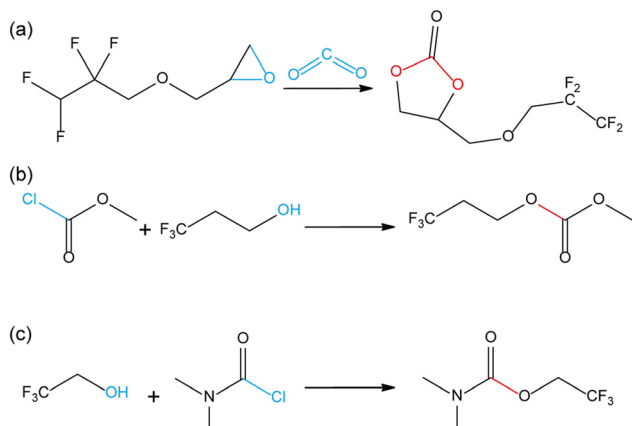


Fig. 8 (a) Synthesis of fluorinated PC derivatives through the cycloaddition and esterification reaction. (b) Synthesis of fluorinated MPC. (c) Synthesis of fluorinated *N,N*-carbamates. Fig. 8b and c are redrawn based on ref. 179 and 40, respectively.

also involves an S_N2 -type substitution.^{182,183} For instance, the fluorinated cyclic phosphate, 2-(2,2,2-trifluoroethoxy)-1,3,2-dioxaphos-pholane 2-oxide (TFEP) can be obtained through the reaction between 2,2,2-trifluoroethanol and 2-chloro-1,3,2-dioxaphospholane 2-oxide with the aid of triethylamine (Fig. 10a).¹⁸⁴

There are five traditional methods to synthesize sulfones including the oxidation of sulfides or sulfoxides, aromatic sulfonylation, alkylation/arylation of sulfonates, and addition

to alkenes and alkynes (Fig. 10b).¹⁸⁵ Among them, the oxidation of sulfides or sulfoxides is the most widely used approach, including the preparation of fluorinated sulfones. Here, the synthesis of TFEMS can serve as an example. As shown in Fig. 10c, two steps are involved, including the reaction of alkyl iodides with sodium mercaptide and the oxidation of thioether intermediates by hydrogen peroxide.⁹⁸ Another common strategy to synthesize fluorinated solvents is aromatic sulfonylation, in which the sulfonyl halide or sulfonic acid reacts with a molecule with active H (arene and amine) in the presence of a suitable Lewis or Brønsted acid catalyst. For example, Fu *et al.* developed a series of *N,N*-dialkyl perfluoroalkanesulfonamides with *N,N*-dialkylamine and the corresponding perfluoroalkanesulfonyl chloride (Fig. 10d).¹⁸⁶

Alternatively, the reaction between the Grignard reagent and sulfonic anhydride also provides a practical route to prepare fluorinated sulfones in a decent yield. As depicted in Fig. 10e, the carbanion in the dialkylmagnesium nucleophilic attacks the S atom in trifluoromethanesulfonic anhydride (TFMSA) to produce trifluoromethyl isopropyl sulfone (FMIS).¹⁸⁷ To the best of our knowledge, no other methods have been reported for the synthesis of fluorinated sulfones for Li-based cells. In this case, it is suggested that further efforts be devoted to employing alkylation/arylation of sulfonates and addition to alkenes and alkynes for the synthesis of new fluorinated sulfones to enrich this field.

3.2.4 Synthesis of fluorinated nitriles. Although various methods have been reported for the synthesis of nitriles, the dehydration of amides seems to be the most promising due to

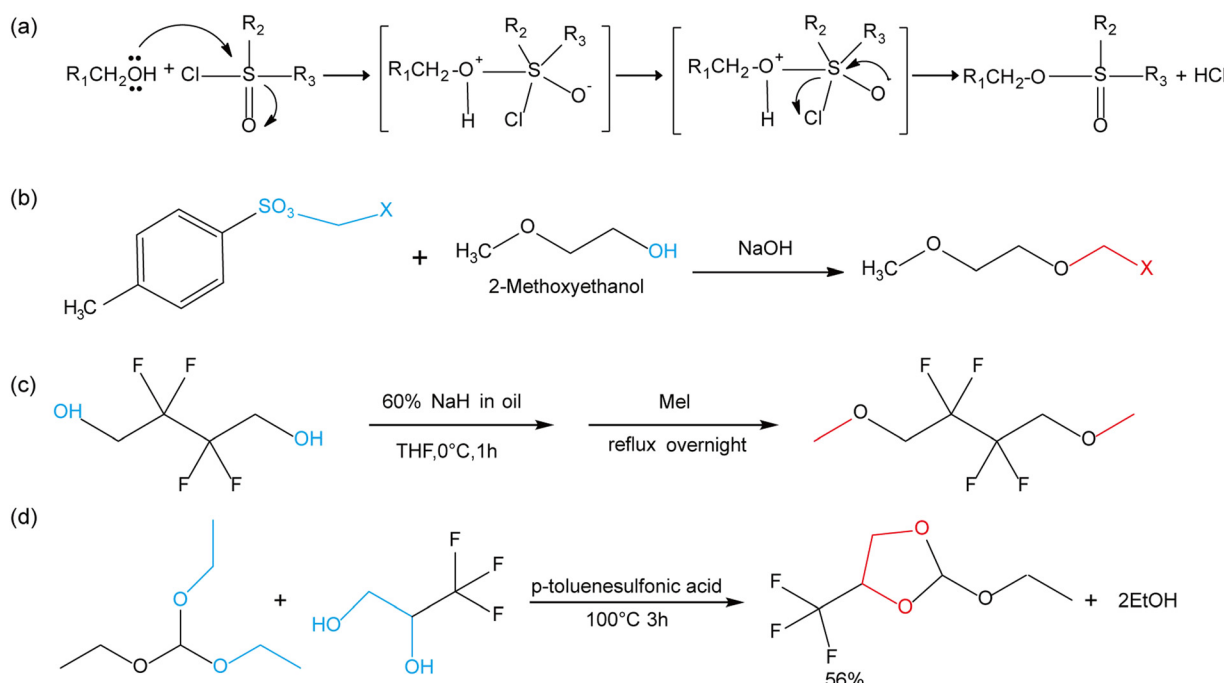


Fig. 9 (a) Reaction mechanism of Williamson ether synthesis. The synthesis scheme of partially fluorinated EME (b), FDMB (c), and cFTOF (d). Fig. 9b–d are redrawn based on ref. 101, 91, and 89, respectively.

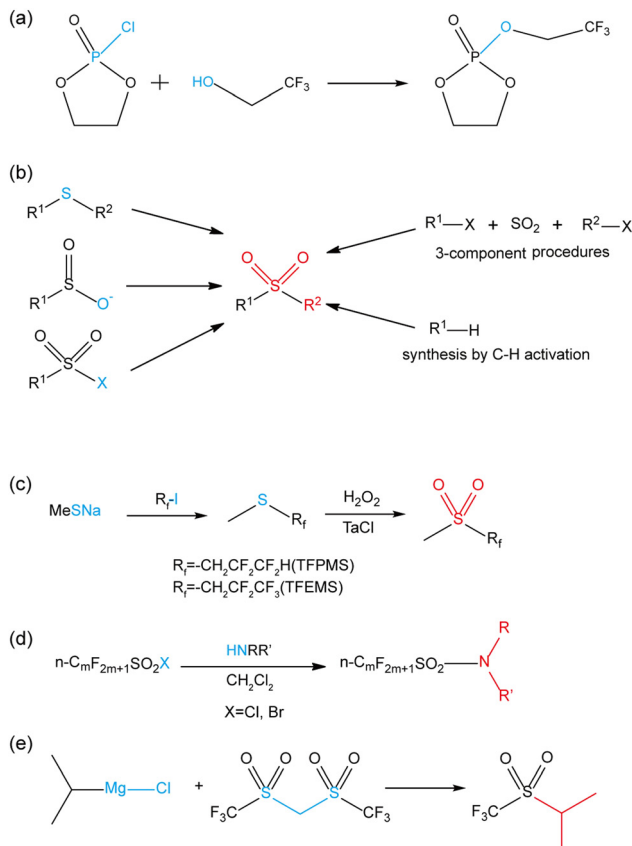


Fig. 10 (a) Synthetic route of TFPMS. (b) Five traditional methods for synthesizing sulfones. (c) Synthetic routes for TFEMMS. (d) General synthesis process for *N,N*-dialkyl perfluoroalkanesulfonamides. (e) Substitution reaction of TFMSA and dialkylmagnesium. Fig. 10b–e are redrawn based on ref. 185, 98, 186, and 187, respectively.

its efficient and benign reaction route.¹⁸⁸ Simple heating at high temperature, dehydrating agents, and catalysts can trigger the dehydration of amides to produce nitriles (Fig. 11a). In fact, dehydration reagents (P_2O_5 , $AlCl_5$, etc.) and catalysts (transition metals, organo-catalysts, etc.) are often needed to overcome the issue of harsh temperature. A typical example is the synthesis of 3-trifluoromethyladiponitrile (ADN- CF_3), where the reaction is accessible to occur under a facile reaction condition with the help of a dehydration reagent (P_4O_{10}) (Fig. 11b).¹⁵⁴

Due to the development of active catalysts, computer-aided synthesis routes, and modern purification techniques, more and more fluorinated electrolyte solvents have been exploited and evaluated. In general, the synthesis of new C–F bonds through fluorination is facile for industrial production, while the substrate scope and corresponding products are restricted. On the contrary, the modification of fluorinated molecules seems to be more versatile without the use of harsh conditions and equipment. However, the selectivity and yield of this method need to be further improved. Modular flow cells should be developed to realize kg-scale synthesis in the future. In this regard, the optimized approach (substrate, catalyst, and solvent) should depend on the molecular structures of the target fluorinated solvents.

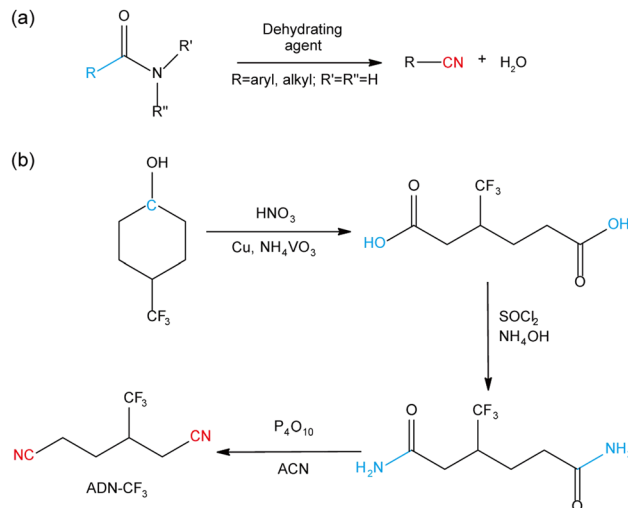


Fig. 11 (a) General route for nitrile synthesis by dehydration of amides. (b) Synthesis route of 3-trifluoromethyladiponitrile (ADN- CF_3). Fig. 11b is redrawn based on ref. 154.

4. Properties and application of fluorinated solvents

4.1 Fluorinated esters

4.1.1 Fluorinated cyclic carbonates. EC has enabled the great success of lithium-ion batteries over the past 30 years as the core and indispensable component for stabilizing the graphite anode. However, its high melting point (T_m), flammability, and relatively low oxidation stability restrict the applications of EC-based electrolytes in many scenarios. Thus, to resolve these issues, various EC derivatives have been developed (Fig. 12). FEC (1-2), one of the most successful EC derivatives, was first reported as a solvent for Li-TiS₂ batteries by Yoshinori *et al.* in 1987.⁶ Benefiting from the low polarizability and high enthalpy of ionization of fluorine, FEC exhibits a lower T_m , less flammability, and higher anodic stability than EC.¹²³ Lower energy levels induce higher oxidation and reduction potentials.¹⁰³ Based on previous research, the specific reduction mechanism of FEC results in the formation of a better (denser) SEI on the anode surface (graphite, silicon, and lithium metal).⁶ This leads to its wide use in improving the interfacial stability of both cathodes and anodes.¹⁸⁹

The physicochemical properties of fluorinated EC derivatives are altered dramatically with a change in fluorine content and position. As reported by Sanchez and co-workers, the melting point, boiling point, and dielectric content of EC derivatives decrease sequentially in the order of EC (1-1) > FEC (1-2) > F₂EC (1-3) > F₃EC (1-5) (Fig. 13a and b).¹⁹⁰ The abnormal melting and boiling points of 2FEC (1-4) imply the importance of the fluorine position. Based on a previous report, the high dielectric constant of EC was ascribed to the intermolecular interactions *via* hydrogen bonds.¹⁹¹ The introduction of fluorine decreases these interactions, and thus reduces their dielectric constant. Besides, the viscosity of fluorinated EC derivatives showed a monotonous decreasing trend with an

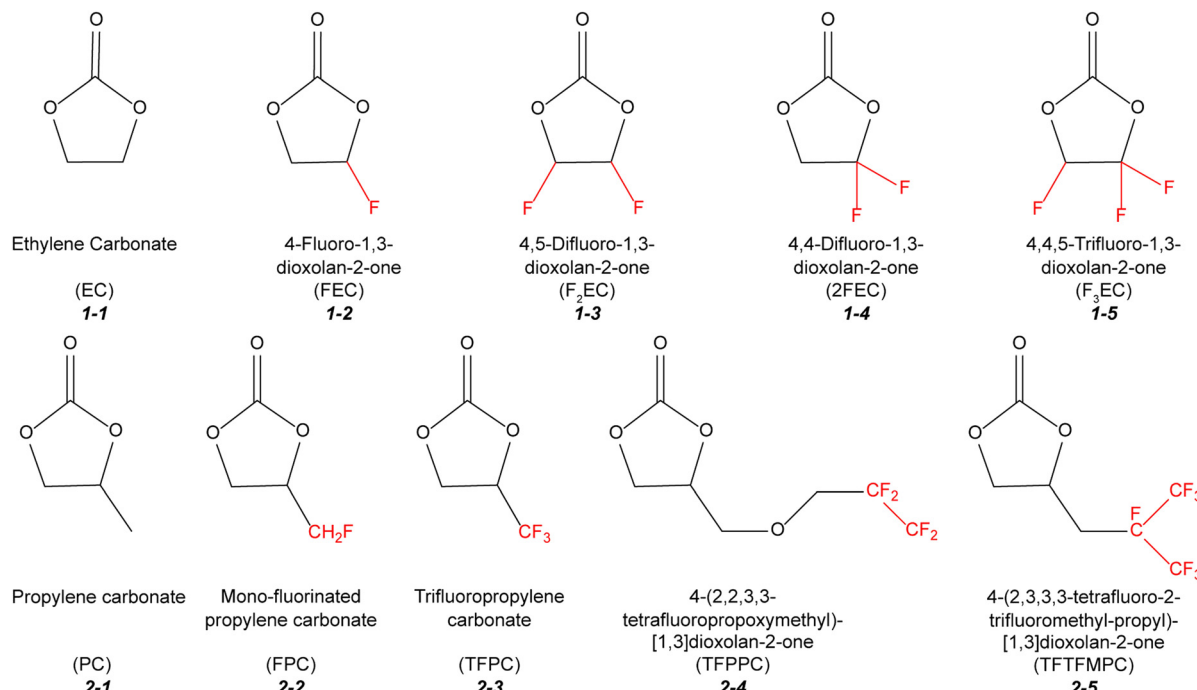


Fig. 12 Molecular structure of cyclic carbonates and their corresponding fluorinated analogs.

increase in fluorine content, which is caused by the lower intermolecular interaction after fluorination. In terms of safety, *i.e.*, thermal properties and flammability, it is expected that fluorinated EC derivatives will exhibit good flame retardance due to the strong capacity of $F\cdot$ radicals to scavenge $H\cdot$

radicals.¹²³ For example, the PC (2-1)/FEC (1-2) electrolyte exhibited a good “self-quench” effect during the flammability test.¹⁹² However, the flash points of EC and its fluorinated analogs decrease monotonically in the order of EC (1-1) > FEC (1-2) > F_2 EC (1-3) (Fig. 13c). The flash point of F_3 EC (1-5) could

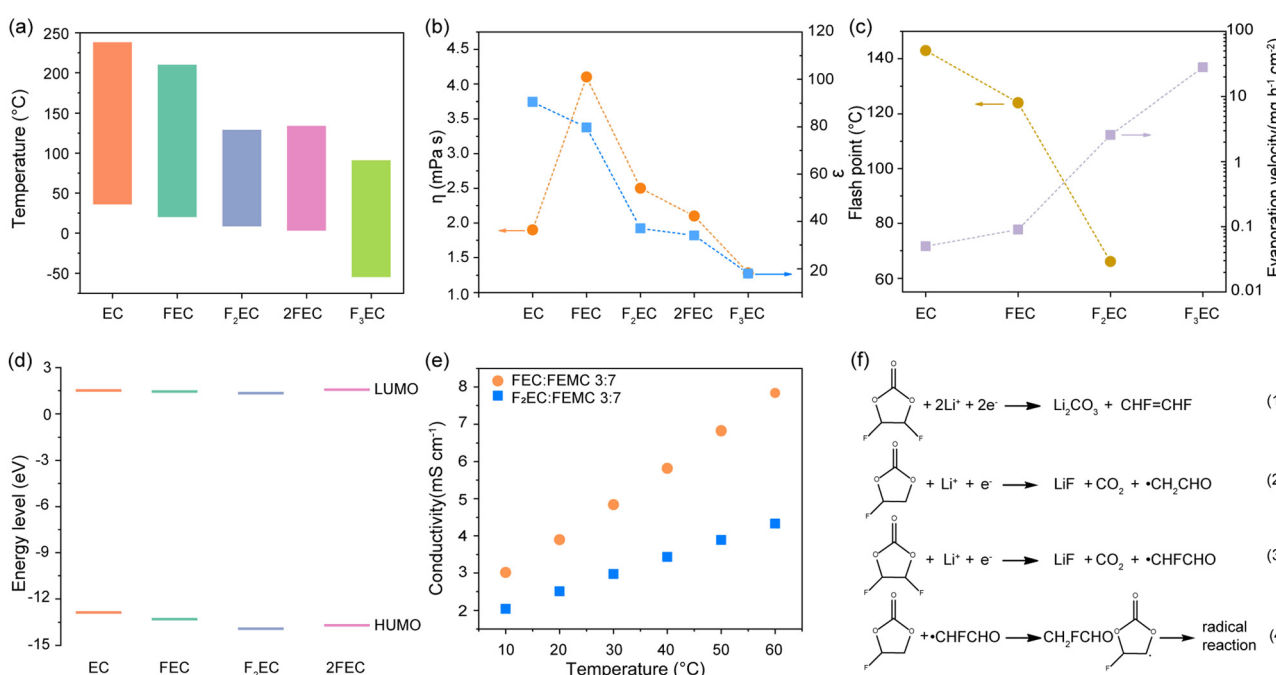


Fig. 13 Properties of EC and its fluorinated derivatives. (a) Melting point and boiling point. (b) Viscosity and dielectric constant at 20 °C. (c) Flash point and evaporation velocity. (d) Calculated HOMO and LUMO energy. (e) Ionic conductivity of FEC (1.0 M LiPF₆) and F_2 EC-based electrolytes at different temperatures. (f) Possible reaction of FEC and F_2 EC on Li anode. Fig. 13a is compiled based on ref. 47. Fig. 13b and c are compiled based on ref. 190. Fig. 13d is compiled based on ref. 193. Fig. 13e is compiled based on ref. 194. Fig. 13f is compiled based on ref. 33.

not be measured given that it is beyond the instrument's detection range. A similar trend was also observed in the evaporation rate of the solvents. In particular, the evaporation rate of F₃EC (1-5) was as high as 28 mg h⁻¹ cm⁻², which is about 500 times higher than that of EC.¹⁹⁰

Besides the monotonous change in physicochemical properties, the energy levels of fluorinated EC derivatives decreased with the increase in fluorine content (Fig. 13d).¹⁹³ Although the anodic stability does not correlate with the HOMO levels of all the solvent molecules, F₂EC (1-3) indeed has higher oxidation potential than FEC and EC. He *et al.* systematically evaluated the anodic stability, conductivity, and electrochemical performance of a series of fluorinated EC-derivatives.¹⁹⁴ Employing LiPF₆ as the lithium salt and trifluoroethyl methyl carbonate (FEMC) as the co-solvent, they found that the voltage stability followed the order of 1 M LiPF₆ F₂EC/FEMC > 1 M LiPF₆ FEC/FEMC > 1 M LiPF₆ EC/FEMC. Besides, they demonstrated that F₂EC-based electrolytes delivered lower ionic conductivity than FEC-based electrolytes at different temperatures (Fig. 13e). However, the full cell (LiNi_{0.5}Mn_{1.5}O₄||graphite) employing F₂EC/FEMC electrolyte displayed improved cycling performance at ambient and high temperatures (55 °C). The subsequent analyses revealed that robust interfacial layers were formed on both the NMC523 cathode and graphite anode in the F₂EC-based electrolyte. Thus, suppressed electrolyte decomposition and transition metal dissolution were achieved. Similar benefits were also found in a lithium metal anode. Zhang *et al.* reported that with the aid of lithium nitrate (LiNO₃), FEC-based electrolytes enabled the formation of an SEI with an abundance of LiF and LiN_xO_y, rendering dendrite-free lithium deposition and ultrahigh CE of 99.96%.¹⁹⁵ Using F₂EC as a co-solvent for FEC electrolyte, the excellent cycling performance of NCM811||Li cells with high cathode loading of 3.4 mA h cm⁻² and low electrolyte usage of 0.7–1.2 μL mg⁻¹_{NCM811} at 30 °C to 55 °C was demonstrated by Aurbach *et al.*³³ The synergistic decomposition of F₂EC and FEC results in more effective passivation on the surface of Li metal anodes. Fig. 13f demonstrates the possible decomposition mechanism and corresponding SEI using dual fluorinated solvents. The SEI layer consisted of flexible polymeric matrices with embedded LiF and ROCO₂Li species. Besides, the favorable effects of F₂EC on SEI could also be extended to the SiO/C anode, as illustrated by Luo *et al.*¹⁹⁶

Alternatively, a higher fluorination degree reduces the solvation power of the solvent and ionic conductivity of the electrolyte. The maximum solubility of LiTFSI in F₂EC and F₃EC (1-5) was only 1.7 and 0.1 M at 30 °C, respectively.¹⁹⁰ Notwithstanding, the Li⁺ transference number and electrochemical aluminum corrosion caused by LiTFSI were improved in the F₂EC electrolyte compared to the FEC-based electrolyte. Furthermore, the reduced melt point and Li⁺-dipole interaction of the fluorinated-EC ensured the potential operation of the batteries over a wide temperature range.¹⁹⁷ Recently, Wang *et al.* illustrated that the de-solvation rate is gradually enhanced with an increase in fluorine content (from EC to F₂EC) due to the lower Li⁺-dipole interaction.¹⁹⁸ Consequently, the cell with

F₂EC-based electrolytes enabled an improved low-temperature performance. It should be noted that these plausible regularities with the degree of fluorination are not applicable to all systems. For example, 4-(2,2,3,3-tetrafluoropropoxymethyl)-[1,3]-dioxolan-2-one (TFPPC (2-4)), a derivative of PC, showed a lower oxidation potential than PC, although the structure of its molecules contained four fluorine (Fig. 12).^{194,199} This phenomenon can be ascribed to the following facts: (1) the tetrafluoroethyl group in HFEEC is far from the carbonate ring, which minimizes the electron-withdrawing effect and (2) the intrinsic low inoxidizability of the ether linkage –CH₂–O–CH₂–.¹⁹⁴

In addition to EC derivatives, the incorporation of fluorine in PC also has unique effects on its physicochemical and electrochemical behavior. For example, mono-fluorinated PC (FPC, 2-2) demonstrates about three times higher dielectric constant than PC (Fig. 14a).⁵³ In contrast, the trifluoropropylene carbonate (TFPC, 2-3) only shows a slightly higher dielectric constant than PC (67 for TFPC and 64.4 for PC). The viscosity of fluorinated PC exhibits the same trend as the dielectric constant.²⁰⁰ The energy level of fluorinated PC derivatives downshifts from PC to FPC to TFPC, implying the higher anodic stability of molecules with a higher fluorine content (Fig. 14b).²⁰¹ In contrast, TFPPC (2-4) and TFTFMPC (2-5) showed a relatively higher HOMO than TFPC (2-3). The longer distance of fluorine from the carbonate ring is the reason behind this phenomenon. Similar to the fluorinated EC, the number of fluorine atoms also significantly affects the solvation ability of fluorinated PC. FPC shows relatively poor capability of solvating Li⁺ due to the lower electron-pair donicity of oxygen atoms. When employed as electrolyte solvents for LIBs, the FPC-based electrolytes exhibit decreased ionic conductivity compared to PC-based electrolytes (Fig. 14c).²⁰² The case is reverse in TFPC (2-3), which shows much higher solvation energy than PC (Fig. 14d).²⁰³ Benefiting from the high degree of dissociation of Li salts, TFPC-based electrolytes deliver a higher ionic conductivity than FPC.

Regarding interfacial compatibility, FPC-based electrolytes exhibited higher anodic stability than PC-based electrolytes, and thus capable of endowing C||LCO cells with prolonged cycling performance.²⁰² Besides, the solvent co-intercalation of PC-based solvents in graphite was efficiently eliminated in a TFPC electrolyte system at the expense of compromises in reversible capacity.²⁰⁴ The stable SEI layer decomposed from TFPC on graphite was responsible for the restrained side reactions in this type of electrolyte.²⁰⁵ A similar reduction reaction with the formation of a stable SEI layer was also observed in 4-(2,3,3,3-tetrafluoro-2-trifluoromethyl-propyl)-[1,3]-dioxolan-2-one (TFTFMPC, 2-5).¹⁷⁵ Furthermore, enhanced safety and widened potential windows could be realized when utilizing TFPC as a co-solvent or additive.^{205,206} The addition of TFPC can make the electrolyte non-flammable.²⁰³ Also, it can endow 5 V-class graphite||LNMO full cells with highly reversible capacity and superb rate performance due to the improved anodic stability. However, the conductivities of binary mixed electrolytes decrease with an increase in the TFPC content due to its high viscosity. Surprisingly, TFPC does not support

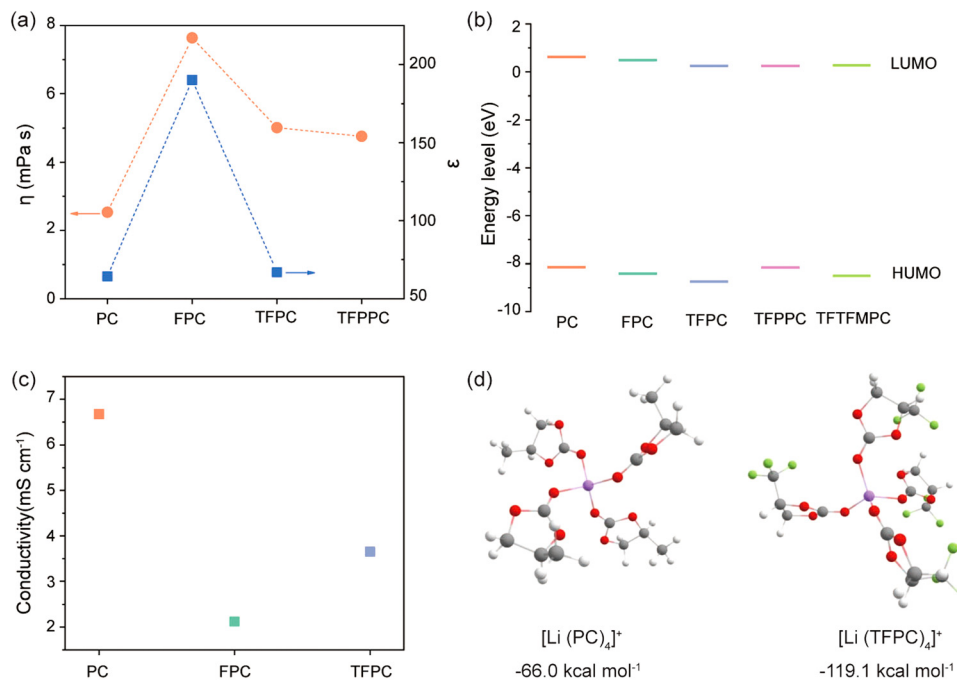


Fig. 14 Properties of PC and its fluorinated derivatives. (a) Viscosity and dielectric constant at 20 °C. (b) Calculated LUMO and HOMO energy (eV). (c) Ionic conductivity of 1 M LiPF₆ in PC, FPC, and TFPC. (d) Optimized structure of $[\text{Li}(\text{PC})_4]^+$ and $[\text{Li}(\text{TFPC})_4]^+$ and their corresponding binding energies. Fig. 14a is compiled based on ref. 53 and 200. Fig. 14b is compiled based on ref. 201. Fig. 14c is compiled based on ref. 202. (d) Reprinted with permission from ref. 203 Copyright 2021, the American Chemical Society.

compatibility with the battery chemistries containing NCM-based cathodes and Li metal anodes, although the voltage of NCM622 is not as high as the LNMO cathode.²⁰⁷ However, the reason behind the contrary results for TFPC in different anode and cathode chemistries is still unclear.

4.1.2 Fluorinated linear carbonates. Compared to cyclic carbonates, linear carbonates have relatively lower viscosity, boiling point, and dielectric content.²⁰⁸ Thus, since the first report by Guyomard *et al.* in 1993, they have been widely adopted as co-solvents to improve the liquidus temperatures and ion conductivity of electrolytes.²⁰⁹ Fig. 15 lists the molecule structure of representative linear carbonates and their fluorinated counterparts. Due to the wide liquidus range (from −75 °C to 126 °C) and low viscosity, diethyl carbonate (DEC, 3-1) has been widely used in commercial electrolytes.²⁰ Partially fluorinated organic molecules can increase the chemical polarity due to the electron-withdrawing effect of fluorine atoms.¹⁶³ Thus, the fluorination of linear carbonates increases their dielectric constants.²¹⁰ For example, the dielectric constant of ethyl (2-fluoroethyl) carbonate (F₁DEC, 3-2) was 6.5, which is larger than that of DEC (2.8).^{190,211} Fig. 16a shows a plot of the dielectric constant of several fluorinated DEC derivatives to comprehensively understand the effect of fluorination on the dielectric constant of DEC.

With an increase in the fluorine content in F₂DEC, the resultant 2,2-difluoroethyl ethyl carbonate (DFDEC, 3-3) and ethyl 2,2,2-trifluoroethyl carbonate (TFDEC, 3-4) showed slightly enhanced dielectric constants of up to 6.6 and 7.1, respectively (Fig. 16a).¹⁹³ When fluorine was introduced in the

α -site, the ethyl (1-fluoroethyl) carbonate (F₁DEC) showed a slightly increased dielectric constant than that of F₂DEC (3-2).¹⁹⁰ The addition of the $-\text{CF}_3$ moiety to the opposite side of F₁DEC (3-5) further elevated the dielectric constant (2,2,2-trifluoroethyl (1-fluoroethyl) carbonate, F₄DEC, 3-6). These results suggest that the electronic polarizability of the solvent is governed by both the position and amount of fluorine.

The viscosity and dielectric constant usually have a consistent trend because they both involve the dipole–dipole interactions of the solvent molecules. Therefore, in all cases, the viscosities of fluorinated DEC were higher than that of DEC (Fig. 16a).²¹⁰ Nevertheless, these associations are not monotonous, given that steric hindrance also affects the viscosity. In particular, the viscosity of TFDEC (3-4) is lower than that of the other fluorinated DEC derivatives. The flash point and boiling point of fluorinated DEC derivatives increased with an increase in the fluorine content (non-linear relationship) (Fig. 16b).¹⁹⁰ Considering the high electron-withdrawing of fluorine, the oxidation stabilities of fluorinated DEC derivatives were elevated as expected (Fig. 16c).^{153,190,210}

Similar to fluorinated cyclic carbonates, all fluorinated DEC derivatives inhibit the degree of ionic dissociation due to the lower electron-pair donicity of oxygen atoms and exhibit suppressed aluminum dissolution due to the formation of a passive layer composed of AlF₃ and AlO_xF_y. This passivation layer can be ascribed to the contact ion pair and ion aggregate in the solvation structures, which contributed to the anion-enriched cathode interphase with the formation of highly stable LiF (Fig. 16d).²¹² The bulk ion transport of

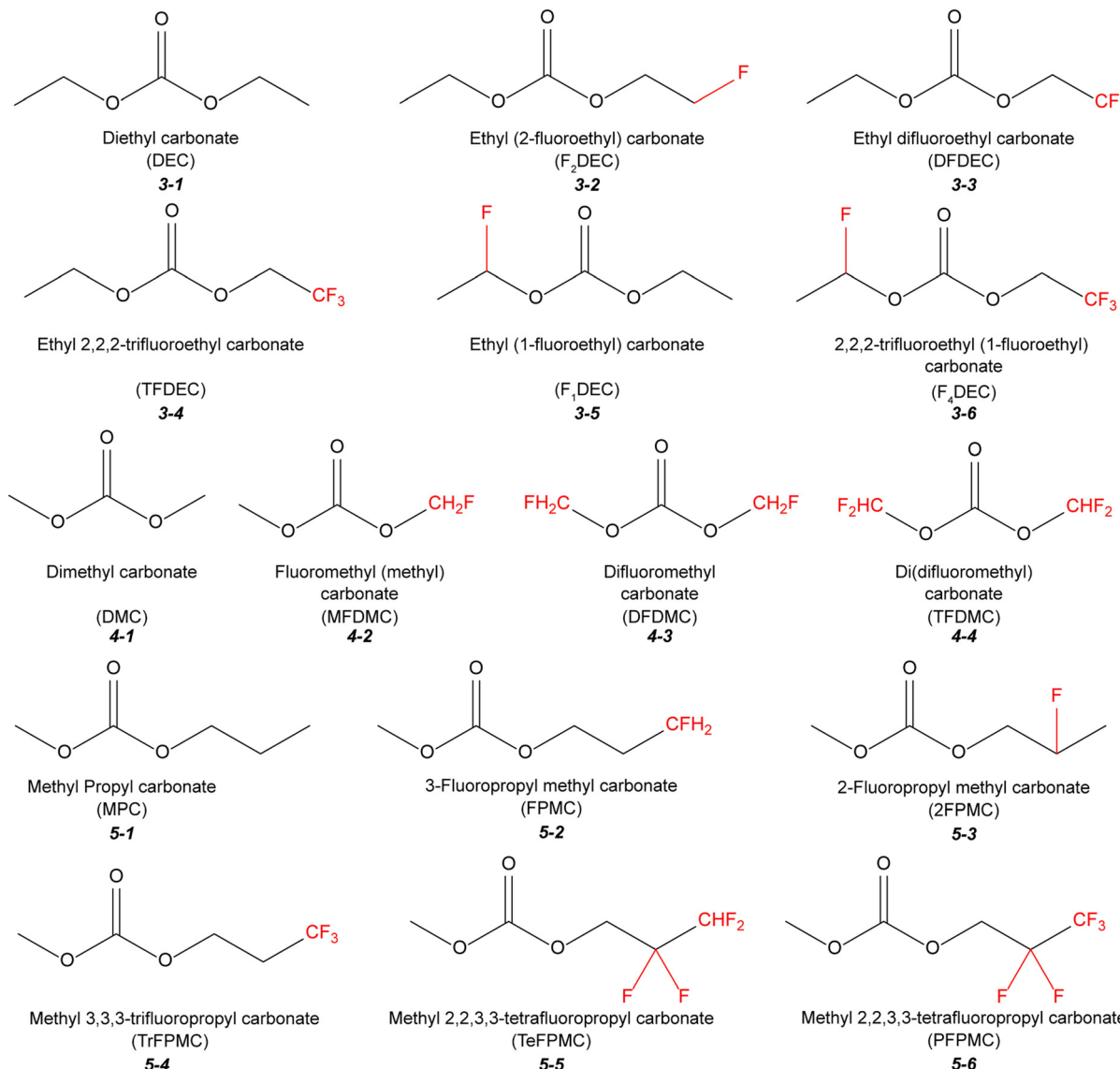


Fig. 15 Molecular structures for representative linear carbonates and their fluorinated derivatives.

F_2DEC (3-2)-based electrolytes was comparable with DEC at ambient temperature.^{190,210} However, when the temperature was below 25 °C, the conductivities of F_2DEC were lower than that of DEC. Meanwhile, the case was reversed when the temperature was elevated, indicating the high active energy of F_2DEC -based electrolytes.²¹¹ Interestingly, the F_1DEC (3-5)-based electrolytes showed a similar ionic conductivity trend, highlighting the importance of viscosity and activity energy in ion transport in bulk electrolytes.

When utilized as a co-solvent in electrolytes, the fluorinated DEC-based electrolyte enables improved interface compatibility, *i.e.*, better cycling stability in Li||LCO half cells.²¹¹ More importantly, fluorinated linear carbonates also function well in elevating the electrochemical performance of LIBs at low-temperatures. Smart *et al.* investigated the low-temperature performance of several multi-component ternary and quaternary carbonate-based electrolyte formulations by incorporating

fluorinated carbonates.¹⁵⁵ Among the fluorinated carbonates, the TFDEC-based electrolytes enabled mesocarbon microbead (MCMB) to show best discharge capacities at -20 °C.

Similar to the fluorinated DEC (3-1), the partially fluorinated dimethyl carbonate (DMC) derivatives also exhibited an increased dielectric constant and viscosity, downshifted HOMO and LUMO energies, higher antioxidant stabilities, and lower ionic conductivities and solvating power than their DMC counterparts (Table 4).^{163,179,210,213,214} Similar results were also be observed in methyl propyl carbonate (MPC, 5-1) and its fluorinated MPC derivatives, as demonstrated by Sasaki *et al.*¹⁷⁹ In particular, TrFPMC (5-4) exhibited higher oxidative decomposition potentials than TeFPMC (5-5), suggesting that the position of fluorine outweighs the quantity of fluorine in determining the anodic stability of these solvents.²¹⁰

4.1.3 Fluorinated cyclic carboxylates. Carboxylate esters were widely applied as co-solvents in electrolytes due to their

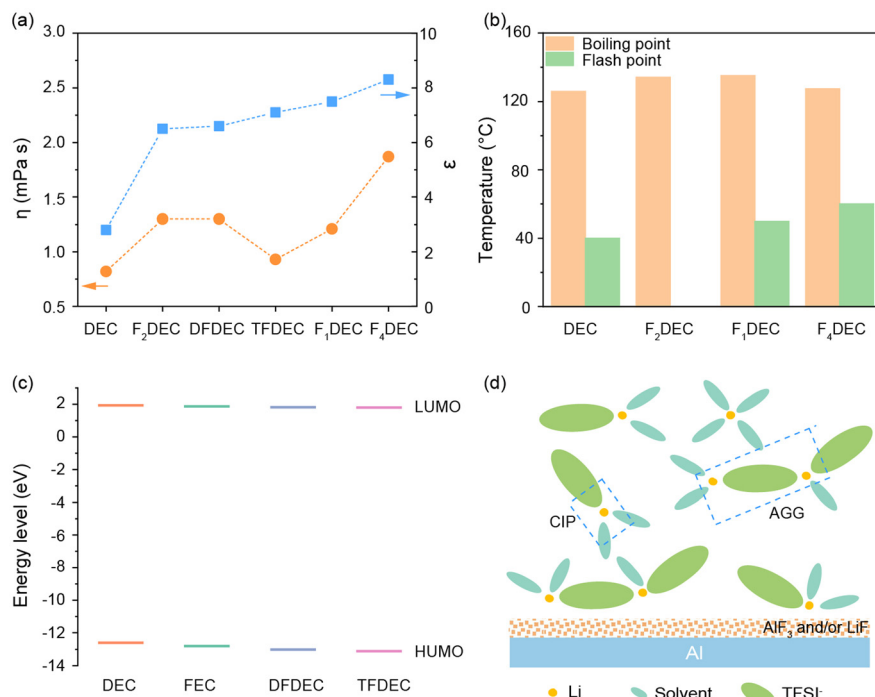


Fig. 16 Properties of DEC and its fluorinated derivatives. (a) Viscosity and dielectric constant at 20 °C. (b) Boiling point and flash points. (c) Calculated LUMO and HOMO energies. (d) Schematic depiction of the passivation mechanism of LiTFSI in fluorinated DEC-based electrolytes on the surface of Al. Fig. 16a and b are compiled based on ref. 193. Fig. 16c is compiled based on ref. 153, 190, and 210.

Table 4 Relevant physicochemical and electrolyte properties of DMC, MPC and their fluorinated derivatives

Name	ϵ	η (cP)	HOMO/LUMO	Oxidation voltage ^a (V)	Conductivity (mS cm ⁻¹)	DN
DMC (4-1)	3.12	0.63	-8.24/-0.07	5.55	5.99	—
MFDMC (4-2)	8.96	0.91	-8.71/-0.01	6.07	4.21	—
DFDMC (4-3)	13.5	1.36	-9.14/-0.39	6.18	2.39	—
TFDMC (4-4)	10.6	0.99	-9.18/-0.58	—	—	—
MPC (5-1)	2.87	0.89	—	5.31 ^b	2.32	12
FPMC (5-2)	7.18	1.86	—	5.48	2.24	11
2FPMC (5-3)	7.43	1.86	—	5.46 ^b	1.61	—
TrFPMC (5-4)	7.65	1.87	—	5.81	1.19	9
TeFPMC (5-5)	8.88	3.00	—	5.48	0.50	4
PFPMC (5-6)	6.31	1.42	—	5.81	0.53	6

Note: the values of ϵ , η , and conductivity are collected at 25 °C. The data of HOMO/LUMO of solvent is obtained from Ref. 214 with the same calculation method. ^a The value of oxidation voltage is decided at the onset of anodic density increase significantly. ^b Electrolyte: 1 M LiPF₆ in the corresponding solvents.

low melting point and viscosity. The ionic conductivities and service temperature range of electrolytes containing carboxylate esters (even with low usage) were significantly enhanced.⁴⁷ Smart *et al.* reported that the prototype cell with 1 M LiPF₆ EC/EMC/MP (2:6:2 in volume) as the electrolyte not only showed six-times higher capacity than the cells with the control electrolyte but also was capable of supporting operation at moderate rates under an extremely low temperature of -60 °C.²¹⁵ However, their average stability against oxidation and inability to form a protective SEI indicate that

carboxylate esters cannot be utilized as single solvents for electrolytes.²¹⁶

Similar to fluorinated carbonates, researchers introduced fluorine in carboxylate esters to address these issues. Taking γ GBL (6-1), which has good solubility for LiBOB, as an example, the introduction of fluorine significantly elevated the melting point of α -FGBL (6-2) and β -F- γ -BL (6-3), suggesting that the high electron-withdrawing ability of F increases the intermolecular interaction of the aromatic ring of GBL (Table 5).^{163,164} Meanwhile, the permittivity, density, and viscosity of fluorinated GBL became much higher than that of γ GBL. The FGBL_{mix}-based electrolytes (α -FGBL: γ -F- γ -BL = 3:7 in moles) exhibited lower ionic conductivity in different lithium salts. Although the fluorination lowers the bulk ion transport, the interfacial compatibility with lithium metal anode is improved. Compared to the deterioration of Li plating/stripping in the γ GBL-based electrolyte, the FGBL_{mix}-based electrolyte, regardless of the lithium salt, showed excellent cycling stability and higher CE for more than 100 cycles.¹⁰⁵ The improved lithium metal compatibility could be extended to binary EC-FGBL_{mix} electrolytes. However, the resistance of the SEI using the FGBL_{mix}-based electrolyte was still high, resulting in the poor cycle performance of the Li||LCO cells.

4.1.4 Fluorinated linear carboxylates. Fig. 17 depicts the representative linear carboxylates and their fluorinated derivatives. The carbon-chain length (molecular weight) and the position isomerism of fluorine significantly affect the physical and electrochemical properties of fluorinated linear carboxylate

Table 5 Molecule and electrolyte properties of γ GBL and α -FGBL

Name	Structure	ϵ	η (cP)	Density (g mL ⁻¹)	Ionic conductivity (mS cm ⁻¹ , 30 °C)			Decomposition voltage ^a (V vs. Li ⁺ /Li)	
					LiClO ₄	LiBF ₄	LiPF ₆	Reduction	Oxidation
γ GBL (6-1)		39.1	1.75	1.125	11.7	8.36	13.1	0.66	6.1
α -FGBL (6-2)		72.6	3.35	1.303	5.14	3.98	5.98	2.12	6.4
γ -F- γ -BL (6-3)		80.3	3.9	1.3					5.9

^a Electrolyte: 1 M LiPF₆ in corresponding solvents. ϵ , η , and density of different solvents are determined at 25 °C.

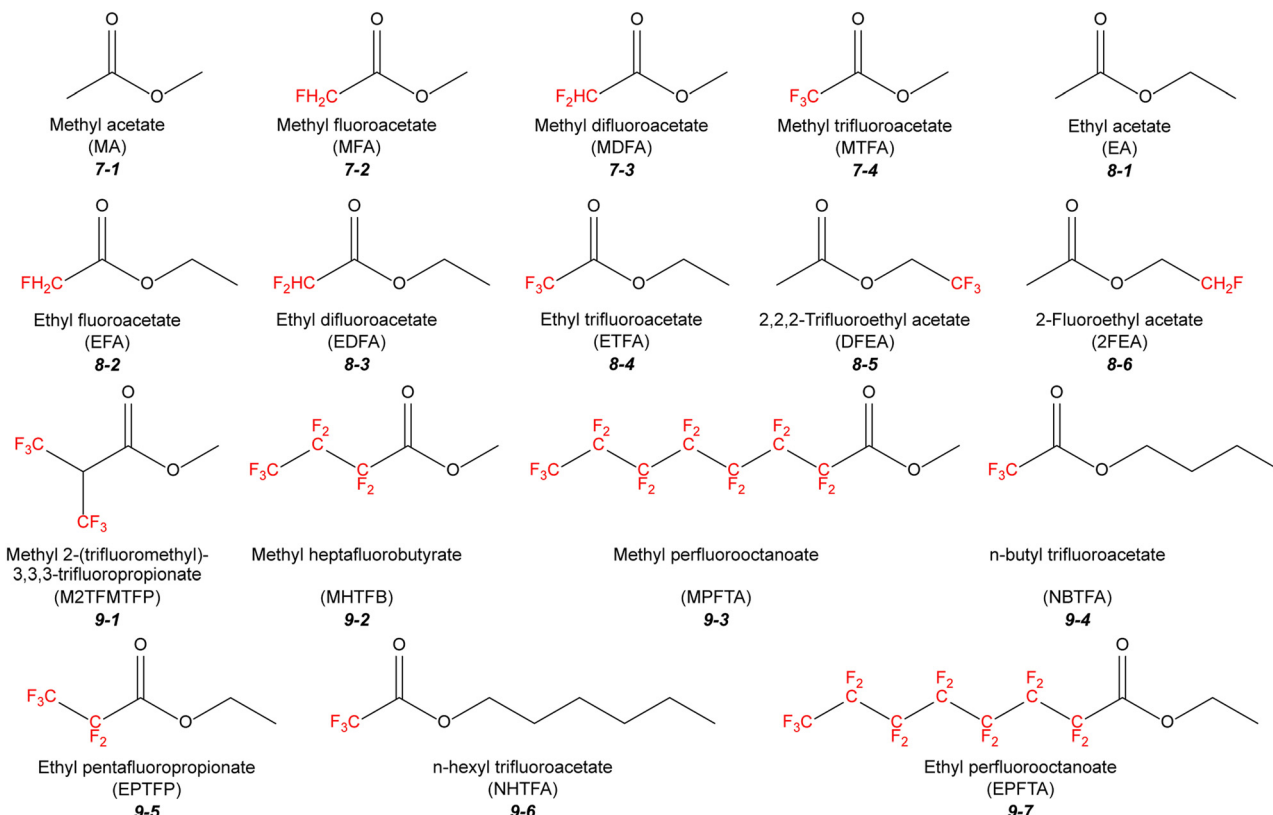


Fig. 17 Chemical structures of linear carboxylates and their fluorinated derivatives.

esters. Lu *et al.* systematically studied four trifluoroacetates (MTFA (7-4), ETFA (8-4), NBTFA (9-4), and NHTFA (9-6)) as a co-solvent for low-temperature LIBs.²¹⁷ The basic properties of these solvents are listed in Table 6.^{47,193,217} According to this table, the following can be concluded: (1) the ability to dissociate LiPF₆ salt decreases with an increase in the carbon-

chain length of trifluoroacetates; (2) the length of the carbon-chain in trifluoroacetates has no contribution to the viscosity and ionic conductivity of the electrolyte at low temperature; and (3) the trifluoroacetates with long carbon-chains deteriorate the electrochemical performance of graphite in terms of polarization potential and de-intercalation capacity (Fig. 18a and b).

Table 6 Physical properties of (fluorinated) linear carboxylates

Name	mp/bp (°C)	Density (g mL ⁻¹)	ϵ	η (cP, 25 °C)	HOMO	LUMO
MA (7-1)	-98/57	0.93	6.7	0.36	-12.21	1.85
MFA (7-2)	-35/104	1.17	18	1.2	-12.58	1.71
MDFA (7-3)	/86	1.26	—	—	-12.90	1.67
MTFA (7-4)	-78/43	—	—	—	-12.2 ^a	-0.0147 ^a
EA (8-1)	-84/77	0.89	6.0	0.43	-12.09	1.87
EFA (8-2)	/121.6 (758 torr)	1.09	15	0.89	-12.47	1.75
EDFA (8-3)	/100	1.24	—	—	-12.78	1.73
ETFA (8-4)	-78/62	—	—	—	-11.98 ^a	-0.082 ^a
2FEA (8-6)	/119.3 (763 torr)	1.09	7.8	0.97	-12.46	1.75
M2TFMTPP (9-1)	/89	1.45	—	—	—	—
MHTFB (9-2)	-86/80	1.47	—	—	—	—
MPFTA (9-3)	/158	1.63	—	—	—	—
NBTFAs (9-4)	<75/104	—	—	—	-11.78 ^a	-0.079 ^a
NHTFA (9-6)	<75/143	—	—	—	-11.39 ^a	-0.078 ^a
EPFTA (9-7)	/74 (18 torr)	1.62	—	—	—	—

^a The values are deduced from corresponding ref. 217 (RHF/6-311+G(2d,p)), while the rest are obtained from ref. 193 (HYPERCHEM 7).

Consequently, a criterion for the selection of trifluoroacetate-based electrolytes for low-temperature operation is proposed, where the length of the carbon-chain in the alcohol group of trifluoroacetate should be as short as possible, which was also reported by Nakajima *et al.* It was found that the fluoroester with low molecular weight could produce higher charge

capacities at 0 °C and -4 °C than that of the control electrolytes and other fluoroester-mixed electrolytes.²¹⁸

Nambu *et al.* selected two monofluorinated carboxylates, 2-fluoroethyl acetate (2FEA, 8-6) and ethyl fluoroacetate (EFA, 8-2), as representatives to understand the effect of position isomerism.²¹⁹ The α -fluorinated ethyl acetate (EFA) resulted in a higher dielectric constant but lower viscosity than that of the γ -fluorinated one (2FEA, 8-6). The CE of the Li||LCO cells using the fluorinated carboxylate-based electrolytes with EC as a co-solvent decreased in the order of EC-2FEA > EC-EA > EC-EFA. Considering that the electrochemically reduced potential of the fluoroesters was more positive than that of EC, the poor cycling efficiency of these cells could be ascribed to the poor SEI formed with fluorinated carboxylates.²¹⁸ In this case, the additives, such as VC and LiBOB, could improve the interface compatibility of fluorinated carboxylates.²²⁰ However, specific performance compromises were usually induced, such as lower ionic conductivity or sluggish rate response.⁴⁷ Xia *et al.* deliberately circumvented the instability of fluorinated carboxylates with graphite and lithium by employing LTO as the anode.²²¹ The formulated electrolyte containing 0.6 M LiTFSI in ethyl trifluoroacetate (ETFA, 8-4) exhibited a wide electrochemical window and remained liquid at an extremely low temperature of -120 °C. The weak affinity between Li⁺ and ETFA contributed to fast de-solvation process at low temperature. The LMO||LTO full cells could deliver high capacity retention (91%) at -40 °C (Fig. 18c and d) but compromised energy density due to the high potentials of the LTO anode.

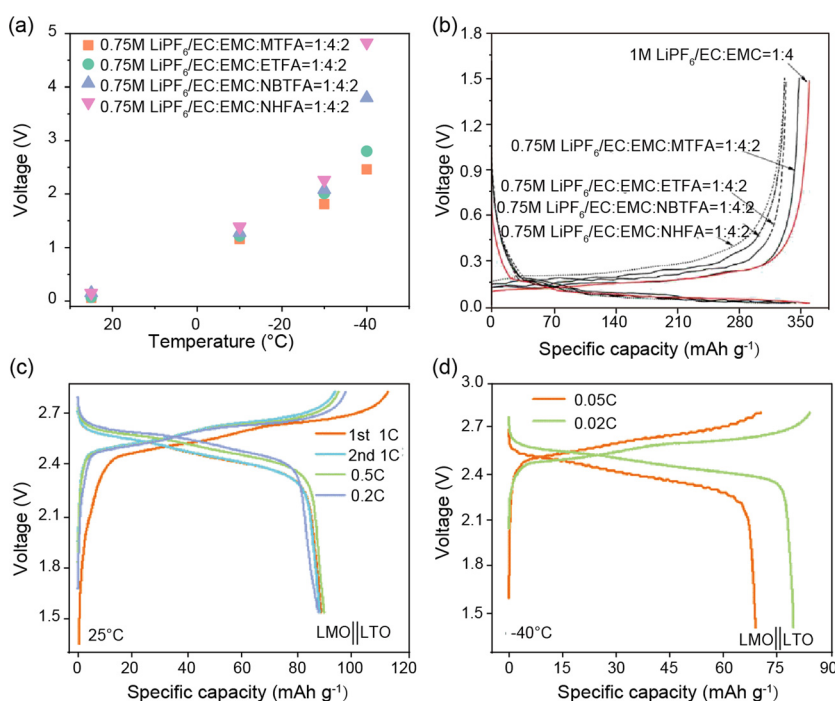


Fig. 18 Electrochemical performance with different fluorinated carboxylate-based electrolytes. (a) Polarization potential of Li||graphite cells at different temperatures. (b) Charge–discharge curve of Li||graphite cells in different electrolytes in the 5th cycle. Discharge/charge profiles of LMO||LTO cells in ETFA electrolytes at 25 °C (c) and -40 °C (d). Fig. 18a is compiled based on ref. 217. (b) Reprinted with permission from ref. 217 Copyright 2013 Elsevier. (c and d) Reprinted with permission from ref. 221 Copyright 2020, The Royal Society of Chemistry.

4.2 Fluoro-ethers

Cyclic or linear ethers deliver moderate dielectric constants and low viscosities. They exhibit good lithium metal anode compatibility and have been utilized as alternative candidates in formulating electrolytes since the 1980s. However, three intractable issues, including high vapor pressure, low voltage window, and co-intercalation into graphite, should be carefully managed before their application in Li-based batteries. Fluorination also triggered widespread research in ether chemistry due to the higher antioxidation and improved interface compatibility of fluorinated solvents.

4.2.1 Fluorinated linear ethers. Similar to fluorinated esters, many factors, including the fluorine content, type of fluorinated groups, building block connectivity, and solvation structure, have essential effects on the properties of fluorinated ethers. Fig. 19 and Table 7 list the chemical structures and basic parameters of linear ethers and their fluorinated analogs, respectively. It is clearly indicated that the dielectric constants of partially fluorinated ethers were almost independent of the fluorine content. For example, the **fluorinated 1-ethoxy-2-methoxyethane (EME, 10-1)** and **1,2-diethoxyethane (DEE, 11-1)** derivatives showed an identical dielectric constant, although it was larger than their non-fluorinated counterparts.¹⁰¹

However, the incorporation of fluorine increased the viscosities of the fluorinated solvents in the order of difluorinated ethers > monofluorinated ethers > trifluorinated ethers > nonfluorinated counterparts. The DN values and oxidative decomposition voltages (except DFEME, 10-3) of the blended EC-Fluorinated ethers were related to the fluorine content, *i.e.*, a higher fluorine content led to lower DN values and higher anodic stability. Regarding the influence of different fluorinated groups, Yue *et al.* pointed out that the solvent with the $-CF_3$ group exhibited much lower viscosity than that with the $-CF_2CF_2H$ group.¹⁰²

Besides, the fluorine content and fluorinated groups also dictated the ionic transport in the electrolyte. On the one hand, for the solvents with the same carbon skeleton, the ionic conductivities of fluorinated ether-based electrolytes decrease with an increase in fluorine content. Thus, by iteratively tuning the number of fluorine atoms, Bao *et al.* demonstrated that the ion transport in fluorinated DEE (ionic conductivity and interfacial transport) changed significantly.⁹⁰ An apparent decreasing trend in the ionic conductivity of the DEE-based electrolytes was observed, following the order of DEE (11-1) \gg F4DEE (11-6) \cong F3DEE (11-4) $>$ F5DEE (11-7) \gg F6DEE (11-8). The interfacial conduction of these electrolytes, extracted from

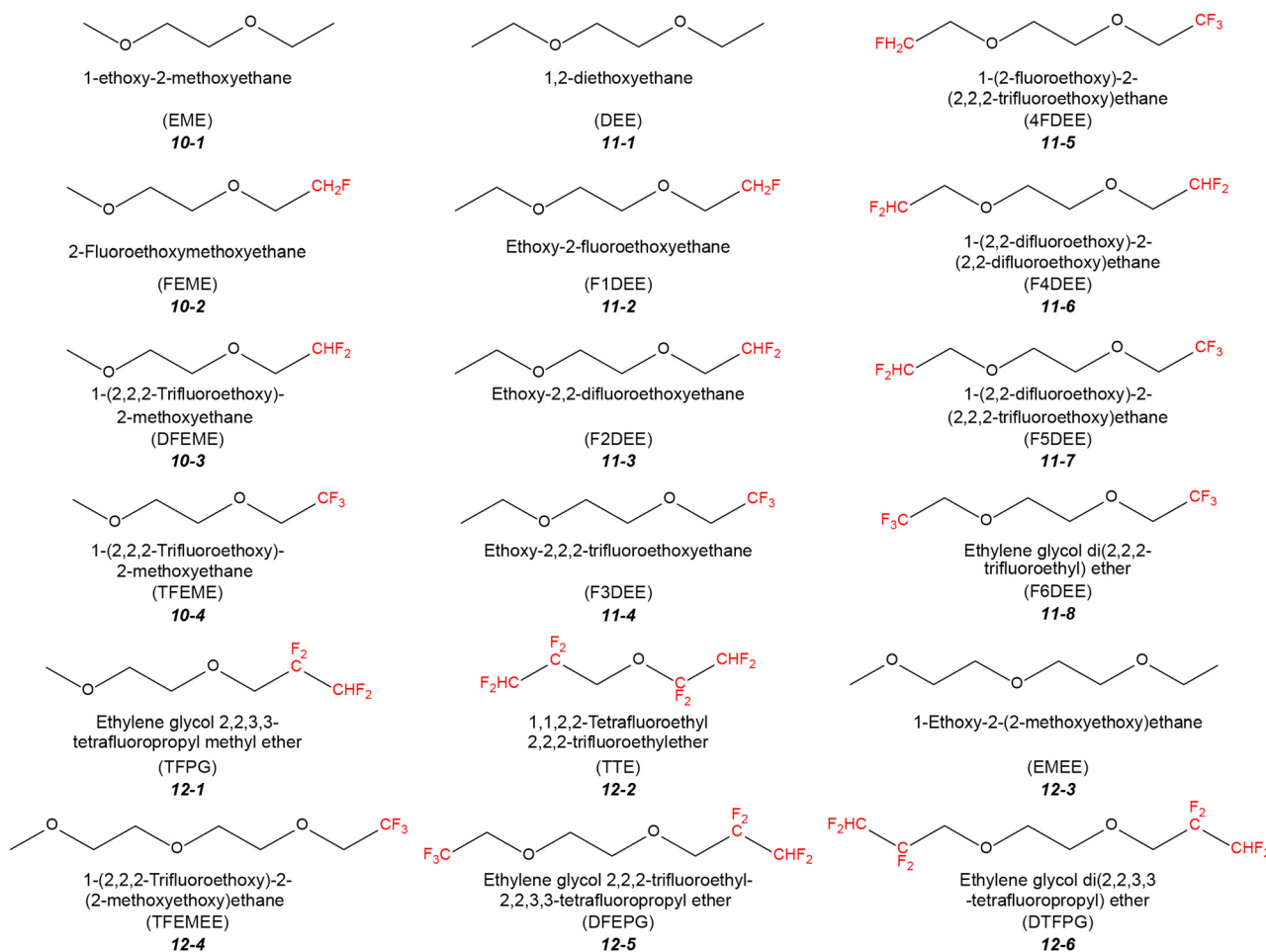


Fig. 19 Chemical structures of representative linear ethers and their fluorinated derivatives.

Table 7 Basic parameters of linear ether and their fluorinated analogs

Name	Density (g mL ⁻¹)	η (cP, 25 °C) solvent/ electrolyte	DN	BP/FP	E_{ox} (V)	Ionic conductivities (mS cm ⁻¹ , 25 °C)
EME 10-	0.85	5.7	0.52/	19.0	—	4.21 ^b 8.03
1	1.01	17	1.0/	17.1	—	4.63 ^b 9.79
FEME 10-2	1.10	17	1.1/	15.0	—	3.99 ^b 4.18
DFEME 10-3	1.15	17	0.79/	14.4	—	4.85 ^b 2.55
TFEME 10-4	1.15	17	0.6/1.46 ^a	13.2 122/ <25	—	4.28 ^a 11.0 ^a
DEE 11-1	0.84	5.0	0.6/1.46 ^a	13.2 122/ <25	—	4.28 ^a 11.0 ^a
F1DEE 11-2	0.97	14	1.1/	12.3	—	4.55 7.16
F2DEE 11-3	1.05	14	1.1/	9.9	—	4.67 2.17
F3DEE 11-4	1.07	14	0.85/2.21 ^a	9.6 161/ 31	—	4.81 6.18 ^a
4FDEE 11-5	—	24	1.66/	—	—	3.34
F4DEE 11-6	1.24	—	/6.97 ^a	—	180/ >6 ^a	4.76 ^a
F5DEE 11-7	1.29	—	/3.39 ^a	—	186/ >6 ^a	5.01 ^a
F6DEE 11-8	1.40	—	/3.61 ^a	—	161/ >6 ^a	4.48 ^a

^a In the η , E_{ox} , and ionic conductivities represents 1.2 M LiFSI in the corresponding solvent, whereas the rest is 1 M LiPF₆ in the corresponding solvent. ^b In the E_{ox} is obtained using platinum as the working electrode at a scan rate of 5 mV s⁻¹, whereas the rest is obtained from Li||Al half cells.

the overpotential of Li||Li symmetric cells, exhibited the same trend, *i.e.*, higher ionic conductivity contributed to faster ion motion (Fig. 20a). On the other hand, a higher -CF₂CF₂H group content in the fluorinated ethers resulted in lower ionic conductivity.¹⁰² The ionic conductivity of 1 M LiTFSI-DMC/F6DEE (**11-8**) (1:1 in volume) was 2.12 mS cm⁻², which is lower than that of 1 M LiTFSI-DMC/TFPG (**12-1**) (1:1 in volume).

The fluorinated groups also significantly affect the solvation structure of the electrolyte, which consequently can alter its ion transport and electrochemical features. In contrast to F6DEE (**11-8**), the Li⁺ solvation sheath in -CHF₂-containing electrolytes has more solvent molecules capable of dispelling the electron-dense FSI⁻ anions away from Li⁺, thus improving ionic transport (Fig. 20b).⁹⁰ Coincidentally, when further replacing the high electron-withdrawing -CHF₂ groups with -CH₂F, the resulting **4FDEE (11-5)**-based electrolytes also exhibit increased ionic conductivities than F6DEE (**11-8**).²²² Besides the change in ionic transport, the fluorine content and the types of fluorinated functional groups can also regulate the redox reaction of the soluble intermediates, such as polysulfide. Mandal *et al.* demonstrated that the solvent molecules with -CF₃ groups exhibited lower polysulfide solubility and faster reaction kinetics than that with -CF₂CF₂H groups (Fig. 20c),¹⁰² which can be explained by the low donor ability and permittivity of the all-fluorinated solvents.^{134,223}

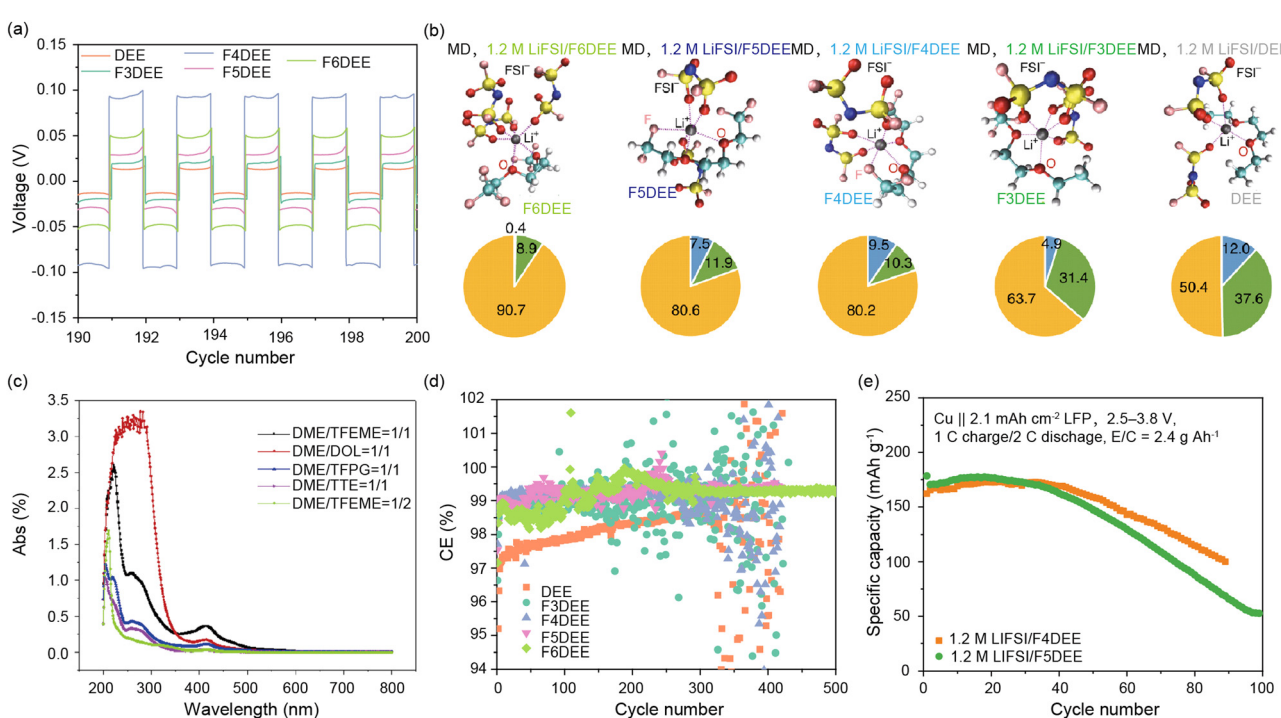


Fig. 20 Electrochemical performance and polysulfide solubility of fluorinated linear ether electrolytes in lithium metal batteries. (a) Long-term cycling of Li||Li symmetric cells with different ether-based electrolytes. (b) Most probable solvation structures of the first Li⁺ solvation sheath from molecular dynamics (MD) simulations and the distribution of different Li⁺ solvates. (c) UV-vis spectra of Li₂S₆-saturated 1 M LiTFSI solutions with different solvent combinations. (d) CE of Li||Cu half cells with different ether-based electrolytes. (e) Cycling stability of Cu||LFP full cells with 1.2 M LiTFSI/F4DEE and 1.2 M LiTFSI/F5DEE as the electrolytes. The data in Fig. 20a, d, and e are from ref. 90. (b) Reprinted with permission from ref. 90 Copyright 2022, Springer Nature. (c) Reprinted with permission from ref. 102. Copyright 2018, Elsevier.

Regarding interfacial compatibility, all these fluorinated ether electrolytes, especially trifluoro-ethers, exhibit higher cycling stability and CE than their non-fluorinated counterparts in Li metal-based cells.⁸⁴ Besides, trifluorinated ethers with shorter carbon-chain lengths delivered a higher CE at the same fluorine content. In the case of fluorinated ether sandwiched with fluorinated groups, the solvents with higher ion transportability exhibited better interfacial compatibility. Benefiting from the improved ion conduction, the F5DEE (11-7) and F4DEE (11-6) electrolytes showed fast activation and high CE of Li metal stripping/plating without sacrificing oxidative stability (Fig. 20d).⁹⁰ More importantly, F5DEE (11-7) and F4DEE (11-6) enabled pouch cells to show excellent cycling performance under realistic testing conditions (Fig. 20e).

Recently, Amanchukwu *et al.* revealed the effects of building block connectivity and ion solvation on physical and electrochemical properties in fluorinated ethers by designing a series of fluoroether compounds with fluorinated end groups (Fig. 21a).⁸³ They reported that these fluoroethers exhibited anomalous oxidative stabilities, which increased when the weight fraction of fluorine decreased (Fig. 21b and c). The type and connectivity of the building blocks also affected the oxidative stability. With a similar fluorine weight fraction of 0.42, the antioxidation potential of E5F2 (13-6) was higher than that of E6F1 (13-7). The ionic conductivity also exhibited similar trends, where the lower the fluorine content, the higher the ionic conductivity until reaching a certain limit of fluorine weight fraction (Fig. 21d). Raman and nuclear magnetic resonance (NMR) spectroscopy disclosed that the free solvent

fraction in the electrolyte was responsible for the unexpected ionic conductivity and oxidative stability (Fig. 21e). It should be emphasized that in all cases, the fluorinated ethers containing a $-CF_2CF_3$ group showed higher oxidative stability but lower ionic conductivity than the fluorinated ethers containing a $-CF_3$ group with the same building blocks. However, these fluorinated ether electrolytes still exhibit poor ionic conductivity and large overpotential, which result in sluggish interfacial transport and poor rate capability for practical applications.

4.2.2 Fluorinated cyclic ethers. Although fluorinated cyclic ether derivatives have been synthesized, their practical application is relatively rare. Fig. 22a lists the molecular structure of fluorinated cyclic ethers that can be applied in electrolytes due to their improved anodic stability. However, the viscosity and thermostability of these solvents should be considered before their application. Recently, a fluorinated cyclic ether, 2-ethoxy-4-(trifluoromethyl)-1,3-dioxolane (cFTOF, 15-2), was synthesized by Zhou *et al.*, who demonstrated that the asymmetric addition of the $-CF_3$ moiety in the cyclic ether can lower the electron density of the oxygen atoms located on the ring component, resulting in decreased solvation ability, thus increasing the content of FSI anions in the solvation structure (Fig. 22b, top two).⁸⁹ Raman spectra proved the rich-anion Li-ion solvation structure, where nearly all the FSI anions were present in the contact-ion pair (CIP) (Fig. 22c and d). Consequently, the 1 M LiFSI/cFTOF electrolytes delivered a high Li-ion transference number (0.78), high voltage window (> 6 V), and good compatibility with the Li anode (LiF-rich SEI layer and dense Li deposition). Notably, a compromise in ionic

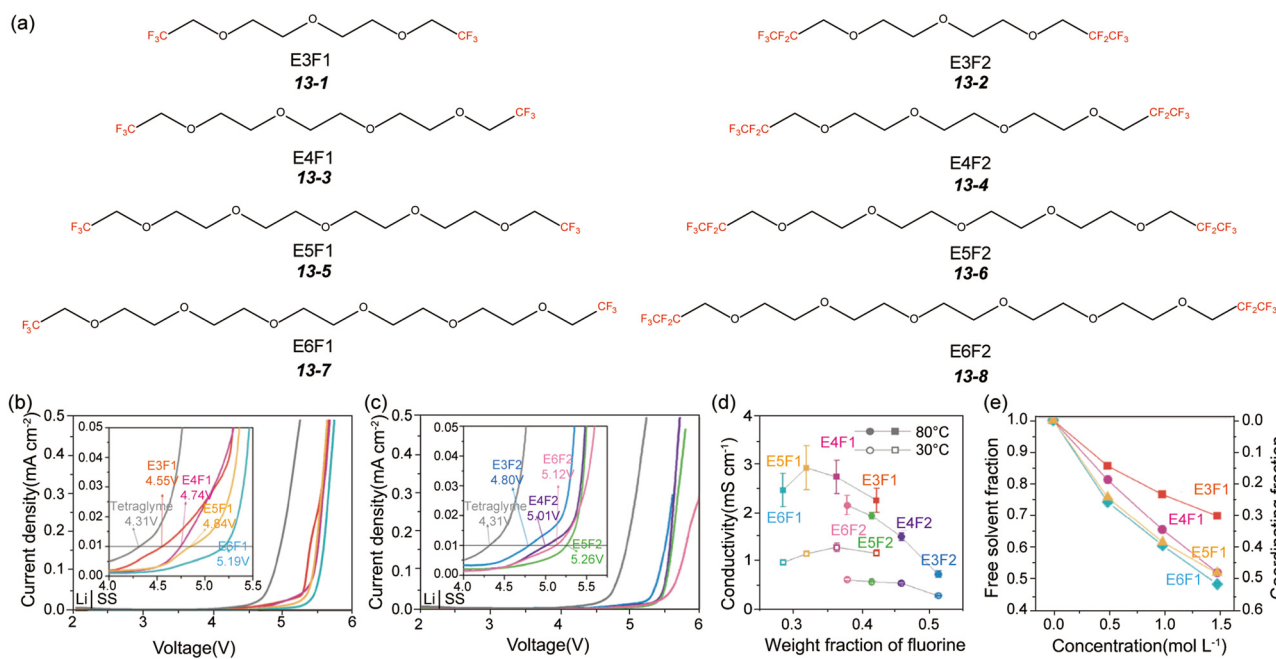


Fig. 21 Electrochemical performance of fluorinated ethers with building blocks of various lengths. (a) Molecular structures of fluorinated ethers with different fluorinated end groups and the number of ethylene oxide units. (b and c) Oxidation potential of various fluorinated ethers. (d) Ionic conductivity of fluorinated ethers ($30\text{ }^\circ\text{C}$ and $80\text{ }^\circ\text{C}$) as a function of fluorine weight fraction. (e) Relationship between free solvent fraction and the LiFSI concentration in F1-type solvents. (b–e) Reprinted with permission from ref. 83. Copyright 2021, the American Chemical Society.

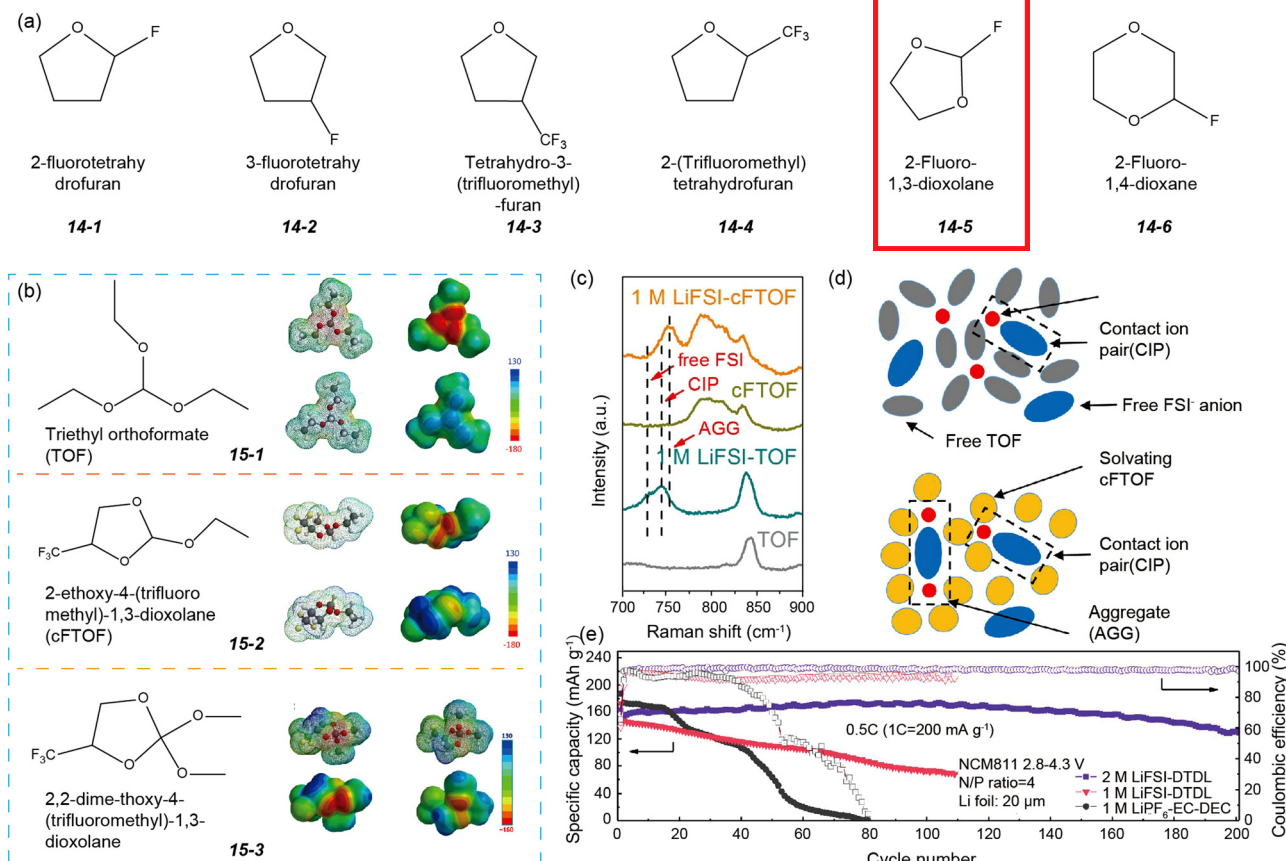


Fig. 22 Molecular electrostatic potential, solvation structures, and electrochemical performance of fluorinated cyclic ethers. (a) Molecular structures of some representative fluorinated cyclic ethers. (b) Electrostatic potential (ESP) calculations of TOF, cFTOF, and DTDL. (c) Raman spectra of TOF and cFTOF and their formulated electrolytes. (d) Schematic diagram of the solvation structures of TOF and cFTOF-based electrolytes. (e) Cycling performance of NCM811||Li full cell employed with different electrolytes. (b) Reprinted with permission from ref. 88 and 89. Copyright 2022, John Wiley & Sons, Inc and 2022, Springer Nature. (c and d) Reprinted with permission from ref. 89. Copyright 2022, John Wiley & Sons. (e) Reprinted with permission from ref. 88. Copyright 2022, Springer Nature.

conductivity and viscosity was observed in cFTOF-based electrolytes due to an anion-rich solvation structure. Recently, Zhao *et al.* reported the preparation of a new ether, 2,2-dimethoxy-4-(trifluoromethyl)-1,3-dioxolane (DTDL, 15-3), which contained both cyclic and linear fluorinated ether groups.⁸⁸ Similar to 15-2, DTDL (15-3) also showed electron density concentrated on O atoms, providing a location to achieve unique rich-anion solvation structures (Fig. 22b, bottom). Therefore, the NCM811||Li full cell employed with the DTDL-based electrolyte exhibited robust cycling performance even with a small negative/positive capacity (N/P) ratio (Fig. 22e).

4.3 Fluorinated sulfones

In contrast to carbonates and ethers, sulfones are often employed in high-voltage electrolytes.^{224,225} The oxidation decomposition voltage of tetramethylene sulfone (TMS, 16-1) reached 5.5 V vs. Li⁺/Li.²²⁶ The strong electron-withdrawing nature of sulfonyl group (S=O) with high polarity, on the one hand, results in high inoxidizability of sulfone and sufficient dissociation of lithium salts; on the other hand, it endows sulfone with high viscosity and poor wettability toward the

electrodes and separators.¹⁷⁶ Meanwhile, sulfones have poor anode compatibility, especially towards the Li metal anode, on which a high resistive SEI layer accompanied by shuttled RSO₂⁻ and RSO₃⁻ species were formed, resulting in a sharp increase in charge transfer resistance.^{227,228}

The introduction of fluorine in sulfone is also an important means to improve its performance. Inspired by the improved SEI chemistry of fluorinated alkyl molecules, Xu *et al.* synthesized a partially fluorinated asymmetric linear sulfone, 3,3,3-trifluoropropylmethyl sulfone (FPMS, 20-3).²²⁹ Although its high melting point (56 °C) excludes its use as a single solvent, the SEI-forming ability of FPMS is indeed improved with well-maintained anodic stability, even in the presence of linear carbonates. In particular, the ionic conductivity of these sulfone + DMC binary electrolytes is comparable with that of commercial carbonate-based electrolytes at 50 °C.²³⁰ The cyclic 1,3-propane sultone (PS, 17-1) has better interfacial chemistry (SEI layer) than TMS (16-1). However, its reduction products, mainly Li₂SO₃, may deteriorate the capacity retention of full cells.²³¹ The incorporation of fluorine elevates the anodic stability and increases the reduction potential of the resulting

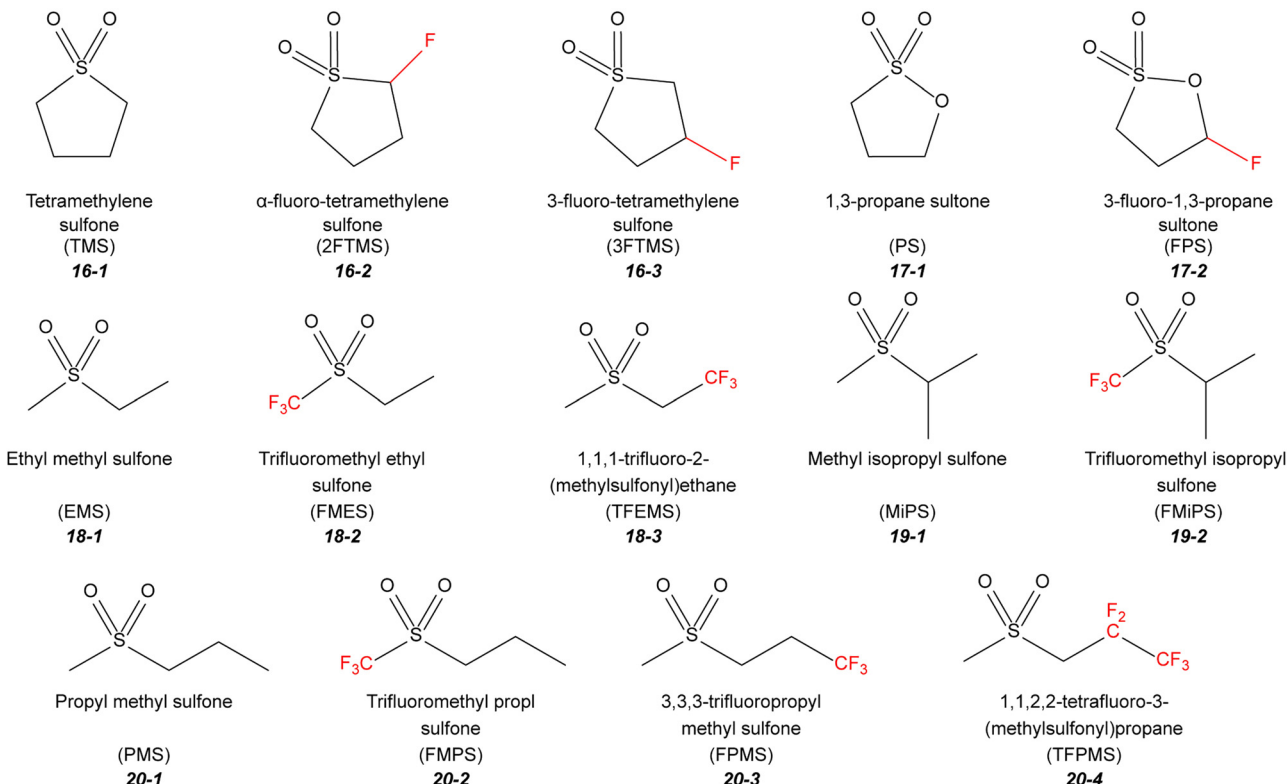


Fig. 23 Molecular structures of sulfones and their fluorinated derivatives.

solvent 3-fluoro-1,3-propane sultone (FPS, 17-2).²³² Fluorosulfolane (3FTMS, 16-3), an analogue to FEC, was proposed by Sasaki in 2002. However, the parameters and applications of this new solvent are unknown (Fig. 23).

Fluorination affects the physical and electrolyte properties of sulfones, different from esters and linear ethers. The fluorinated sulfones exhibit lower viscosity and contact angle toward the separator than their non-fluorinated counterparts (Table 8). However, fluorination results in a lower boiling point. The SEI formed by fluorinated sulfone is still ineffective to support the repeated graphite anode cycles, as demonstrated by Zheng *et al.*¹⁸⁷ In particular, fluorination does not always enhance the anodic stability of sulfones.¹⁰⁴

Du *et al.* studied the oxidation potential of sulfones and fluorinated sulfones *via* quantum chemical calculations.¹⁰⁴ They pointed out that the oxidation potential of fluorinated

sulfones was correlated with the fluorination position and molecular structure. Replacing one H atom in TMS (16-1) with a fluorine atom, the charge of the C atoms connected directly to the O=S=O bond became more positive or negative, depending on the position of fluorine. If the F is at the α -site, the Coulombic repulsive between the C and S atoms increases, causing lengthened C-S bonds (Fig. 24). On the contrary, Coulombic attraction between the C and S atoms exists at the other sites of sulfone (3-FTMS, 16-3). The longer S-C bonds are prone to breakage during oxidation. Therefore, 2-FTMS (16-2) has a lower oxidation decomposition potential than TMS.

Similar to cyclic sulfones, the fluorination positions (α -CF₃ and non- α -CF₃) also induce different anodic stability on linear sulfones. In contrast to non- α -CF₃ fluorination methyl isopropyl sulfone (FEMS), α -trifluoromethyl isopropyl sulfone (FMES, 18-2) has a higher oxidation potential, which may be ascribed to

Table 8 Basic properties of different sulfones

Sulfone	TMS 16-1	EMS 18-1	FMES 18-2	MIS 19-1	FMIS 19-2	MPS 20-1	FMPS 20-2	FPMS 20-3
bp (°C)	285	240	141	238	150	130 (15 torr)	152	—
Viscosity ^a (cP)	7.97	4.53	1.17	5.73	1.20	—	—	—
Contact angle	74	71	24	66	28	—	23	—
Conductivity ^b (mS cm ⁻²)	1.75	1.63	1.39	1.20	0.99	—	0.45	—
E_{ox}	6.22	6.34	6.76	5.91	6.28	6.29	6.70	6.73
E_{re}	0.85	0.80	1.43	0.98	1.68	0.79	1.51	0.98
HOMO	-7.90	-8.10	-8.84	-7.93	-8.78	-8.06	-8.78	-8.55
LUMO	-0.37	-0.41	-0.62	-0.36	-0.45	-0.36	-0.45	-0.52

All data obtained from ref. 187. ^a The viscosity of various solvents at 40 °C. ^b The conductivity of the solvent containing 0.5 M LiPF₆ at 20 °C.

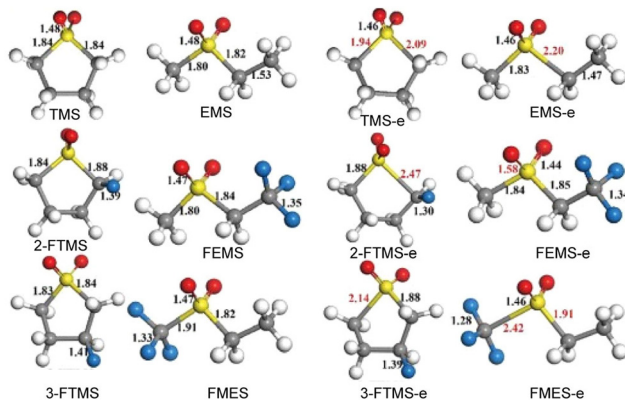


Fig. 24 Optimized geometric structures and bond lengths of TMS, EMS, FTMS, and FEMS before and after oxidation. Reprinted with permission from ref. 104 Copyright 2021, Elsevier.

the different routes during oxidation. Referring to fluorinated methyl isopropyl sulfone (MiPS, **19-1**), the α -fluorinated FIMS undergoes a spontaneous chemical reaction during oxidation, resulting in continuous bond elongation or rupture. FMiPS (**19-2**) delivered a lower oxidation potential (5.9 V) than MiPS (**19-1**, 6.1 V). However, the fluorinated propyl methyl sulfone (from **20-2** to **20-4**) had similar oxidation potentials, regardless of the position of the $-\text{CF}_3$ group.

Recently, Amine *et al.* explained the importance of fluorinated sites in fluorinated sulfones.⁹⁸ They declared that the polarity of the sulfonyl group decreased drastically when the trifluoromethyl group was located at the traditional α position, resulting in lower ionic conductivity. Alternatively, the $-\text{CF}_3$ group showed a trivial electron-withdrawing effect on the sulfonyl group when it was located in the γ position. By introducing the F-containing group at the β position, transition metal dissolution could be reduced, and balance among anodic stability, ionic conductivity, and reductively stability toward graphite achieved. In particular, 1,1,2,2-tetrafluoro-3-(methylsulfonyl)propane (TFPMS, **20-4**) showed flame retardancy. Hence, a “golden middle way” strategy is proposed to design β -fluorinated sulfones for high-voltage LIBs.

4.4 Fluorinated phosphorous solvents

4.4.1 Fluorinated linear phosphate. Organic phosphates, such as triethyl phosphate (TEP, **21-1**), have been incorporated in conventional electrolytes as flame-extinguishing agents to improve battery safety.^{121,123,233} The most conspicuous issue of phosphates is their poor ability to form a protective SEI film on graphitic anodes,³² which causes the collapse of the laminar structure of graphite and the continuous decomposition of the electrolyte. Also, organic phosphates have to be used at low doses (less than 10% either by weight or volume) to balance the safety and performance of batteries. Unfortunately, the risk of combustion accidents remains as long as volatile components are present in the electrolyte.^{234,235} This necessitates improvement of the interface compatibility of phosphates to meet the requirement to serve as the primary solvent for Li-based

batteries. Fig. 25 shows the representative fluorinated linear phosphates for Li-based batteries.

Considering that fluorinated substituents in esters or ethers may favor SEI on the anode and reduce the solvent viscosity, Xu *et al.* systemically studied a novel fluorinated alkylphosphate, tris(2,2,2-trifluoroethyl)phosphate (TFP, **22-2**).²³⁶ The trade-off between electrolyte non-flammability and performance in the battery was well resolved in TFP. They further evaluated the influence of fluorination degree on the physical properties, flammability, and electrochemical stability.⁷⁹ Similar to fluorinated EC, the boiling points of fluorinated alkyl phosphates monotonically decreased with the degree of fluorination (Table 9). Three fluorinated alkyl phosphates exhibited much higher melting points than the TEP reference. The higher fluorination degree of the alkyls yielded higher flame retarding efficiency. The baseline electrolytes (1 M LiPF₆ in EC/EMC (1 : 1 by volume)) containing only 20% TFP or BMP (**22-3**) were considered completely non-flammable. Both TFP and BMP showed improved cathodic stability. Despite certain compromises in ionic conductivity, the presence of TFP in the baseline electrolyte made little difference in electrochemical stability on carbonaceous anodes.

Winter and co-workers surprisingly found that the anodic stability was lowered with an increase in the phosphate content and fluorination degree.²³⁷ Interestingly, the partially fluorinated BMP (**21-3**) offered both optimal electrochemical performance and non-flammability in graphite||Li half cells, NCM||Li half cells, and graphite||NCM full cells. Shifting to fluorinated tripropyl phosphate (TPrP, **23-x**) derivatives, they further studied the influence of fluorination degree of organophosphates on the flammability and electrochemical performance.²³⁸ As expected, a clear trend could be verified in ionic conductivities of the formulated electrolytes, *i.e.*, a higher phosphate content in the electrolytes resulted in lower ionic conductivity (Fig. 26a). In comparison with fluorinated TEP, the monotonous behavior between the fluorination degree and ionic conductivity, flammability, and anodic stability was not observed for the fluorinated TPrP (**23-1**). For example, the 5F-TPrP (**23-4**)-based electrolyte was even more conductive and favored anodic stability than other fluorinated TPrP-based electrolytes. 3F-TPrP (**21-2**) delivered better flame-retarding efficiency than 4F-TPrP (**23-3**) (Fig. 26b). Furthermore, 5F-TPrP showed a thicker CEI and shorter SET than the branched $-\text{CF}_3$ (HfIP, **22**).²³⁹ These results underscored that the fluorine position plays a crucial role in the properties of fluorinated TPrP (**23-1**). Although they showed improved compatibility towards both electrodes, all the fluorinated phosphates were far from satisfactory, and thus efforts are still needed to develop new solvents or strategies.

4.4.2 Fluorinated cyclic phosphate. Cyclic ethylene ethyl phosphate (EEP, **24-1**) was first employed by Ota *et al.* as an electrolyte additive to improve the interphase compatibility of TMP with graphite.²⁴⁰ The SEI layer created by EEP could efficiently suppress the continuous and uncontrolled decomposition of TMP on the graphite surface. The EEP in carbonate electrolytes could not only improve the initial Coulombic

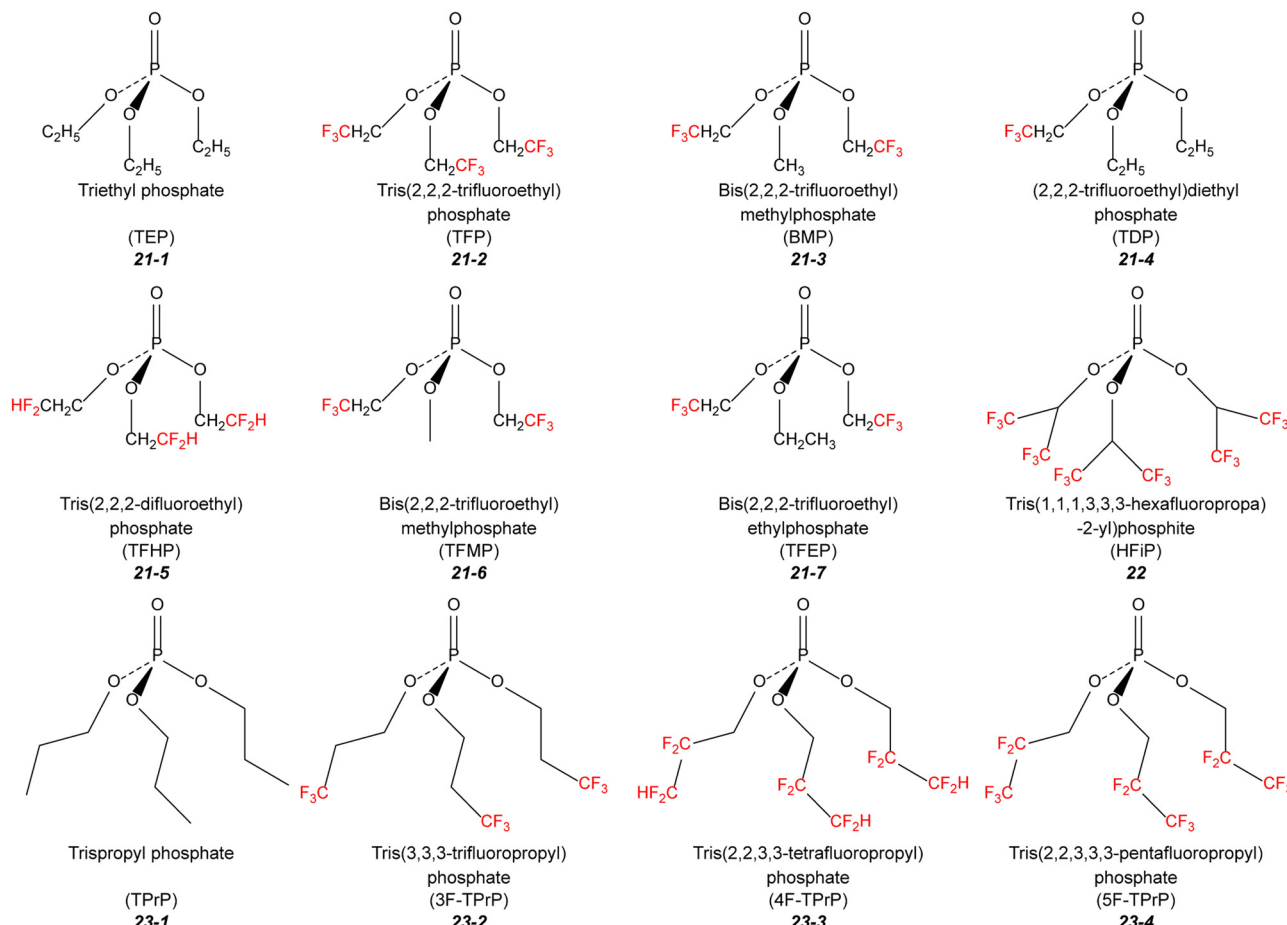


Fig. 25 Molecular structures of linear phosphates and their fluorinated phosphates.

Table 9 Properties of representative linear phosphates and their fluorinated derivatives

Name	bp (°C)	mp (°C)	fp (°C)	ε (20 °C)	η (mPa s ⁻¹ , 25 °C)	HOMO	LUMO
TEP (21-1)	215	-56.4	117	13	1.6	-6.51	0.73
TFP (21-2)	178	-19.6	148	10.5	4.6	-7.85	-0.50
BMP (21-3)	203	-22.5	—	12	—	—	—
TDP (21-4)	210	—	—	15	—	—	—

efficiency and cycling stability of graphite and NCM electrodes, but also serve as a specific flame inhibitor and overcharge protector to enhance the safety of batteries.²⁴¹ Su *et al.* reported that the fluorinated cyclic phosphate ester, 2-(2,2,2-trifluoroethoxy)-1,3,2-dioxaphospholane 2-oxide (TFEP, 24-2) enabled higher protection effectiveness of the cathode than EEP and other fluorination cyclic phosphates (Fig. 27a).¹⁸⁴ Surface and electrolyte composition analyses conducted with XPS and NMR suggested that the cathode surface after cycling was covered with an F and P-rich CEI, preventing continuous electrolyte decomposition and transition metal dissolution. The possible reaction mechanism is proposed in Fig. 27b. The P=O bond in the TFEP underwent nucleophilic attack by the oxygen center

on the cathode surface, causing the ring-opening polymerization of TFEP, thus producing a protective CEI consisting of LiP_xO_yF_z and polyphosphoesters.²⁴² Zheng *et al.* further applied TFEP as a co-solvent for LIBs.¹¹⁸ The formulated electrolyte, 0.95 M LiFSI TFEP/FEMC (1 : 3 by volume), exhibited excellent non-flammability and capacity retention in graphite||Li-Ni_{0.5}Mn_{1.5}O₄ cells with slight compromise in ionic conductivity and viscosity (Fig. 27c). Furthermore, these electrolytes showed excellent current collector dissolution resistance at high voltage. Postmortem analyses through XPS peak devolution illustrated that the inorganic-rich (AlF₃ and LiF) interface layer decreased the side reactions between the imide salt and Al (Fig. 27d).

4.4.3 Fluorinated phosphites. In contrast to phosphates, phosphites are intrinsically susceptible to oxidation, and thus usually used as additives in electrolyte formulations.²⁴³ The poor oxidation state of phosphites can scavenge the notorious HF and modify the CEI to improve the interfacial stability of high-voltage cathodes.²⁴⁴ Nevertheless, their highly flammable and resistive interphase layer limits their wide application. Fortunately, the fluorinated phosphites show excellent flame retardancy and unique interphase on both electrodes (Fig. 28).¹²³ Zhang *et al.* reported that the addition of 15 wt%

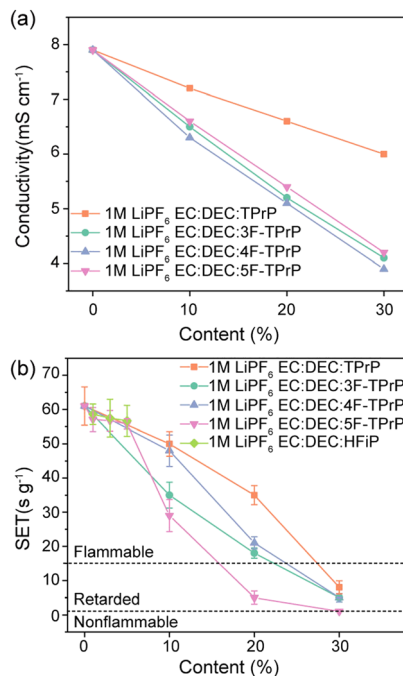


Fig. 26 Ion transport and flame-retarding properties of fluorinated linear phosphate-based electrolytes. (a) Ionic conductivities of different electrolytes. (b) SET measurements of various electrolytes. Fig. 26a is compiled based on ref. 238. (b) Reprinted with permission from ref. 237 and 238. Copyright 2017, Elsevier and Copyright 2018, IOP Publishing, Ltd.

tris(2,2,2-trifluoroethyl) phosphite (TTFP, 25-1) could make carbonates non-flammable, with a slight compromise in ionic conductivity.²⁴⁵ The additional benefits were that TTFP not only participated in the formation of an SEI layer, suppressing the co-intercalation of PC into graphite, but also improved the high-temperature (60 °C) performance of full cells with graphite anodes.

Alternatively, He *et al.* systematically analyzed the function of TTFP (25-1) additives on the protection of an NCM523 cathode and illustrated that the formed organophosphate passivation layer with high Li⁺ ion mobility was capable of effectively isolating the cathode surface from the electrolyte.²⁴⁶ Based on the XPS results, they deduced that the fluorinated alkyl in the TTFP molecule prevented its complete mineralization to orthophosphates, which was the main reason for the formation of the resistive interphase layer for TEP (21-1). Similar flame-retarding properties and interphase protective effects were also achieved in Li-S chemistry employing pPAN@S as the cathode. Wang *et al.* reported that the presence of TTFP (25-1) not only served as a flame retardant but also delivered high Li-ion conductive interphase on the pPAN@S cathode.²⁴⁷ Consequently, more than a 10-fold diffusion coefficient of Li-ion and accelerated redox kinetics were achieved simultaneously, and a stable electrochemical performance of over 750 cycles at 10C was realized.

Aspern *et al.* selected two cyclic phosphites, 2-(2,2,3,3,3-pentafluoropropoxy)-1,3,2-dioxaphospholane (PFPOEPi, 25-3) and 2-(2,2,3,3,3-Pentafluoropropoxy)-4-(trifluoro-methyl)-1,3,2-

dioxaphospholane (PFPOEPi-1CF₃, 25-4), as additives for high-voltage LIBs.²⁴⁸ Similar to TFEP (25-1), these cyclic phosphites were capable of polymerizing on the cathode surface to participate in CEI formation. Compared to PFPOEPi (25-3), the extra -CF₃ groups may retard the polymerization dynamics of PFPOEPi-1CF₃ (25-4), resulting in the formation of a thicker CEI with higher LiF content. Therefore, the cells with PFPOEPi-1CF₃ (25-4) additives showed higher impedance and decreased cycling performance than that containing PFPOEPi (25-3).

4.5 Fluorinated nitriles

Nitriles have high electronic polarizability with good solvating properties due to the electron-rich cyano (C≡N) groups.^{249,250} They can coordinate with transition metal (TM) ions, such as nickel/cobalt/manganese, to generate a layer of -C≡N-TM complexes on the aggressive cathode surfaces, on which the catalytic activity of metal sites are deactivated.^{251–254} An electrochemical double-layer capacitor with more than 7.8 V vs. Li⁺/Li was afforded by adiponitrile- and glutaronitrile-based electrolytes, as demonstrated by Ue *et al.*²⁵⁵ Therefore, the high anodic stability nitriles represent promising candidates for applying 5 V high-voltage cathodes.²⁵⁶ However, nitriles have poor compatibility with graphite and lithium metal.⁴⁷ In this case, Co-solvents or additives are required in nitrile-based electrolytes. However, the incorporation of fluorine into nitriles only slightly affects their interfacial compatibility. Fortunately, the aluminum dissolution induced by imide salts was effectively mitigated in fluorinated nitriles. Oldiges *et al.* reported that 3-(trifluoromethyl)adiponitrile (ADN-CF₃, 26-2) afforded suppressed aluminum dissolution in the presence of the TFSI⁻ anion compared with its non-fluorinated counterpart adiponitrile (ADN, 26-1), as shown in Fig. 29b and c.¹⁵⁴ They found that the high viscosity and low permittivity of ADN-CF₃ resulted in increased Li⁺-TFSI⁻ coordination and stronger Li⁺-solvent interactions, and thus slowed down the diffusion of TFSI⁻ and lowered the solubility of Al(TFSI)_x, which were identified as critical parameters for reducing aluminum dissolution (Fig. 29d).

4.6 Fluorinated carbamates

In contrast to other types of solvents, carbamates have received relatively little attention due to their undesirable SEI-forming ability (large resistive and unprotective SEI).⁶ Smart *et al.* first used fluorinated carbamates as co-solvents to formulate ternary and quaternary electrolytes for LIBs.¹⁵⁵ They found that the introduction of carbamates caused higher polarization and higher interface resistance at low temperatures, and hence lowered the charge capacity of MCMB-carbon electrodes. Bolloli *et al.* revealed the physicochemical and electrochemical properties of a class of fluorinated carbamates.⁴⁰ As shown in Table 10, the fluorinated carbamates exhibit a higher melting point and lower boiling point than their non-fluorinated counterparts. Similar to fluorinated linear carbonates, the introduction of fluorine also increased the dielectric constant and viscosity of carbamates. With the addition of 1 M LiTFSI in these carbamates, the non-fluorinated carbamate-based

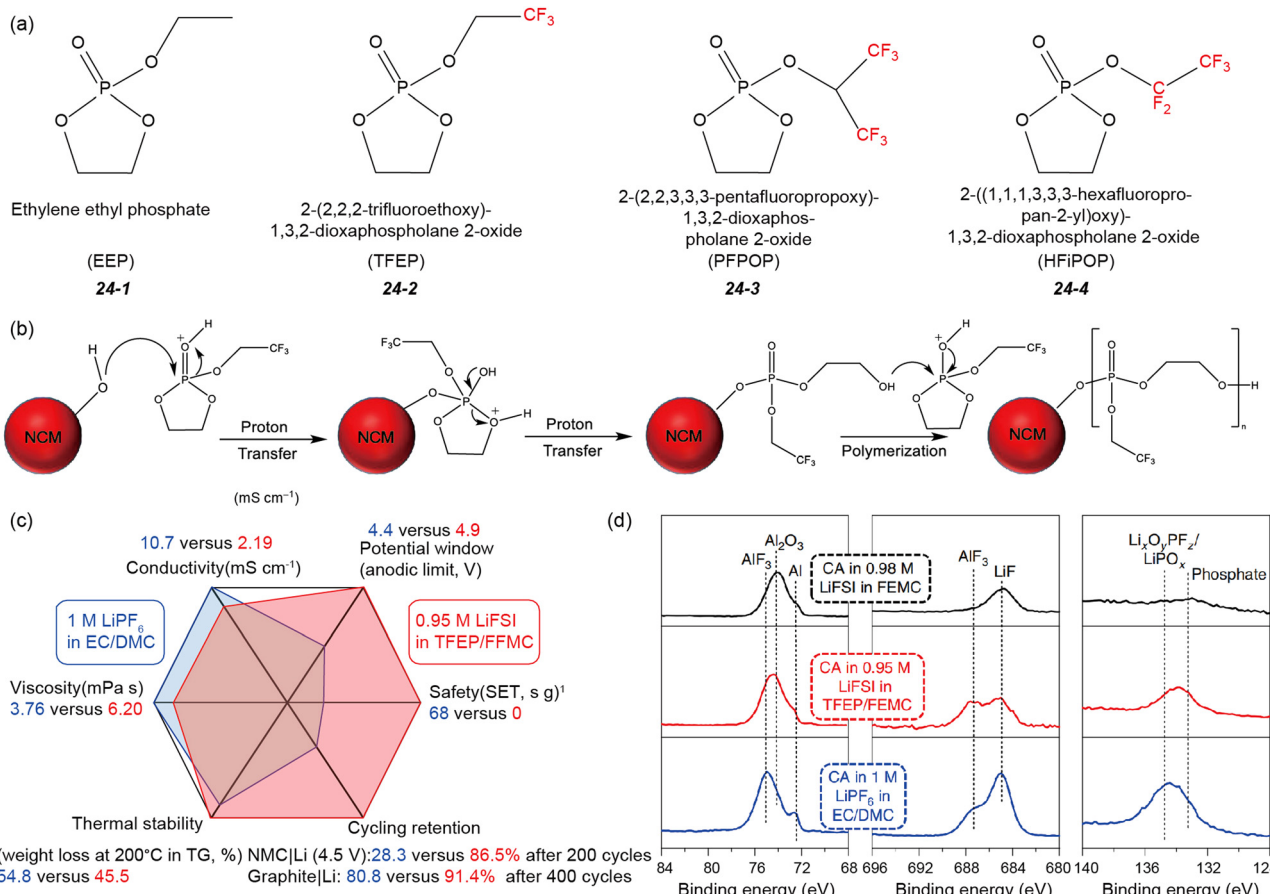


Fig. 27 Molecular structures and functions in batteries of cyclic phosphates and their fluorinated phosphates. (a) Molecular structures of EEP, TFEP, PFPOP, and HFiPOP. (b) Proposed mechanism of the ring-opening polymerization of TFEP. (c) Comparison of the properties and performances of TFE-based electrolytes and EC/DMC-based electrolytes. (d) XPS spectra of post-mortem Al current collector after the chronoamperometry tests. Fig. 27b is compiled based on ref. 184. (c and d) Reprinted with permission from ref. 118. Copyright 2020, Springer Nature.

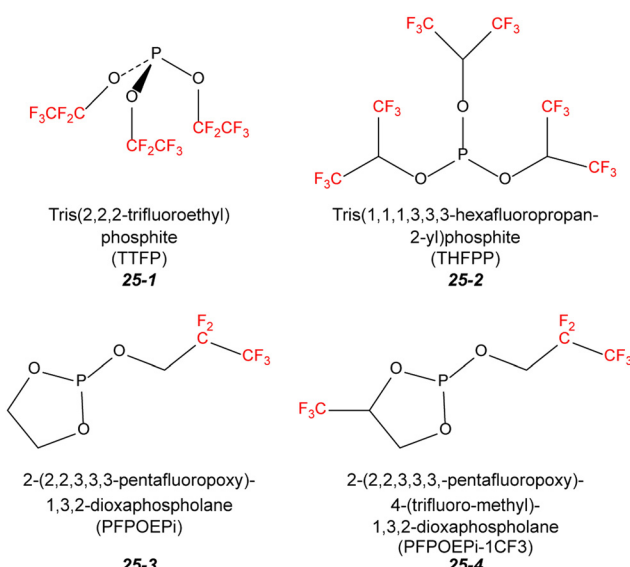


Fig. 28 Chemical structures of representative fluorinated phosphites.

electrolytes showed higher ionic conductivity and lower anodic stability than the fluorinated ones.

Alternatively, the continuous anodic Al corrosion is well mitigated in fluorinated carbamates, especially in the 27-7-based electrolytes, where a protective AlF_3 layer with sufficient thickness was formed on the current collector. However, the low ionic conductivity of the 27-7-based electrolytes (about 0.3 mS cm^{-1}) and inferior interphase layer caused the NMC111||Li half cells to show a low rate performance and Coulombic efficiency compared to that with the 27-5-based electrolytes. Thus, more efforts should be devoted to optimizing the solvent mixtures or molecular structures to decouple the interphase chemistry and ionic transport capacity.

Due to the high electronegativity of fluorine, most fluorinated solvents demonstrate low capabilities of solvating Li^+ , which can reduce the de-solvation barriers and favor the formation of an anion-derived interface on the working electrode. This is beneficial for the stability and safety of solvents by scavenging $\text{H}\cdot$ radicals through $\text{F}\cdot$ radicals. Furthermore, the Al dissolution caused by imide anions (FSI^- and TFSI^-) can be suppressed in electrolytes by forming a passivation layer

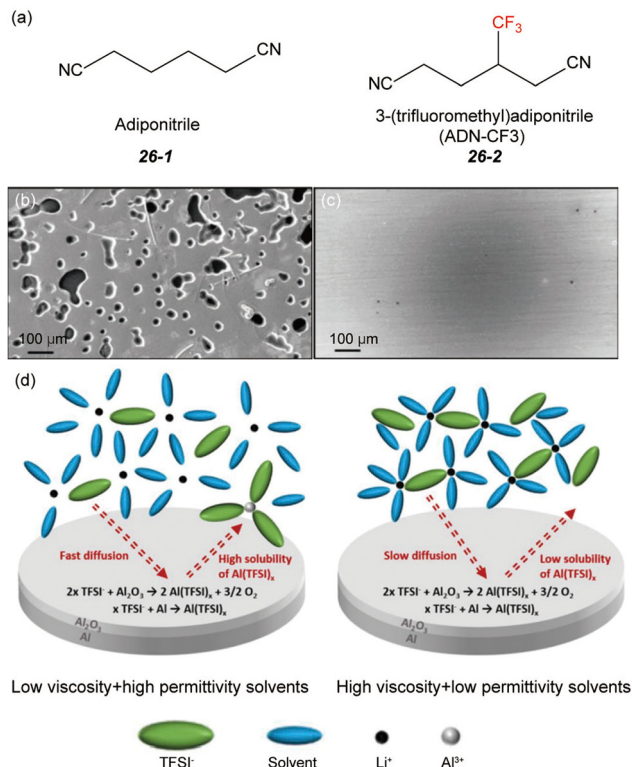


Fig. 29 Molecule structures and Al current collector dissolution behaviors of nitriles and their fluorinated phosphates. (a) Chemical structures of ADA and ADN–CF₃. SEM images of Al electrodes after constant-voltage charging at 5 V vs. Li⁺/Li for 72 h in 1 M LiTFSI/ADN electrolyte (b) and 1 M LiTFSI/ADN–CF₃ electrolyte (c). (d) Schematic descriptions of the possible mechanism of aluminum dissolution within ADN (left) and AND–CF₃ (right) based electrolytes. (b-d) Reprinted with permission from ref. 154. Copyright 2018, IOP Publishing, Ltd.

such as AlF₃. However, the physical properties and oxidative stability are vastly different, depending on the type of fluorinated solvent. Besides these advantages, fluorination generally lowers the bulk transport in electrolytes, deteriorating the fast charging properties. Thus, considering various application demands, careful consideration of the fluorine content and position should be conducted to design and predict new fluorinated solvents. Alternatively, tuning the coordination structure of fluorinated solvents with Li⁺ by changing the fluorine content represents another promising way to improve the properties of electrolytes. The C–F bond shows strong interaction with Li ions, while the affinity between the –CF₃ bond and the Li ion is weak. Therefore, more efforts are needed in this direction to design fluorinated molecules with well-balanced properties.

5. Grafting ester or ether functional groups in fluorinated solvents

The most conspicuous merit of esters and ethers is their high solvation to guarantee the capacity to dissolve lithium salts. Accordingly, the modification of ester or ether groups on

perfluoro molecules can combine both merits, rendering much-improved performances in specific cases. For example, fluorinated 1,4-dimethoxylbutane (FDMB) was found to offer the combined advantages of the Li metal anode compatibility of the ether and high-voltage tolerance of the fluorinated solvent.⁹¹ Also, Wong *et al.* described that grafting carbonate with hydrofluoroethers resolved the dilemma of solubility and ionic conduction of hydrofluoroethers with non-flammability.²⁵⁷ Another significant advantage of esters or ethers is their good interphase compatibility with anode materials. Several ether-modified phosphates and sulfones were designed and exhibited improved SEI-forming ability.^{258,259} However, it should be noted that the additional segments made the solutions more viscous and less conductive. Obviously, the concept of integrating two or more types of solvents is one of the most promising directions to design advanced electrolytes for LIBs. In this section, we highlight the change in interphase compatibility and ion transport of ester or ether-modified perfluoro-solvents.

5.1 Carbonate-grafted hydrofluoroethers

The application of hydrofluoroethers (HFE) as a co-solvent or additive dates back to about 20 years ago. Arai *et al.* described the use of nonafluorobutyl ether as a flame retardant to develop an inherently safe electrolyte for LIBs.²³⁵ Since then, many researchers have used different HFE to formulate advanced electrolytes. Recently, the low viscosity and nonflammability of HFE triggered hot research on developing localized high-concentration electrolytes (LHCE).⁹⁴ However, the poor solvating power of HFE makes the mixed electrolyte prone to undergo phase separation at high salt concentrations or makes it challenging to eradicate undesirable parasitic reactions of unstable solvents.²⁶⁰ Besides, the safety of HFE-based electrolytes may be unsatisfactory because fire incidents are suppressed rather than eliminated as long as highly flammable organic solvents are still present.²⁶¹ Thus, tailoring HFE molecules to dissolve sufficient lithium salts is highly desirable. Fig. 30 shows the chemical structure of the reported carbonate-grafted hydrofluoroethers.

To the best of our knowledge, Wong *et al.* were the first to report the synthesis of methyl carbonate-functionalized perfluoropolyether (PFPE-DMC, 28-1).²⁵⁷ They found that the inherently non-flammable PFPE-DMC could solvate LiTFSI, and the resulting electrolytes delivered unprecedented transference numbers (close to 1). Although the conductivity was low ($\sim 2.5 \times 10^{-6} \text{ S cm}^{-1}$), the PFPE-DMC-based electrolytes showed high compatibility with LiNMC cathodes, emphasizing the viability of these materials for practical application (Fig. 31a and b). Olson *et al.* further improved the ion transport in DMC-terminated PFPE electrolytes by employing ethoxylated-PTPE (EO-PTPE).²⁶² They believed that in the resultant solvents, EO-PFPE-DMC (28-2), the ethylene oxide units supported ion dissociation and increased conductivity, while the fluorinated carbon backbones ensured high thermal stability and sufficient cation transference numbers. Besides, higher degrees of terminated moieties favored ion transport. Upon mixing with LiTFSI

Table 10 Basic parameters of carbamates and their fluorinated counterparts

Solvent	Molecular structure	mp (°C)	bp (°C)	Density (g cm ⁻³ , 20 °C)	ε (20 °C)	η (mPa s ⁻¹ , 20 °C)	HOMO (eV)
<i>N,N</i> -Dimethylethyl carbamate (27-1)		< -50	141	0.97 ± 0.03		10.45 ± 0.09 1.00 ± 0.03	-10.22
<i>N,N</i> -Dimethylisopropyl carbamate (27-2)		< -50	136	0.93 ± 0.02		8.12 ± 0.07 1.18 ± 0.08	—
<i>N,N</i> -Diethylethyl carbamate (27-3)		< -50	161	0.91 ± 0.02		8.65 ± 0.02 1.41 ± 0.03	—
2,2,2-Trifluoroethyl <i>N,N</i> -dimethyl-carbamate (27-4)		-26	135	1.24 ± 0.04		12.25 ± 0.04 1.26 ± 0.05	-10.66
1,1,1,3,3,3-Hexafluoropropan-2-yl <i>N,N</i> -dimethyl-carbamate (27-5)		4	130	1.38 ± 0.02		9.2 ± 0.2 2.02 ± 0.06	-10.94
2,2,2-Trifluoroethyl <i>N,N</i> -diethyl-carbamate (27-6)		< -50	154	1.14 ± 0.03		11.4 ± 0.2 1.78 ± 0.10	—
1,1,1,3,3,3-Hexafluoro-propan-2-yl <i>N,N</i> -diethylcarbamate (27-7)		-15	149	1.29 ± 0.04	n.a.	2.27 ± 0.08	-10.65

Reprinted with permission from ref. 40. Copyright 2015, the American Chemical Society.

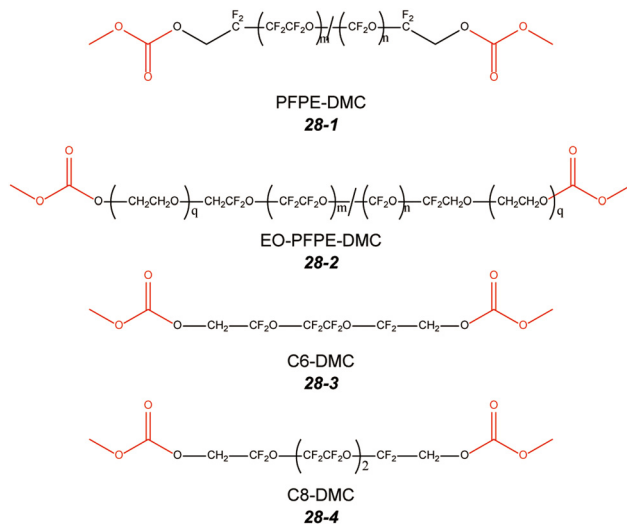


Fig. 30 Molecular structures of carbonate-functionalized perfluoropolymers.

salts, the electrolyte with EO-PFPE showed an order of magnitude higher conductivity than non-ethoxylated PFPE at room temperature (5×10^{-5} S cm⁻¹ vs. 5×10^{-6} S cm⁻¹). However, the conductivity of PFPE-based electrolytes is still too low to compete with commercial electrolytes. In this case, it can be further improved through the rational design of novel electrolytes with larger polar end groups and lowering the molecular weight of the backbones.

Chintapalli *et al.* studied the ion transport properties of a series of electrolytes with different end-group terminated PFPE to clarify the relationship between continuum scale and microscopic ion transport properties of PFPE electrolytes.²⁶³ A non-dimensional parameter, β , was proposed to describe the microscopic diffusivities and conductivity (eqn (7)).

$$\beta = \frac{\sigma RT}{F^2 c(D_+^{\text{NMR}} + D_-^{\text{NMR}})} \quad (7)$$

where σ is the ionic conductivity of the electrolyte, F is the faradaic constant, R is the gas constant, T is temperature, and D_+^{NMR} and D_-^{NMR} represent the diffusion coefficients of cations and anions under nuclear magnetism, respectively.

In the electrolytes with high β values, such as ethoxylated PFPE, the microscopic and continuum transference numbers were similar. Conversely, in electrolytes with low β values, a significant deviation of these two indexes was observed. Timachova *et al.* further revealed the ion transport mechanism of perfluoropolyether electrolytes.²⁶⁴ They believed that ion hopping between clusters was responsible for the ion transport in the electrolytes with a low β . Shah examined the effect of anion size on the Li⁺ ion transport properties of PFPE electrolytes by using a family of lithium salts, *i.e.*, LiFSI, LiTFSI, and LiBETI.²⁶⁵ They reported that a smaller anion (LiFSI) exhibited higher conductivity in C6-DMC (28-3) and C8-DMC (28-4) (Fig. 31c and d, respectively).

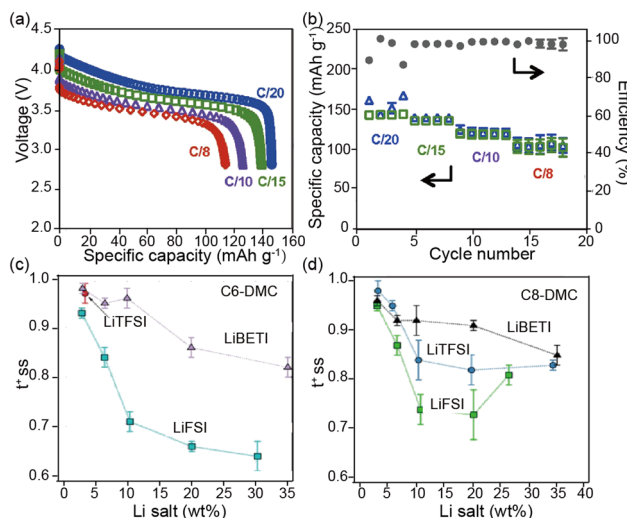


Fig. 31 Electrochemical performance of batteries with carbonate-functionalized perfluoropolyether-based electrolytes. (a) Discharge profiles of Li||LiNMC cells with DMC-PFPE-based electrolytes. (b) Cycling stability of Li||LiNMC cells with DMC-PFPE-based electrolytes at different charge-discharge rates. Conductivity of the Li-ion for C6-DMC (c) and C8-DMC (d) at different lithium salt contents. (a and b) Reprinted with permission from ref. 257 Copyright, 2014 National Academy of Sciences. (c and d) Reprinted with permission from ref. 265 Copyright 2017, IOP Publishing.

5.2 Ether-grafted hydrofluoroethers

Ether modification is another effective way to increase the capability of hydrofluoroethers to solvate Li^+ . The fluorine-rich backbone and ether end-groups have high compatibility with lithium metal, exhibiting tremendous potential for application in next-generation lithium metal batteries.

Amanchukwu *et al.* developed a series of novel ether-modified HFE by varying the length and types of ether end-group, as well as the length of fluorinated backbones for Li||NCM811 cells (Fig. 32).²⁶⁶ All the ether-modified HFE exhibited useful physical and electrochemical features including low glass transition, sufficient ionic conductivity, high lithium transference number, and elevated oxidative voltage (Table 11). Using NMR and molecular dynamics (MD) simulations, Olson *et al.* revealed that more extended ether groups and lower weight of backbone led to higher ionic conductivity.²⁶² Surprisingly, the NMC811 cathode with a high loading of 4 mg cm^{-2} delivered over 100 charge/discharge cycles in 1 M LiFSI/DEG-FTriEG (29-4) electrolyte.

5.3 Ether-grafted fluorine-containing molecules

Combining the high-voltage tolerance of fluorinated alkyl chains and favorable lithium anode compatibility of ethers, a novel fluorinated solvent, FDMB (**30-1**), was proposed by Yu *et al.*⁹¹ FDMB inherited the benefits of DME, exhibiting low viscosity and high ability to conduct Li⁺ ions. Meanwhile, several critical drawbacks of DME, such as low boiling point and high flammability, were well avoided. Paired with 1 M LiFSI, the resulting electrolyte delivered a high oxidation potential (>6 V vs. Li⁺/Li) and excellent Li cycling CE (~99.52%) with fast activation in Li||Cu cells. Combining MD simulations, DFT calculations, and NMR characterization, it was determined that the unique Li–F interaction in the electrolytes contributed to a high anion/solvent ratio in the solvation sheath, leading to high compatibility with the Li anode and high oxidation resistance (Fig. 33b). Furthermore, this unique coordination could permanently regulate the SEI structure and Li packing morphology in anode-free Cu||NMC

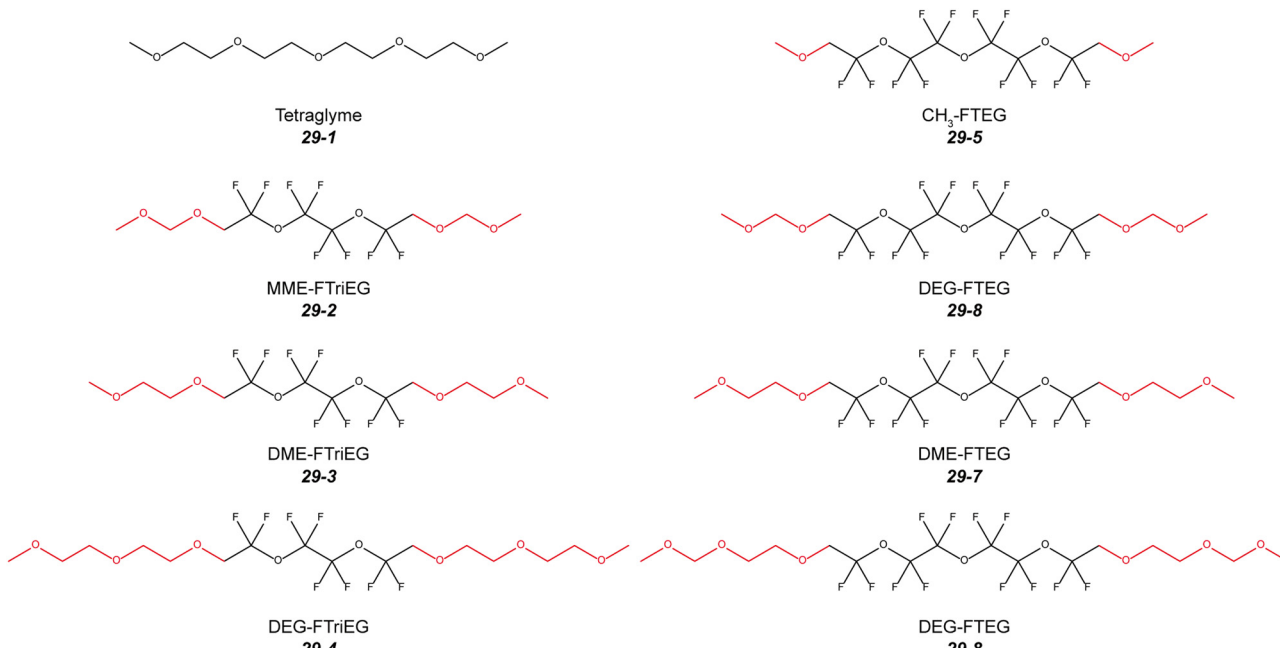


Fig. 32 Molecular structures of the representative ether-modified fluorinated triethylene glycol (FTriEG) and fluorinated tetraethylene glycol (FTEG).

Table 11 Physicochemical properties of ether-modified FTriEG and FTE and their formulated electrolytes

Compound	Glass transition (°C)	Ionic conductivity (mS cm ⁻²) 0.1 M/1 M LiFSI	Lithium transference number	Oxidative voltage ^a (V)	Oxidative voltage ^b (V)
Tetraglyme (29-1)	N/A	0.2/2.5	0.40	4.0	3.9
MME-FTriEG (29-2)	-21.5	4.8×10^{-4} /	0.54	5.6	5.4
DME-FTriEG (29-3)	-21.2	2.6×10^{-2} / 2.4×10^{-1}	0.44	5.4	4.8
DEG-FTriEG (29-4)	-21.5	8.1×10^{-2} / 2.7×10^{-1}	0.57	5.4	5.1
MME-FTEG (29-5)	-21.1	2.4×10^{-4} /	0.64	5.6	5.7
DME-FTEG (29-6)	-20.8	7.2×10^{-3} / 9.1×10^{-2}	0.46	5.8	4.9
DEG-FTEG (29-7)	-21.5	4.3×10^{-2} / 2.4×10^{-1}	0.56	5.6	4.7

^a Oxidation voltage obtained from potentiostatic hold measurements of 0.1 M LiFSI electrolytes at 30 °C. ^b Oxidation voltage obtained from the linear sweep voltammetry for 0.1 M LiFSI electrolytes.

cells, endowing them a high specific energy (325 W h kg⁻¹) and reasonable capacity retention (80% for 100 cycles) in anode-free pouch cells (Fig. 33c–e). It should be mentioned that although FDMB delivered an encouraging electrochemical performance, its high interfacial resistance and relatively low conductivity need to be solved for its application in actual batteries.

Wang *et al.* synthesized a series of FDMB analogs with a gradually prolonged -CF₂- backbone (Fig. 33a).²⁶⁷ DME was selected as the co-solvent to decrease the ionic and interfacial

resistance. They formulated several electrolytes with different FDMB or its analogs to DME ratios and demonstrated that the electrochemical performance of these electrolytes was not all related to the fluorination and fluorinated molecule content. The optimized electrolyte, 1 M LiFSI/6FDMH (30-3)-DME, exhibited a high CE of lithium stripping/plating (99.5%) and oxidative potential (6 V). Employing this electrolyte, both a 20 μm Li||NMC532 coin cell and Cu||NMC811 pouch cell delivered interesting long-term cyclability and rate capability under lean electrolyte conditions (Fig. 33f).

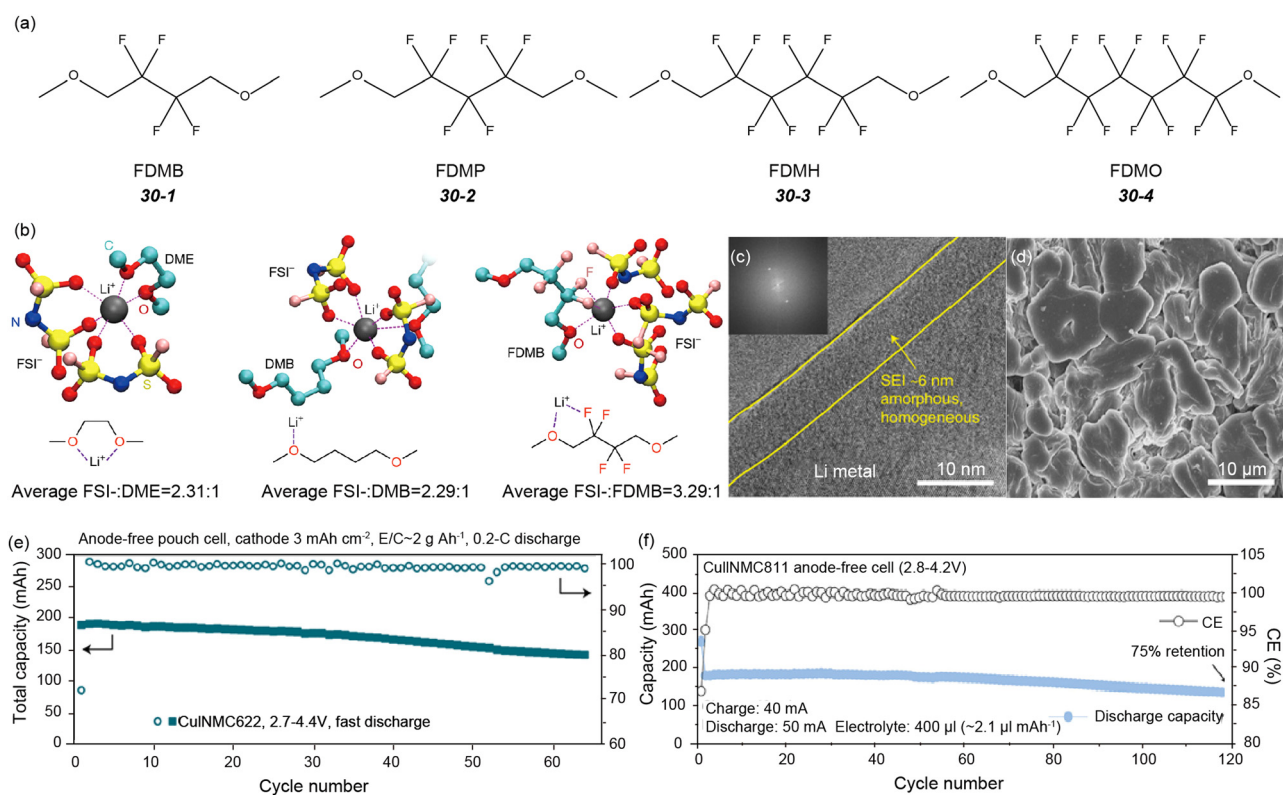


Fig. 33 Molecule design, solvation structures, interface evolution, and anode-free battery applications with ether-grafted fluorinated solvent/electrolyte. (a) Molecular structures of FDMB and its analogs. (b) Coordination structures and corresponding binding ratios of 1 M LiFSI/DME (left), 1 M LiFSI/DMB (middle), and 1 M LiFSI/FDMB (right) based electrolyte. The configuration is deduced from MD simulations. (c) Cryo-TEM image of SEI in 1 M LiFSI/FDMB electrolytes. (d) Li deposition morphology in 1 M LiFSI/FDMB electrolytes after 70 cycles. (e) Cycle stability of Cu||NMC622 pouch cell. (f) Long-term cycling stability of Cu||NMC811 pouch cell at the practical conditions. (b–e) Reprinted with permission from ref. 91. Copyright 2020, Springer Nature. (f) Reprinted with permission from ref. 267. Copyright 2021, John Wiley & Sons, Inc.

5.4 Ether-modified fluorinated cyclophosphazenes

Ethoxy(pentafluoro)cyclotriphosphazene (PFPN, 31-1) was first synthesized by Niecke *et al.* in 1971 (Fig. 34a).²⁶⁸ However, the consideration of PFPN as a flame-retardant additive was first proposed by Xia *et al.*, who found that the presence of only 5 wt% PFPN in 1 M LiPF₆ EC/DMC (3 : 7, v/v) electrolyte could make it non-flammable, which is superior to TMP and TEP in terms of flame-retardant efficiency.²⁶⁹ Benefiting from its low viscosity (1.2 mPa s), PFPN has a slight effect on the conductivity of the electrolyte. The Li||LCO half cells incorporating the PFPN electrolytes showed significantly improved cycling stability than that without PFPN at a high cut-off voltage of 4.5 V. The reason behind the improved cyclability was demonstrated by Ji *et al.*²⁷⁰ The oxidization potential of PFPN was lower than EC and DMC, thus producing an inorganic-rich polymer layer, which efficiently isolated the electrolyte from the cathode, and therefore suppressed its continuous decomposition, and

decreased the interfacial resistance upon the long cycling process. These beneficial interface effects could also be extended to low-temperature and other high-voltage cathodes. Li *et al.* elucidated that 5 wt% PFPN was the optimum amount in formulating electrolytes and confirmed that the N,P-rich CEI layer derived from the oxidization of PFPN could lower the charge transfer resistance and enhance the low-temperature performance of the LCO electrode.²⁷¹ Liu *et al.* found that the addition of PFPN enabled the formation of a compact, uniform, and thinner CEI on LNMO cathodes than the control electrolyte, protecting the cathode from structural destruction and eliminating electrolyte degradation (Fig. 34b and c).²⁷² Furthermore, the reaction mechanism of PFPN at high voltage was proposed based on XPS, ICP, and related spectroscopy analysis. Under high voltage, the unsaturated functionalities of the hexatomic rings in PFPN provided sites for straight chain and octatomic ring polymerization. During this process, inorganic anions (NO₂⁻, NO₃⁻, PO₃⁻, and PO₄⁻) were generated and combined with Li⁺ ions to produce the corresponding interphase with inorganic salts (Fig. 34d). Li *et al.* applied PFPN to NCM811||Li cells, and reported remarkable improvements in their cycle life and thermal stability, benefiting from the stable SEI interphase and radical inhibitors ([P] and [PO]) formed by PFPN on the Li metal surface and high temperature decomposition, respectively.²⁷³

Dagger *et al.* developed another ether-modified fluorinated cyclophosphazene, (phenoxy)-pentafluorocyclotriphosphazene (FPPN, 31-2). They demonstrated that 5% FPPN in EC-based electrolyte reduced the flammability and rendered the MNC111 full batteries better cycling performance than the batteries without FPPN.²⁷⁴ Feng *et al.* showed that FPPN could electro-polymerize at 5.05 V (vs. Li⁺/Li), and thus serve as an overcharge protector for 5 V-class cathodes.²⁷⁵ Recently, Gu and co-workers analyzed the influence of FPPN on a graphite anode in a GBL-based electrolyte. It was found that FPPN adversely affected the initial CE and discharge capacity of the graphite||LiNi_{0.5}Co_{0.2}Mn_{0.3}O₂ full cells, unless an extra LiDFOB additive was added to improve the interfacial properties.²⁷⁶

Overall, through the rational design of structures, the grafting of ether or ester functional groups on fluorinated solvents can achieve an intriguing balance between ion transport and electrolyte stability. The modified solvents with high fluorine ratio and specific coordination structure of Li–F interactions are pursued. Besides high stability toward the electrodes, their intrinsically low flammable features favor the development of next-generation battery chemistries with both high energy density and safety. However, when utilizing this type of solvent as the main component for electrolytes, the density and molar mass are two important factors that need to be considered, given that a high density can decrease the energy density, while a sizeable molar mass of solvents can reduce the power density of cells. In practical rechargeable batteries, the electrolyte usage is suggested to be less than 3 g A⁻¹. Thus, applying fluorinated solvents (except for FDMB, 30-1) in high-energy-density batteries without low-density co-solvents is problematic. Meanwhile, the ionic conductivities of electrolytes should be as high

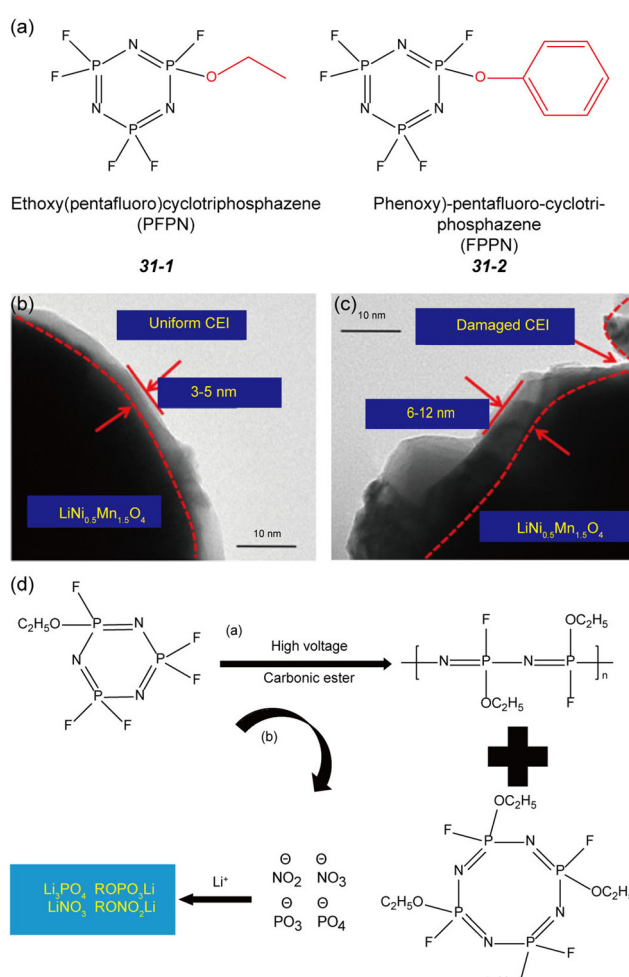


Fig. 34 Characteristics of CEI using electrolytes with PFPN and FPPN additives. (a) Chemical structures of PFPN and FPPN. TEM images of LiNMO cathodes after 100 cycles in the electrolyte with (b) and without (c) PFPN. (d) Possible reaction mechanism of PFPN additive on the cathode surface. (b and c) Reprinted with permission from ref. 272. Copyright 2018, Elsevier. Fig. 31d is compiled based on ref. 273.

as possible to meet the fast charging and energy output requirements. However, the ionic conductivities of electrolytes discussed in this chapter are lower than that of the commercial EC-based electrolytes. Thus, based on the above analysis, the fluorine-containing backbone and ether or ester segment should be as short as possible during the design of this type of emerging fluorinated solvent. Meanwhile, the main groups that can dissolve lithium salts are suggested to be located at the β site to balance the solvating power and stability of fluorinated solvents.

6. Multifunctional group-modified fluorinated solvents

To achieve comprehensive improvements in electrolytes, incorporating more functional groups into one solvent molecule has been proposed recently. In this section, we discuss multi-atom-containing (N, P, F, and S) solvents, highlighting their physicochemical properties and electrolyte properties for Li-based cells.

6.1 Amide-containing phosphates

Phosphates show distinguished self-extinguishing properties but suffer from poor interphase compatibility with carbonaceous and metallic anodes. In this case, although fluorination can ameliorate the severe reductive decomposition of phosphates on the anode surface, the improvements are still far from satisfactory. Shiga *et al.* compared the thermal stability of two types of fluorinated phosphoric acid ester amides (PNMeMe (32-1) and PNMePh (32-2)) toward charged $\text{LiNi}_{0.8}\text{Co}_{0.15}\text{Al}_{0.05}\text{O}_2$ (Table 12).²⁷⁷ The introduction of a phenyl group in the amino group delivered better thermal stability than fluorinated alkyl phosphates. However, Li-ion intercalation into graphite was still not entirely irreversible in PNMePh electrolytes, even with a high salt concentration and extra aid of VC.

6.2 Fluorinated sulfonamides

Perfluoroalkanesulfonamides are commonly utilized in pesticides, surfactants, and biological fields due to their chemical/thermal stability and high miscibility. The earliest use of perfluoroalkanesulfonamides in electrolytes dates back to 2001 in a European patent, where perfluoroalkanesulfonamides were employed as non-flammable solvents to increase

the safety of LIBs.²⁷⁸ To elucidate the relationship between the fundamental physicochemical properties and molecular structure–property of perfluoroalkanesulfonamides, Fu *et al.* synthesized a series of *N,N*-dialkyl perfluoroalkanesulfonamides.¹⁸⁶ As summarized in Table 13, with the same perfluoroalkyl chains, the melting point of these new solvents decreases with the longer alkyl chains, indicating that larger amino segments lower the packing efficiency of the molecule, while maintaining low van der Waals interactions. Alternatively, with a given *N*-alkyl substituent, the melting point increases with the lengthening of the perfluoroalkyl chain (except for 34-2 and 34-3), suggesting strengthened van der Waals interactions. In particular, 34-2 and 34-3 exhibited lower melting points than 33-2 and 33-3, indicating that their melting points are dictated by the flexibility of the perfluoroalkyl chains. Besides, substituting the alkyl group with an alkoxyalkyl group could lower the melting point, where less than 10 °C was obtained even for a long perfluoroalkyl chain ($n\text{-C}_8\text{F}_{17}$). With an increase in the length of the perfluoroalkyl and alkyl chains, the viscosities and dielectric constants of these solvents showed a regular change, *i.e.*, longer chains led to larger viscosities and lower dielectric constant. In particular, *N,N*-dimethyl-trifluoromethanesulfonamide (DMT, 33-1) represents the most promising solvent and has been applied in various scenarios.

Shyamsunder *et al.* found that the relatively hydrophobic DMT (33-1) could work collaboratively with a low ion-pairing salt to suppress the shuttle effect in Li–S batteries (Fig. 35a).²⁷⁹ Furthermore, DMT showed high resistance to the nucleophilic attack of peroxide and superoxide, enabling Li–O₂ cells with stable cycles for more than 90 times without obvious capacity decay (Fig. 35b–f).²⁸⁰ Recently, Xue *et al.* demonstrated that the 1 M LiFSI/DMT electrolyte could operate in an $\text{LiNi}_{0.8}\text{Mn}_{0.1}\text{Co}_{0.1}\text{O}_2$ cathode with a high cut-off voltage of 4.7 V, showing highly reversible Li metal stripping and plating.²⁸¹ The detailed characterizations, including morphology, surface chemistry, and gaseous product analyses, suggested that the LiF-like inorganic components in the interphase layer (SEI and CEI) were responsible for the decoupling of anodic and cathodic stability, *i.e.*, the lower TM dissolution and gas evolution on the cathode side and compact Li deposition with low pulverization on the anode side (Fig. 35g–j). Consequently, the ultra-high-voltage lithium–metal cells could retain good cycling stability under

Table 12 Physicochemical properties of PNMeMe and PNMePh

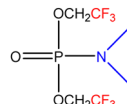
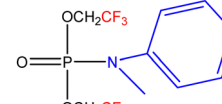
Compound	PNMeMe 32-1	PNMePh 32-2
Structure		
mp (°C)	10	< -50
bp (°C)	190	313 (94 °C at 0.02 kPa)
η (mPa s)	4.3	7.7
ϵ	10.4	8.1
Saturation concentration (LiFSI : PNRR' molar ratio)	0.52–0.54	0.50–0.52

Table 13 Basic parameters of *N,N*-dialkyl perfluoroalkanesulfonamides

Name Structure	mp (°C)	ρ (g cm ⁻³) 25 °C	η (mPa s, ε) 25 °C	(25 °C)
33-1	-39.6	1.382	1.48	22.98
33-2	-41.4	1.304	1.50	22.58
33-3	-43.0	1.277	1.57	20.42
33-4	-33.7	1.270	4.18	19.48
34-1	-3.3	1.469	1.99	21.80
34-2	-49.3	1.398	1.99	20.67
34-3	-54.2	1.376	2.04	17.10
34-4	-23.5	1.362	5.10	16.04
35-1	34.5	—	—	—
35-2	5.2	1.539	4.12	15.90
35-3	-3.6	1.450	4.35	14.66
35-4	-17.3	1.402	10.2	13.82
36-1	64.3	—	—	—

Table 13 (continued)

Name Structure	mp (°C)	ρ (g cm ⁻³) 25 °C	η (mPa s, ε) 25 °C	(25 °C)
36-2	43.1	—	—	—
36-3	7.1	1.612	9.90	12.87
36-4	-13.8	1.560	21.1	11.63
37-1	99.6	—	—	—
37-2	69.3	—	—	—
37-3	49.2	—	—	—
37-4	9.7	1.823	46.3	9.61

Reprinted with permission from ref. 186. Copyright 2013, Elsevier.

Published on 03 April 2023. Downloaded by Tsinghua University on 4/24/2023 3:38:35 AM.

harsh testing conditions (Fig. 35k). Recently, Xu *et al.* further studied the benefit of interface stability on both Li metal and high-voltage cathodes caused by DMT.²⁸² Paired with 1 M LiPF₆, a high-voltage electrolyte that was suitable for a 4.7 V cathode (LCO) was formulated. They demonstrated that the notorious issues of LCO cathodes, including unstable interphase, Co dissolution, electrolyte degradation, and impedance growth, were suppressed in this electrolyte.

Although the element scope for multi-atom-containing solvents is still limited, they provide enormous potential to access desirable electrolyte solvents for different battery applications, especially in Li metal battery chemistries. In these solvents, the multifunctional groups can work collaboratively to realize many attractive features, as follows: (1) improved interface compatibility without compromise in non-flammable properties was achieved through the synergistic effect of P=O, C–F, and C–N–C bonds;²⁷⁷ (2) the strong electron-withdrawing effect of the –CF₃ groups could weaken the Li⁺–solvent interactions, and thus create an anion-rich solvation configuration, benefiting the formation of a stable inorganic-rich interface layer on the

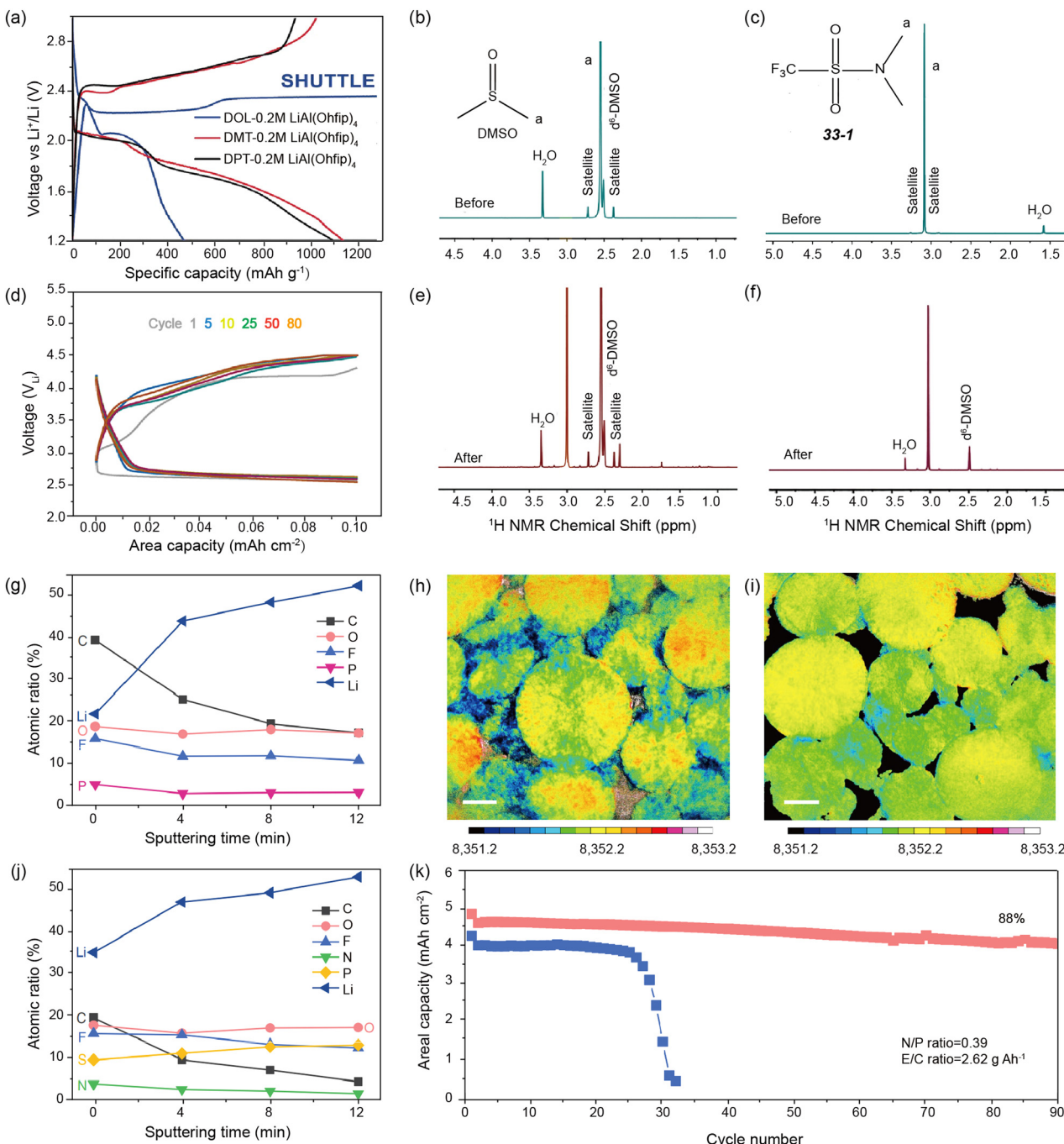


Fig. 35 Applications of DMSO and *N,N*-dimethyl-trifluoromethanesulfonamide (**33-1**)-based electrolyte. (a) Specific capacity–voltage curves of Li–S batteries cycling in different electrolytes. ${}^1\text{H}$ NMR analysis of different electrolytes before and after the chemical stability test: DMSO-based electrolyte before (b) and after (e) chemical stability test; **33-1**-based electrolyte before (c) and after (f) chemical stability test. (d) Galvanostatic discharge–discharge curves of $\text{Li}-\text{O}_2$ cells employed with **33-1**-based electrolytes. Two-dimensional XANES mapping of NCM811 particles cycled in the **33-1**-based electrolyte (h) and commercial electrolyte (i). Scale bars in h and i are 5 μm . Atomic ratio as a function of sputtering time conducted by XPS deep etching in (g) commercial electrolyte and (j) **33-1**-based electrolyte. (k) Cycling stability of NCM811||Li cells with **33-1**-based electrolyte and commercial electrolyte under practical conditions. (a) Reprinted with permission from ref. 279. Copyright 2017, John Wiley & Sons, Inc. (b–f) Reprinted with permission from ref. 280. Copyright 2019, Cell Press. (g–k) Reprinted with permission from ref. 281. Copyright 2021, Springer Nature.

cathode and anode;²⁸¹ and (3) the combination of $\text{O}=\text{S}=\text{O}$, $\text{C}-\text{N}-\text{C}$, and $-\text{CF}_3$ groups could get rid of the attack of peroxide and superoxide in Li–oxygen batteries.²⁸⁰ However,

we emphasize that the density of this type of solvent should be carefully considered for application in practical rechargeable batteries.

7. Solvent selection for different battery applications

In this section, we provide general guidelines for screening fluorinated solvents for different battery chemistries. The top five concerns are highlighted including high voltage, fast charging, Li metal anode, low-temperature, and safety.

7.1 High voltage

As mentioned above, an efficient and straightforward method to improve the energy density of batteries is to increase the working voltage of the electrodes. Therefore, developing high-voltage electrolytes represents an important research field. Although electrolyte oxidation is complicated without unified mechanisms, the primary oxidation components in electrolytes are usually the solvent molecules.^{176,283} Regardless if the high oxidation window derived from intrinsically thermodynamically stable fluorinated solvents or kinetically widened by a forming stable CEI is ignored, the synergistic effect is always present in many electrolyte systems. Many fluorinated solvents, such as carbonates (2-3), sulfones (18-2 and 20-2), and ethers (30-x), have high oxidation voltages of more than 5 V (Fig. 36a).

When paring high-voltage cathode with graphite anodes, the electrolyte oxidation can be mitigated by partially or entirely replacing EC with fluorinated carbonates, sulfones, and

nitriles. It should be noted that the poor reductive stability of sulfone- and nitrile-based solvents require extra film-forming components. The highly catalytic surface of aggressive cathodes will lower the oxidation potential of electrolytes. Thus, the application of these fluorinated solvents is typically lower than 5 V. When paring with Li metal cell chemistries, most of the fluorinated linear ethers discussed in this review have the appropriate qualities in voltage tolerance for 4 V cathodes (11-x). In the case of 5 V-class battery chemistries, fluorinated carbonates (1-2 and 3-4) and sulfones (20-2 and 20-4) may support stable cycling.

7.2 Fast-charging

Fast-charging is a vital characteristic for the application of batteries, especially in vehicles, which needs fast ion transport in both the bulk electrolyte and interfacial layers. In this context, solvents with low viscosity, high dielectric constant, and good film-forming ability are pursued. To date, the charging rates of new fluorinated solvents are often less than 4C, which is the rate when the batteries can be fully charged within 15 min (Fig. 36b). For the battery chemistries with graphite anodes, fluorinated linear carbonates (such as 3-x and 4-x types) and linear carboxylates (such as 8-x and 9-x) are suggested to be included to reduce the viscosity of the electrolyte. Besides, fluorinated EC or PC analogs (such as 1-2, 1-3, 2-2, and

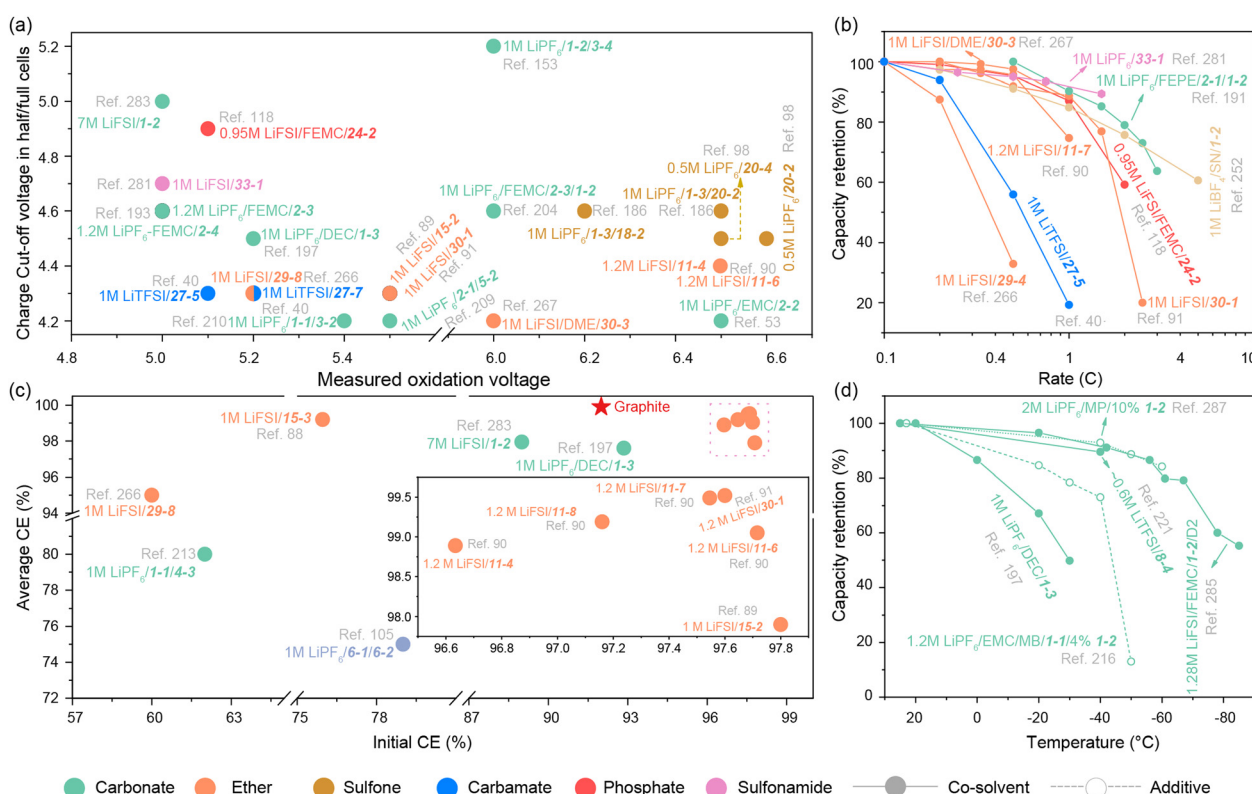


Fig. 36 Key electrochemical parameters with electrolyte containing fluorinated solvents. (a) Oxidation voltage and charge cut-off voltage in cell systems. (b) Charge/discharge rate as a function of capacity retention. (c) Initial and average CE of lithium anode in $\text{Li}||\text{Cu}$ cell in different electrolytes. (d) Capacity retentions of representative electrolytes at different temperatures. MP refers to methyl propionate and D2 is 1,1,2,2-tetrafluoro-1-(2,2,2-trifluoroethoxy)ethane.

2-3) can be added to improve the interface compatibility and ionic conductivity of the electrolyte.

Regarding Li metal batteries, the high charging current density of Li-metal batteries can deteriorate the lithium deposition morphology and form a highly resistive SEI, dramatically increasing the generation of “dead lithium” and the cell impedance.²⁸⁴ Thus, exploiting fast-charging lithium metal batteries requires careful design and coordination of all components of electrolytes to achieve a reasonable trade-off in interfacial stability and ion transport property. Although high Coulombic efficiencies and cycling life have been obtained in many electrolytes with new fluorinated solvents, the charging rates of these systems are still low (Fig. 36b).²⁰⁸ Partially fluorinated ethers (**11-5** and **11-6**) have good solvating power, low viscosity, and good interfacial properties. Furthermore, all-fluorinated ethers or carbonates can efficiently reduce the viscosity and improve the transference number of electrolytes without compromising the electrochemical performance. Mixing partially fluorinated ethers with all-fluorinated ethers or carbonates may meet the requirements in fast-charging electrolytes for lithium metal batteries.

7.3 Li metal anode

Benefiting from the rapid development of materials science, the Li metal anode has been revisited to improve the energy densities of batteries in recent years. To support Li metal batteries over the commercial Li-ion batteries in terms of energy density, the amount of Li anode should be low. Regardless of the safety concern, the CE of Li stripping/plating is one of the most important parameters to evaluate the advancement of electrolytes. Fig. 36c summarizes the CE of representative electrolytes composed of the fluorinated solvents discussed in this review. Most Li employed with fluorinated solvents, especially ethers, have a higher initial CE than graphite. However, the average Li CE in these fluorinated solvents is lower than that of graphite in EC-based electrolytes. Even for the “state-of-the-art” electrolytes with fluorinated solvents, the average Li CE is less than 99.9%, a critical requirement to support the operation of an Li-anode-free battery over 200 cycles with a capacity retention of over 80%. From a cathode point of view, partially fluorinated linear ethers (**11-7** and **11-8**) have potential application in Li-S and 4 V-class batteries. The fluorinated carbonates (**1-2**) and fluorinated sulfonamides (**33-x**, not included in Fig. 36c) can be applied in Li-O₂ batteries due to their high boiling point and high Li CE.

7.4 Low temperature

Solvents with low melting points are a prerequisite for developing low-temperature electrolytes. In the low-temperature zone, the issues associated with ion transport are aggravated, drastically increasing the cell impedance and deteriorating the cell performance. Besides the requirement of fast ion transport in the bulk electrolyte and interface layer, de-solvation barriers have a critical effect on the low-temperature performance of electrolytes.^{39,285} As mentioned in Section 2.2.3, fluorination favors the de-solvation process but lowers the solvating power

of solvents. Therefore, fluorinated solvents are suggested as co-solvents or additives to balance these requirements. The low-temperature performance of a Li metal and graphite anode could be improved by FEC (**1-2**) and DFDEC (**3-3**).^{155,286,287} Fig. 36d show the plot of temperature as a function of capacity retention of different electrolytes with fluorinated solvents. The linear carboxylates, all-fluorinated ethers/carbonates, and FEC (**1-2**) show undisputed advantages in terms of higher capacity retention at low temperatures.

7.5 Safety

Regulating electrolytes from “flammable” to “non-flammable” without sacrificing their basic properties remains a fundamental question. For most of the fire-extinguishing solvents discussed in this review, the undesirable compromise in either flame-retardant efficiency or battery performance inevitably affects the design of non-flammable electrolytes. Despite the promising interfacial passivation ability and flame-retardant efficiency of fluorinated phosphates, some flammable solvents are still needed to balance the overall performance of electrolytes.^{118,234} Recently, locally high-concentration electrolyte strategies provide attractive interfacial compatibility, while remaining flammable by turning the electrolyte structure from a “solvent-rich” to “anion-rich” solvation structure with all-fluorinated ethers.²⁸⁸ However, a large overpotential was observed in these systems. In this regard, replacing TEP (**21-1**) with more interface-friendly flame-retardant solvents, such as TFP (**21-2**), HFIP (**22**), and TFEP (**24-2**), is promising for further investigations.

8. Conclusions and outlook

The excellent compatibility of EC and graphite anodes plays an indispensable role in the commercialization of LIBs. The insatiable appetite for advanced battery chemistries keeps pushing the development of electrode materials toward more challenging areas, which raises more requirements for electrolytes. In this regard, significant efforts have been made to exploit new electrolytes containing new solvents, salts, and additives. In contrast to the non-sustainable effects of additives and lithium salts in a standard concentration (1 M), liquid solvents possess a higher ratio, and thus play a more prominent in dictating the overall performance of electrolytes. Therefore, designing and synthesizing new solvent molecules constitute a vital research territory for next-generation battery chemistries.

The advent of fluorinated solvents will keep motivating research and commercial interest in energy storage science. The introduction of fluorine atoms in solvent molecules, regardless of the number and position, can result in different physical and chemical properties than their non-fluorine-contained counterparts, thus broadening the application of electrolytes. One of the most significant barriers in electrolyte selection and longevity is electrolyte instability. Incorporating fluorine can overcome these barriers by lowering the HOMO of the electrolyte, dispelling the solvents from the aggressive

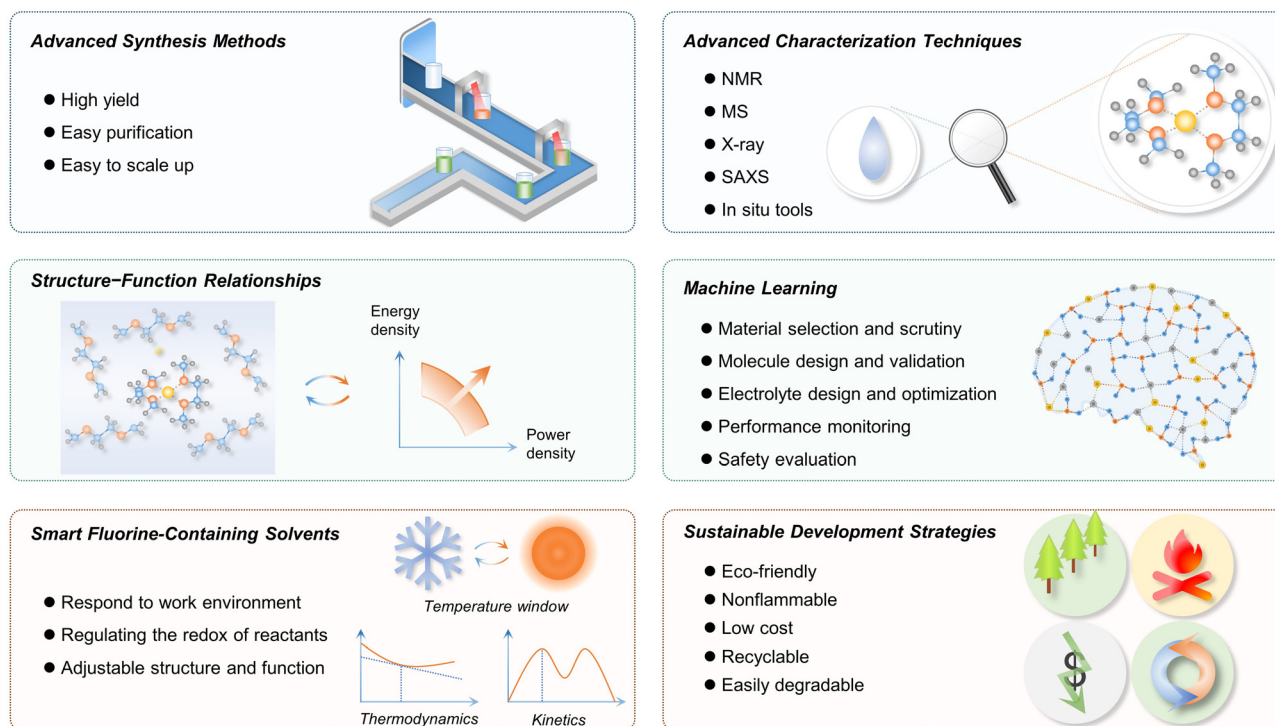


Fig. 37 Possible scientific and engineering directions for new fluorinated solvents for Li-based batteries.

electrode surface, or forming an LiF-rich interfacial layer. For example, fluorinated ether can decouple the poor anodic stability from the desirable lithium metal compatibility. Safety is another important factor that needs to be considered in designing electrolytes. Fortunately, the fluorion radicals decomposed from gaseous fluorides can scavenge hydrogen radicals ($\text{H}\cdot$) to suppress the combustion chain branching reactions.²⁸⁹ Therefore, the development of fluorinated solvents is an important frontier.

Considering the vital role of fluorine in impacting several variables of small organic molecules, a specialized research area, fluorine chemistry, has received great attention in the past few years. Prompted by the demand in cell chemistries, different methods for introducing fluorine and fluorinated groups in cell solvents have been actively investigated and developed. Meanwhile, **theoretical and mechanism research assisted by the rapid development of computational science and characterization techniques** have been used to propose and verify new findings about fluorinated solvents, such as the unique coordination structure of Li–F interactions. However, although remarkable progress has been made in exploiting new fluorinated solvents, some scientific and engineering issues still remain to be resolved (Fig. 37).

(1) Advanced synthesis methods

The yield is one of the most critical factors in evaluating a synthetic method. To date, the synthesis and processing of fluorinated solvents are still plagued by low productivity. Most reported methods involve multi-step reaction paths and tedious procedures for their separation and purification. Therefore,

more efforts must be devoted to developing novel synthesis techniques, including concise but effective synthetic routes, highly active catalysts, and advanced refining processes. The practicality and scale of the synthesis method are other essential factors that need to be considered. Although the performance of recently reported fluorinated solvents is close to or even surpasses industry requirements, their synthesis methods are still unsuitable for high-volume manufacturing. Reagents with high cost, toxicity, and safety concerns, such as NaH, will inevitably pose many limitations in industry.

(2) Advanced characterization techniques

Benefiting from constantly updated *in situ* and operando methodologies, a profound and more comprehensive understanding of fluorine atoms on the physical and chemical properties of solvent molecules, the solvation structure change of electrolytes, and the interfacial chemistries has been achieved. For example, recently, the prevalent cryo-analytical electron microscopy represents important progress in the observation of the SEI structure.^{290,291} Meanwhile, liquid-state nuclear magnetic resonance (NMR), Raman spectroscopy, and small-angle X-ray scattering (SAXS) have been developed to decipher local and whole molecular bonding of electrolytes.^{292,293} However, many previous reports only highlighted the static solvation structures of bulk electrolytes and their interfacial chemistries after cycled. Thus, a critical gap remains in observing the dynamic evolution of electrodes, electrolytes, and interfaces in a working cell with accuracy at the meso-/microscale, such as the process of desolvation and Li^+ transport across interphases. Besides, the specific features

of liquid electrolytes also pose several challenges. For example, stimulated Raman scattering (SRS) was utilized to investigate the ion transport/depletion and dendrite growth in a symmetric cell with gel-electrolyte.^{294,295} However, applying this advanced technique in liquid electrolytes is problematic due to the influence of convection and electro-osmotic effects. Therefore, more smartly designed *in situ* cells and new analytical approaches with non-invasive features should be developed. Besides, coupling multiple characterization techniques (such as *in situ* SEM) should be strongly considered given that it can provide multi-dimensional information on working cells.

(3) Structure–function relationships

Although the development of new fluorinated solvents is pursued, more efforts are still needed to give insight into their structure–function relationships, which can push the boundaries of electrolyte chemistry into more scientific territories. Currently, the most plausible rules and conclusions discussed above are derived from experimental studies involving a “trial-and-error” process. The complex chemistries and bonding types of solvation structure, SEI components, the synergistic effect of electrolyte compounds, and the electrochemical stability of the solvents towards electrode materials are responsible for the main barrier in constituting authentic structure–function relationships between solvent chemistries and electrochemical performance.

(4) Machine learning

Computational methodologies (such as first principles molecular dynamics simulations) based on thermodynamics and kinetics phenomenological equations have successfully tackled many intractable issues in electrolyte chemistries.²⁹⁶ However, their passive nature compels additional human labeling or supervision requirements, limiting the innovative screening or prediction of new solvent molecules that go beyond those currently known. Machine learning (ML) represents a state-of-the-art tool for data aggregation and deep learning algorithms.²⁹⁷ Recent work verified that ML can serve as an unsupervised method to analyze and recommend suitable electrode materials by scanning the repositories present in the published literature.²⁹⁸ Meanwhile, ML molecular dynamics (MLMD), with the advantage of the accuracy of *ab initio* molecular dynamics (AIMD) and the computation efficiency of classical molecular dynamics (CMD), has been applied successfully in the study of solid-state electrolytes to realize the unsupervised discovery of potential solid electrolytes with high ionic conductivity^{299,300} and satisfactory dendrite suppression ability.³⁰¹ However, due to the disordered structure of fluorinated electrolytes, unveiling and predicting the physicochemical properties, solvation structures, and interface compatibilities of electrolytes are challenging and lacking. In this regard, training machine learning to construct fundamental knowledge or principles for the rational design and validation of emerging fluorinated molecules, electrolyte recipe design and optimization, and cell management and monitoring

can accelerate the progress for the development of next-generation safe energy storage batteries.

(5) Smart fluorinated solvents

It is expected that smart electrolytes with self-adaptability may be more promising in the future. As the work conditions change, some electrolyte components in the smart electrolyte can dynamically respond as the supervisor for flame retardant or thermal runaway management, to be temperature-responsive, and as the mediator for regulating the redox of intermediates in some cell systems, such as Li-S and Li-O₂ batteries. Switching to the subject of this review, *i.e.*, fluorinated solvents, in the smart era, solvent molecules with the function of changeable steric hindrance and molecular orientation, as well as the ability to scavenge undesirable species (HF and dissolved TMs) are needed.

(6) Sustainable development strategy

Although fluorinated solvents for different cell chemistries have been constantly updated, their potential environmental impacts, especially in production, storage, application, and recycling, are typically overlooked. Compared to non-fluorinated organic molecules, the degradation of fluorinated organics significantly differs from one to another. For example, molecules with a high degree of fluorination have extremely high structure stability, making them difficult to degrade in the environment. Therefore, more attention needs to be focused on the use of fluorinated solvents in manufacturing and their recycling process to reduce the seriousness of fluorine pollution.

With persistent cooperation and dedication, new progress in electrolytes is being made daily. Meanwhile, the rapid development of cutting-edge characterization techniques (cryogenic focused ion beam, X-ray absorption spectroscopy, neutron diffraction, *etc.*) and computational science (artificial intelligence and machine learning) will undoubtedly assist in resolving the above-mentioned issues. We can envision a future in which highly stable and promising fluorinated solvents can be rationally designed to encourage progress in advanced lithium-based cell chemistries.

Author contributions

Conceptualization, Y.-K. Wang, Q. Zhao, and J. Chen; data curation, Y.-K. Wang, Z.-M. L; visualizaiton, Z.-M. Li, Y.-M. Hou, Q. Zhang, and Z.-M. Hao; writing – original draft, Y. Wang; writing – review & editing, Y. Wang, Y. Lu, Q. Zhao, K. Zhang, and F.-J. Li; software, Y.-X. Ni, resources, Z.-H. Yan, Y. Lu; supervision, J. Chen.

Conflicts of interest

There are no conflicts to declare.

Acknowledgements

This work was supported by the National Key R&D Program of China (2022YFB2402200), National Natural Science Foundation of China (22121005, 22020102002, 21835004), Frontiers Science Center for New Organic Matter of Nankai University (63181206), and Haihe Laboratory of Sustainable Chemical Transformations.

References

- M. V. Reddy, G. V. Subba Rao and B. V. R. Chowdari, *Chem. Rev.*, 2013, **113**, 5364–5457.
- Z. Wang, Z. Sun, J. Li, Y. Shi, C. Sun, B. An, H.-M. Cheng and F. Li, *Chem. Soc. Rev.*, 2021, **50**, 3178–3210.
- T. Liu, J. P. Vivek, E. W. Zhao, J. Lei, N. Garcia-Araez and C. P. Grey, *Chem. Rev.*, 2020, **120**, 6558–6625.
- H. Gao and B. M. Gallant, *Nat. Rev. Chem.*, 2020, **4**, 566–583.
- M. Winter, B. Barnett and K. Xu, *Chem. Rev.*, 2018, **118**, 11433–11456.
- K. Xu, *Chem. Rev.*, 2004, **104**, 4303–4418.
- Q. Liu, X. Su, D. Lei, Y. Qin, J. Wen, F. Guo, Y. A. Wu, Y. Rong, R. Kou, X. Xiao, F. Aguesse, J. Bareño, Y. Ren, W. Lu and Y. Li, *Nat. Energy*, 2018, **3**, 936–943.
- M. Ben Yahia, J. Vergnet, M. Saubanère and M.-L. Doublet, *Nat. Mater.*, 2019, **18**, 496–502.
- E. Hu, X. Yu, R. Lin, X. Bi, J. Lu, S. Bak, K.-W. Nam, H. L. Xin, C. Jaye, D. A. Fischer, K. Amine and X.-Q. Yang, *Nat. Energy*, 2018, **3**, 690–698.
- P. Yan, J. Zheng, J. Liu, B. Wang, X. Cheng, Y. Zhang, X. Sun, C. Wang and J.-G. Zhang, *Nat. Energy*, 2018, **3**, 600–605.
- G. M. Hobold, J. Lopez, R. Guo, N. Minafra, A. Banerjee, Y. S. Meng, Y. Shao-Horn and B. M. Gallant, *Nat. Energy*, 2021, **6**, 951–960.
- P. Zou, Y. Sui, H. Zhan, C. Wang, H. L. Xin, H.-M. Cheng, F. Kang and C. Yang, *Chem. Rev.*, 2021, **121**, 5986–6056.
- S.-J. Tan, W.-P. Wang, Y.-F. Tian, S. Xin and Y.-G. Guo, *Adv. Funct. Mater.*, 2021, **31**, 2105253.
- X. Li, R. Zhao, Y. Fu and A. Manthiram, *eScience*, 2021, **1**, 108–123.
- H. Ma, F. Cheng, J. Chen, J. Zhao, C. Li, Z. Tao and J. Liang, *Adv. Mater.*, 2007, **19**, 4067–4070.
- B. Peng, F. Cheng, Z. Tao and J. Chen, *J. Chem. Phys.*, 2010, **133**, 034701.
- A. Huang, Y. Ma, J. Peng, L. Li, S.-L. Chou, S. Ramakrishna and S. Peng, *eScience*, 2021, **1**, 141–162.
- S. Zhang, S. Li and Y. Lu, *eScience*, 2021, **1**, 163–177.
- C. Wei, Y. Zhang, Y. Tian, L. Tan, Y. An, Y. Qian, B. Xi, S. Xiong, J. Feng and Y. Qian, *Energy Storage Mater.*, 2021, **38**, 157–189.
- M. Li, C. Wang, Z. Chen, K. Xu and J. Lu, *Chem. Rev.*, 2020, **120**, 6783–6819.
- Z. Wang, H. Zhang, J. Xu, A. Pan, F. Zhang, L. Wang, R. Han, J. Hu, M. Liu and X. Wu, *Adv. Funct. Mater.*, 2022, **32**, 2112598.
- A. N. Tran, T.-N. Van Do, L.-P. M. Le and T. N. Le, *J. Fluorine Chem.*, 2014, **164**, 38–43.
- F. Wu, S. Fang, M. Kuenzel, A. Mullaliu, J.-K. Kim, X. Gao, T. Diemant, G.-T. Kim and S. Passerini, *Joule*, 2021, **5**, 2177–2194.
- J. Wan, J. Xie, X. Kong, Z. Liu, K. Liu, F. Shi, A. Pei, H. Chen, W. Chen, J. Chen, X. Zhang, L. Zong, J. Wang, L.-Q. Chen, J. Qin and Y. Cui, *Nat. Nanotechnol.*, 2019, **14**, 705–711.
- J. Dai, C. Yang, C. Wang, G. Pastel and L. Hu, *Adv. Mater.*, 2018, **30**, 1802068.
- K. Fu, Y. Gong, B. Liu, Y. Zhu, S. Xu, Y. Yao, W. Luo, C. Wang, S. D. Lacey, J. Dai, Y. Chen, Y. Mo, E. Wachsman and L. Hu, *Sci. Adv.*, 2017, **3**, e1601659.
- T. Krauskopf, F. H. Richter, W. G. Zeier and J. Janek, *Chem. Rev.*, 2020, **120**, 7745–7794.
- B. Tang, Y. Zhao, Z. Wang, S. Chen, Y. Wu, Y. Tseng, L. Li, Y. Guo, Z. Zhou and S.-H. Bo, *eScience*, 2021, **1**, 194–202.
- S. Yuan, T. Kong, Y. Zhang, P. Dong, Y. Zhang, X. Dong, Y. Wang and Y. Xia, *Angew. Chem., Int. Ed.*, 2021, **60**, 25624–25638.
- B. Flamme, G. Rodriguez Garcia, M. Weil, M. Haddad, P. Phansavath, V. Ratovelomanana-Vidal and A. Chagnes, *Green Chem.*, 2017, **19**, 1828–1849.
- X. Cao, Y. Xu, L. Zhang, M. H. Engelhard, L. Zhong, X. Ren, H. Jia, B. Liu, C. Niu, B. E. Matthews, H. Wu, B. W. Arey, C. Wang, J.-G. Zhang and W. Xu, *ACS Energy Lett.*, 2019, **4**, 2529–2534.
- Z. Zeng, V. Murugesan, K. S. Han, X. Jiang, Y. Cao, L. Xiao, X. Ai, H. Yang, J.-G. Zhang, M. L. Sushko and J. Liu, *Nat. Energy*, 2018, **3**, 674–681.
- E. Markevich, G. Salitra, M. Afri, Y. Talyosef and D. Aurbach, *J. Electrochem. Soc.*, 2020, **167**, 070509.
- F. Yang, Y. Liu, T. Liu, Y. Wang, J. Nai, Z. Lin, H. Xu, D. Duan, K. Yue and X. Tao, *Small Struct.*, 2023, **4**, 2200122.
- N. von Aspern, G.-V. Röschenthaler, M. Winter and I. Cekic-Laskovic, *Angew. Chem., Int. Ed.*, 2019, **58**, 15978–16000.
- N. Xu, J. Shi, G. Liu, X. Yang, J. Zheng, Z. Zhang and Y. Yang, *J. Power Sources Adv.*, 2021, **7**, 100043.
- L. Xia, H. Miao, C. Zhang, G. Z. Chen and J. Yuan, *Energy Storage Mater.*, 2021, **38**, 542–570.
- Z. He, Y. Chen, F. Huang, Y. Jie, X. Li, R. Cao and S. Jiao, *Acta Phys. – Chim. Sin.*, 2022, **38**, 2205005.
- Q. Li, D. Lu, J. Zheng, S. Jiao, L. Luo, C.-M. Wang, K. Xu, J.-G. Zhang and W. Xu, *ACS Appl. Mater. Interfaces*, 2017, **9**, 42761–42768.
- M. Bolloli, J. Kalhoff, F. Alloin, D. Bresser, M. L. Phung Le, B. Langlois, S. Passerini and J.-Y. Sanchez, *J. Phys. Chem. C*, 2015, **119**, 22404–22414.
- R. J. C. Brown and R. F. C. Brown, *J. Chem. Educ.*, 2000, **77**, 724–731.
- S. Prahlada Rao and S. Sunkada, *Reson.*, 2007, **12**, 43–57.
- R. Abramowitz and S. H. Yalkowsky, *Pharm. Res.*, 1990, **7**, 942–947.
- A. R. Katritzky, R. Jain, A. Lomaka, R. Petrukhin, U. Maran and M. Karelson, *Cryst. Growth Des.*, 2001, **1**, 261–265.

- 45 S. H. Yalkowsky, *J. Pharm. Sci.*, 2014, **103**, 2629–2634.
- 46 J. C. Dearden, *Sci. Total Environ.*, 1991, **109–110**, 59–68.
- 47 K. Xu, *Chem. Rev.*, 2014, **114**, 11503–11618.
- 48 M. Takehara, N. Tsukimori, N. Nanbu, M. Ue and Y. Sasaki, *Electrochemistry*, 2003, **71**, 1201–1204.
- 49 E. M. King, M. A. Gebbie and N. A. Melosh, *Langmuir*, 2019, **35**, 16062–16069.
- 50 A. Jouyban, S. Soltanpour and H.-K. Chan, *Int. J. Pharm.*, 2004, **269**, 353–360.
- 51 J. Y. Kim, D. O. Shin, T. Chang, K. M. Kim, J. Jeong, J. Park, Y. M. Lee, K. Y. Cho, C. Phatak, S. Hong and Y.-G. Lee, *Electrochim. Acta*, 2019, **300**, 299–305.
- 52 N. Yao, X. Chen, X. Shen, R. Zhang, Z. H. Fu, X. X. Ma, X. Q. Zhang, B. Q. Li and Q. Zhang, *Angew. Chem., Int. Ed.*, 2021, **60**, 21473–21478.
- 53 N. Nanbu, K. Takimoto, K. Suzuki, M. Ohtake, K. Hagiwara, M. Takehara, M. Ue and Y. Sasaki, *Chem. Lett.*, 2008, **37**, 476–477.
- 54 C.-C. Su, M. He, R. Amine, Z. Chen and K. Amine, *Angew. Chem., Int. Ed.*, 2018, **57**, 12033–12036.
- 55 C.-C. Su, M. He, R. Amine, T. Rojas, L. Cheng, A. T. Ngo and K. Amine, *Energy Environ. Sci.*, 2019, **12**, 1249–1254.
- 56 J. Chen, Q. Li, T. P. Pollard, X. Fan, O. Borodin and C. Wang, *Mater. Today*, 2020, **39**, 118–126.
- 57 Z. Peng, X. Cao, P. Gao, H. Jia, X. Ren, S. Roy, Z. Li, Y. Zhu, W. Xie, D. Liu, Q. Li, D. Wang, W. Xu and J.-G. Zhang, *Adv. Funct. Mater.*, 2020, **30**, 2001285.
- 58 O. O. Postupna, Y. V. Kolesnik, O. N. Kalugin and O. V. Prezhdo, *J. Phys. Chem. B*, 2011, **115**, 14563–14571.
- 59 L. Xing, X. Zheng, M. Schroeder, J. Alvarado, A. von Wald Cresce, K. Xu, Q. Li and W. Li, *Acc. Chem. Res.*, 2018, **51**, 282–289.
- 60 H. Tsunekawa, A. Narumi, M. Sano, A. Hiwara, M. Fujita and H. Yokoyama, *J. Phys. Chem. B*, 2003, **107**, 10962–10966.
- 61 C. M. Burba and R. Frech, *J. Phys. Chem. B*, 2005, **109**, 15161–15164.
- 62 Z. Chen, H. H. Wang, D. R. Vissers, L. Zhang, R. West, L. J. Lyons and K. Amine, *J. Phys. Chem. C*, 2008, **112**, 2210–2214.
- 63 S. Wei, S. Choudhury, Z. Tu, K. Zhang and L. A. Archer, *Acc. Chem. Res.*, 2018, **51**, 80–88.
- 64 T. Li, X.-Q. Zhang, P. Shi and Q. Zhang, *Joule*, 2019, **3**, 2647–2661.
- 65 Y.-S. Hu and Y. Lu, *ACS Energy Lett.*, 2020, **5**, 3633–3636.
- 66 X. Cao, X. Ren, L. Zou, M. H. Engelhard, W. Huang, H. Wang, B. E. Matthews, H. Lee, C. Niu, B. W. Arey, Y. Cui, C. Wang, J. Xiao, J. Liu, W. Xu and J.-G. Zhang, *Nat. Energy*, 2019, **4**, 796–805.
- 67 T. Li, X.-Q. Zhang, N. Yao, Y.-X. Yao, L.-P. Hou, X. Chen, M.-Y. Zhou, J.-Q. Huang and Q. Zhang, *Angew. Chem., Int. Ed.*, 2021, **60**, 22683–22687.
- 68 A. B. Gunnarsdóttir, C. V. Amanchukwu, S. Menkin and C. P. Grey, *J. Am. Chem. Soc.*, 2020, **142**, 20814–20827.
- 69 L. Xu, S. Tang, Y. Cheng, K. Wang, J. Liang, C. Liu, Y.-C. Cao, F. Wei and L. Mai, *Joule*, 2018, **2**, 1991–2015.
- 70 J. B. Goodenough and K.-S. Park, *J. Am. Chem. Soc.*, 2013, **135**, 1167–1176.
- 71 J. B. Goodenough and Y. Kim, *Chem. Mater.*, 2010, **22**, 587–603.
- 72 X. Fan, L. Chen, X. Ji, T. Deng, S. Hou, J. Chen, J. Zheng, F. Wang, J. Jiang, K. Xu and C. Wang, *Chem.*, 2018, **4**, 174–185.
- 73 W. Xu, X. Chen, F. Ding, J. Xiao, D. Wang, A. Pan, J. Zheng, X. S. Li, A. B. Padmaperuma and J.-G. Zhang, *J. Power Sources*, 2012, **213**, 304–316.
- 74 X. Ren, X. Zhang, Z. Shadike, L. Zou, H. Jia, X. Cao, M. H. Engelhard, B. E. Matthews, C. Wang, B. W. Arey, X.-Q. Yang, J. Liu, J.-G. Zhang and W. Xu, *Adv. Mater.*, 2020, **32**, 2004898.
- 75 Z. Luo, H. Zhang, L. Yu, D. Huang and J. Shen, *J. Electroanal. Chem.*, 2019, **833**, 520–526.
- 76 H.-J. Liaw, Y.-H. Lee, C.-L. Tang, H.-H. Hsu and J.-H. Liu, *J. Loss Prev. Process Ind.*, 2002, **15**, 429–438.
- 77 H.-J. Liaw and Y.-Y. Chiu, *J. Hazard. Mater.*, 2006, **137**, 38–46.
- 78 S. Hess, M. Wohlfahrt-Mehrens and M. Wachtler, *J. Electrochem. Soc.*, 2015, **162**, A3084–A3097.
- 79 K. Xu, M. S. Ding, S. Zhang, J. L. Allen and T. R. Jow, *J. Electrochem. Soc.*, 2003, **150**, A161–A169.
- 80 M. S. Whittingham, *US Pat.*, 4009052, 1977.
- 81 R. D. Chambers, *Fluorine in organic chemistry*, CRC press, 2004.
- 82 R. E. Banks, B. E. Smart and J. C. Tatlow, *Springer Science & Business Media*, 2013.
- 83 P. Ma, P. Mirmira and C. V. Amanchukwu, *ACS Cent. Sci.*, 2021, **7**, 1232–1244.
- 84 T. Satoh, N. Nambu, M. Takehara, M. Ue and Y. Sasaki, *ECS Trans.*, 2013, **50**, 127–142.
- 85 L. Chen, X. Fan, E. Hu, X. Ji, J. Chen, S. Hou, T. Deng, J. Li, D. Su, X. Yang and C. Wang, *Chem.*, 2019, **5**, 896–912.
- 86 X. Ren, L. Zou, X. Cao, M. H. Engelhard, W. Liu, S. D. Burton, H. Lee, C. Niu, B. E. Matthews, Z. Zhu, C. Wang, B. W. Arey, J. Xiao, J. Liu, J.-G. Zhang and W. Xu, *Joule*, 2019, **3**, 1662–1676.
- 87 X. Fan, L. Chen, O. Borodin, X. Ji, J. Chen, S. Hou, T. Deng, J. Zheng, C. Yang, S.-C. Liou, K. Amine, K. Xu and C. Wang, *Nat. Nanotechnol.*, 2018, **13**, 715–722.
- 88 Y. Zhao, T. Zhou, T. Ashirov, M. El Kazzi, C. Cancellieri, L. P. H. Jeurgens, J. W. Choi and A. Coskun, *Nat. Commun.*, 2022, **13**, 2575.
- 89 T. Zhou, Y. Zhao, M. El Kazzi, J. W. Choi and A. Coskun, *Angew. Chem., Int. Ed.*, 2022, **61**, e202115884.
- 90 Z. Yu, P. E. Rudnicki, Z. Zhang, Z. Huang, H. Celik, S. T. Oyakhire, Y. Chen, X. Kong, S. C. Kim, X. Xiao, H. Wang, Y. Zheng, G. A. Kamat, M. S. Kim, S. F. Bent, J. Qin, Y. Cui and Z. Bao, *Nat. Energy*, 2022, **7**, 94–106.
- 91 Z. Yu, H. Wang, X. Kong, W. Huang, Y. Tsao, D. G. Mackanic, K. Wang, X. Wang, W. Huang, S. Choudhury, Y. Zheng, C. V. Amanchukwu, S. T. Hung, Y. Ma, E. G. Lomeli, J. Qin, Y. Cui and Z. Bao, *Nat. Energy*, 2020, **5**, 526–533.

- 92 J. Mo, Y. Yao, C. Li, H. Yang, H. Li, Q. Zhang, Z. Jiang and Y. Li, *Chem. Commun.*, 2022, **58**, 12463–12466.
- 93 Y. Zhao, T. Zhou, L. P. H. Jeurgens, X. Kong, J. W. Choi and A. Coskun, *Chem.*, 2023, **9**, 1–16.
- 94 X. Cao, P. Gao, X. Ren, L. Zou, M. H. Engelhard, B. E. Matthews, J. Hu, C. Niu, D. Liu, B. W. Arey, C. Wang, J. Xiao, J. Liu, W. Xu and J.-G. Zhang, *Proc. Natl. Acad. Sci. U. S. A.*, 2021, **118**, e2020357118.
- 95 X.-Q. Zhang, X.-B. Cheng, X. Chen, C. Yan and Q. Zhang, *Adv. Funct. Mater.*, 2017, **27**, 1605989.
- 96 Y.-M. Lee, K.-M. Nam, E.-H. Hwang, Y.-G. Kwon, D.-H. Kang, S.-S. Kim and S.-W. Song, *J. Phys. Chem. C*, 2014, **118**, 10631–10639.
- 97 Z. Chen and K. Amine, *J. Electrochem. Soc.*, 2006, **153**, A1221–A1225.
- 98 C.-C. Su, M. He, J. Shi, R. Amine, Z. Yu, L. Cheng, J. Guo and K. Amine, *Energy Environ. Sci.*, 2021, **14**, 3029–3034.
- 99 Y. Zhang and V. Viswanathan, *J. Phys. Chem. Lett.*, 2021, **12**, 5821–5828.
- 100 J. Xie, S. Y. Sun, X. Chen, L. P. Hou, B. Q. Li, H. J. Peng, J. Q. Huang, X. Q. Zhang and Q. Zhang, *Angew. Chem., Int. Ed.*, 2022, **61**, e202204776.
- 101 Y. Sasaki, G. Shimazaki, N. Nanbu, M. Takeara and M. Ue, *ECS Trans.*, 2009, **16**, 23–31.
- 102 Z. Yue, H. Dunya, S. Aryal, C. U. Segre and B. Mandal, *J. Power Sources*, 2018, **401**, 271–277.
- 103 L. Hu, Z. Zhang and K. Amine, *Electrochem. Commun.*, 2013, **35**, 76–79.
- 104 F. Du, T. Ye, Y. Wu, G. Guo, Z. Xie, Y. Zhang, F. Xiao and J. Liu, *Chem. Phys.*, 2021, **551**, 111328.
- 105 M. Takehaea, R. Ebara, N. Nanbu, M. Ue and Y. Sasaki, *Electrochemistry*, 2003, **71**, 1172–1176.
- 106 J. Wang, W. Huang, A. Pei, Y. Li, F. Shi, X. Yu and Y. Cui, *Nat. Energy*, 2019, **4**, 664–670.
- 107 D. Luo, M. Li, Y. Zheng, Q. Ma, R. Gao, Z. Zhang, H. Dou, G. Wen, L. Shui, A. Yu, X. Wang and Z. Chen, *Adv. Sci.*, 2021, **8**, e2101051.
- 108 N. Zhang, T. Deng, S. Zhang, C. Wang, L. Chen, C. Wang and X. Fan, *Adv. Mater.*, 2022, **34**, e2107899.
- 109 Q. Li, G. Liu, H. Cheng, Q. Sun, J. Zhang and J. Ming, *Chemistry*, 2021, **27**, 15842–15865.
- 110 X. Dong, Z. Guo, Z. Guo, Y. Wang and Y. Xia, *Joule*, 2018, **2**, 902–913.
- 111 K. Hirata, T. Kawase and Y. Sumida, *J. Electrochem. Soc.*, 2020, **167**, 140534.
- 112 K. Park, S. Yu, C. Lee and H. Lee, *J. Power Sources*, 2015, **296**, 197–203.
- 113 X. Wang, E. Yasukawa and S. Mori, *Electrochim. Acta*, 2000, **45**, 2677–2684.
- 114 T. Ma, G. L. Xu, Y. Li, L. Wang, X. He, J. Zheng, J. Liu, M. H. Engelhard, P. Zapol, L. A. Curtiss, J. Jorne, K. Amine and Z. Chen, *J. Phys. Chem. Lett.*, 2017, **8**, 1072–1077.
- 115 A. Gabryelczyk, S. Ivanov, A. Bund and G. Lota, *J. Energy Storage*, 2021, **43**, 103226.
- 116 E. Yoon, J. Lee, S. Byun, D. Kim and T. Yoon, *Adv. Funct. Mater.*, 2022, **32**, 2200026.
- 117 I. A. Shkrob, K. Z. Pupek and D. P. Abraham, *J. Phys. Chem. C*, 2016, **120**, 18435–18444.
- 118 Q. Zheng, Y. Yamada, R. Shang, S. Ko, Y.-Y. Lee, K. Kim, E. Nakamura and A. Yamada, *Nat. Energy*, 2020, **5**, 291–298.
- 119 F. Lin, J. Wang, H. Jia, C. W. Monroe, J. Yang and Y. NuLi, *J. Power Sources*, 2013, **223**, 18–22.
- 120 Y. Yin, Y. Yang, D. Cheng, M. Mayer, J. Holoubek, W. Li, G. Raghavendran, A. Liu, B. Lu, D. M. Davies, Z. Chen, O. Borodin and Y. S. Meng, *Nat. Energy*, 2022, **7**, 548–559.
- 121 S.-J. Tan, J. Yue, X.-C. Hu, Z.-Z. Shen, W.-P. Wang, J.-Y. Li, T.-T. Zuo, H. Duan, Y. Xiao, Y.-X. Yin, R. Wen and Y.-G. Guo, *Angew. Chem., Int. Ed.*, 2019, **58**, 7802–7807.
- 122 X. Mönnighoff, P. Murmann, W. Weber, M. Winter and S. Nowak, *Electrochim. Acta*, 2017, **246**, 1042–1051.
- 123 K. Deng, Q. Zeng, D. Wang, Z. Liu, G. Wang, Z. Qiu, Y. Zhang, M. Xiao and Y. Meng, *Energy Storage Mater.*, 2020, **32**, 425–447.
- 124 J. Hou, L. Wang, X. Feng, J. Terada, L. Lu, S. Yamazaki, A. Su, Y. Kuwajima, Y. Chen, T. Hidaka, X. He, H. Wang and M. Ouyang, *Energy Environ. Mater.*, 2023, **6**, e12297.
- 125 D. Du, Z. Zhu, K. Y. Chan, F. Li and J. Chen, *Chem. Soc. Rev.*, 2022, **51**, 1846–1860.
- 126 N. Giri, M. G. Del Popolo, G. Melaugh, R. L. Greenaway, K. Ratzke, T. Koschine, L. Pison, M. F. Gomes, A. I. Cooper and S. L. James, *Nature*, 2015, **527**, 216–220.
- 127 J. G. Riess, *Artif. Cells, Blood Substitutes, Immobilization Biotechnol.*, 2005, **33**, 47–63.
- 128 S. S. Zhang and J. Read, *J. Power Sources*, 2011, **196**, 2867–2870.
- 129 W.-J. Kwak, S. Chae, R. Feng, P. Gao, J. Read, M. H. Engelhard, L. Zhong, W. Xu and J.-G. Zhang, *ACS Energy Lett.*, 2020, **5**, 2182–2190.
- 130 Q. Zhao, Y. Zhang, G. Sun, L. Cong, L. Sun, H. Xie and J. Liu, *ACS Appl. Mater. Interfaces*, 2018, **10**, 26312–26319.
- 131 Y. Wang, R. Zhang, Z. Sun, H. Wu, S. Lu, J. Wang, W. Yu, J. Liu, G. Gao and S. Ding, *Adv. Mater. Interfaces*, 2020, **7**, 1902092.
- 132 Y. Wang, R. Zhang, Y.-C. Pang, X. Chen, J. Lang, J. Xu, C. Xiao, H. Li, K. Xi and S. Ding, *Energy Storage Mater.*, 2019, **16**, 228–235.
- 133 C. W. Lee, Q. Pang, S. Ha, L. Cheng, S. D. Han, K. R. Zavadil, K. G. Gallagher, L. F. Nazar and M. Balasubramanian, *ACS Cent. Sci.*, 2017, **3**, 605–613.
- 134 J. Zheng, G. Ji, X. Fan, J. Chen, Q. Li, H. Wang, Y. Yang, K. C. DeMella, S. R. Raghavan and C. Wang, *Adv. Energy Mater.*, 2019, **9**, 1803774.
- 135 X. Wang, Y. Tan, G. Shen and S. Zhang, *J. Energy Chem.*, 2020, **41**, 149–170.
- 136 N. Azimi, Z. Xue, I. Bloom, M. L. Gordin, D. Wang, T. Daniel, C. Takoudis and Z. Zhang, *ACS Appl. Mater. Interfaces*, 2015, **7**, 9169–9177.
- 137 U. Košir, I. Kralj Cigić, J. Markelj, S. Drvarič Talian and R. Dominko, *Electrochim. Acta*, 2020, **363**, 137227.
- 138 N. Azimi, Z. Xue, N. D. Rago, C. Takoudis, M. L. Gordin, J. Song, D. Wang and Z. Zhang, *J. Electrochem. Soc.*, 2014, **162**, A64–A68.

- 139 H. Lu, Y. Zhu, Y. Yuan, L. He, B. Zheng, X. Zheng, C. Liu and H. Du, *J. Mater. Sci.: Mater. Electron.*, 2021, **32**, 5898–5906.
- 140 P. Liu, L. Yang, B. Xiao, H. Wang, L. Li, S. Ye, Y. Li, X. Ren, X. Ouyang, J. Hu, F. Pan, Q. Zhang and J. Liu, *Adv. Funct. Mater.*, 2022, **32**, 2208586.
- 141 J.-i Yamaki, H. Takatsuji, T. Kawamura and M. Egashira, *Solid State Ionics*, 2002, **148**, 241–245.
- 142 T. Yoon, M. S. Milien, B. S. Parimalam and B. L. Lucht, *Chem. Mater.*, 2017, **29**, 3237–3245.
- 143 R. Jung, M. Metzger, F. Maglia, C. Stinner and H. A. Gasteiger, *J. Electrochem. Soc.*, 2017, **164**, A1361–A1377.
- 144 B. Rowden and N. Garcia-Araez, *Energy Rep.*, 2020, **6**, 10–18.
- 145 U. Mattinen, M. Klett, G. Lindbergh and R. Wreland Lindström, *J. Power Sources*, 2020, **477**, 228968.
- 146 N. Galushkin, N. N. Yazvinskaya and D. N. Galushkin, *J. Electrochem. Soc.*, 2019, **166**, A897–A908.
- 147 H. Q. Pham, Ł. Kondracki, M. Tarik and S. Trabesinger, *J. Power Sources*, 2022, **527**, 231181.
- 148 J. Langdon, R. Sim and A. Manthiram, *ACS Energy Lett.*, 2022, **7**, 2634–2640.
- 149 T. Noguchi, T. Hasegawa, H. Yamauchi, I. Yamazaki and K. Utsugi, *ECS Trans.*, 2017, **80**, 291–303.
- 150 D. J. Xiong, L. D. Ellis, R. Petibon, T. Hynes, Q. Q. Liu and J. R. Dahn, *J. Electrochem. Soc.*, 2016, **164**, A340–A347.
- 151 J. Xia, K. J. Nelson, Z. Lu and J. R. Dahn, *J. Power Sources*, 2016, **329**, 387–397.
- 152 X. Teng, C. Zhan, Y. Bai, L. Ma, Q. Liu, C. Wu, F. Wu, Y. Yang, J. Lu and K. Amine, *ACS Appl. Mater. Interfaces*, 2015, **7**, 22751–22755.
- 153 M. He, L. Hu, Z. Xue, C. C. Su, P. Redfern, L. A. Curtiss, B. Polzin, A. von Cresce, K. Xu and Z. Zhang, *J. Electrochem. Soc.*, 2015, **162**, A1725–A1729.
- 154 K. Oldiges, N. von Aspern, I. Cekic-Laskovic, M. Winter and G. Brunklaus, *J. Electrochem. Soc.*, 2018, **165**, A3773–A3781.
- 155 M. C. Smart, B. V. Ratnakumar, V. S. Ryan-Mowrey, S. Surampudi, G. K. S. Prakash, J. Hu and I. Cheung, *J. Power Sources*, 2003, **119–121**, 359–367.
- 156 J. A. Wilkinson, *Chem. Rev.*, 1992, **92**, 505–519.
- 157 T. Furuya, A. S. Kamlet and T. Ritter, *Nature*, 2011, **473**, 470–477.
- 158 D. J. Adams and J. H. Clark, *Chem. Soc. Rev.*, 1999, **28**, 225–231.
- 159 A. L'Heureux, F. Beaulieu, C. Bennett, D. R. Bill, S. Clayton, F. LaFlamme, M. Mirmehrabi, S. Tadayon, D. Tovell and M. Couturier, *J. Org. Chem.*, 2010, **75**, 3401–3411.
- 160 J. S. Moilliet, *J. Fluorine Chem.*, 2001, **109**, 13–17.
- 161 Y. Tamboli, B. Kashid, R. P. Yadav, M. Rafeeq and A. Y. Merwade, *Org. Process Res. Dev.*, 2020, **24**, 1609–1613.
- 162 M. Kobayashi, T. Inoguchi, T. Iida, T. Tanioka, H. Kumase and Y. Fukai, *J. Fluorine Chem.*, 2003, **120**, 105–110.
- 163 Y. Sasaki, *Electrochemistry*, 2008, **76**, 2–15.
- 164 Y. Sasaki, R. Ebara, N. Nanbu, M. Takehara and M. Ue, *J. Fluorine Chem.*, 2001, **108**, 117–120.
- 165 J. Guo, C. Kuang, J. Rong, L. Li, C. Ni and J. Hu, *Chem. – Eur. J.*, 2019, **25**, 7259–7264.
- 166 P. J. Foth, F. Gu, T. G. Bolduc, S. S. Kanani and G. M. Sammis, *Chem. Sci.*, 2019, **10**, 10331–10335.
- 167 M. Epifanov, P. J. Foth, F. Gu, C. Barrillon, S. S. Kanani, C. S. Higman, J. E. Hein and G. M. Sammis, *J. Am. Chem. Soc.*, 2018, **140**, 16464–16468.
- 168 X. Yang, T. Wu, R. J. Phipps and F. D. Toste, *Chem. Rev.*, 2015, **115**, 826–870.
- 169 M. K. Nielsen, C. R. Ugaz, W. Li and A. G. Doyle, *J. Am. Chem. Soc.*, 2015, **137**, 9571–9574.
- 170 M. K. Nielsen, D. T. Ahneman, O. Riera and A. G. Doyle, *J. Am. Chem. Soc.*, 2018, **140**, 5004–5008.
- 171 L. Conte and G. P. Gambaretto, *J. Fluorine Chem.*, 2004, **125**, 139–144.
- 172 T. Fuchigami and S. Inagi, *Acc. Chem. Res.*, 2020, **53**, 322–334.
- 173 H. Ishii, N. Yamada and T. Fuchigami, *Tetrahedron*, 2001, **57**, 9067–9072.
- 174 M. Hasegawa, H. Ishii and T. Fuchigami, *Tetrahedron Lett.*, 2002, **43**, 1503–1505.
- 175 T. Achiha, T. Nakajima, Y. Ohzawa, M. Koh, A. Yamauchi, M. Kagawa and H. Aoyama, *J. Electrochem. Soc.*, 2009, **156**, A483–A488.
- 176 X. Fan and C. Wang, *Chem. Soc. Rev.*, 2021, **50**, 10486–10566.
- 177 M. North, R. Pasquale and C. Young, *Green Chem.*, 2010, **12**, 1514–1539.
- 178 W. Beichel, P. Klose, H. Blattmann, J. Hoecker, D. Kratzert and I. Krossing, *ChemElectroChem*, 2018, **5**, 1415–1420.
- 179 Y. Sasaki, H. Satake, N. Tsukimori, N. Nanbu, M. Takehara and M. Ue, *Electrochemistry*, 2010, **78**, 467–470.
- 180 E. Fuhrmann and J. Talbiersky, *Org. Process Res. Dev.*, 2005, **9**, 206–211.
- 181 A. Diamanti, Z. Ganase, E. Grant, A. Armstrong, P. M. Piccione, A. M. Rea, J. Richardson, A. Galindo and C. S. Adjiman, *React. Chem. Eng.*, 2021, **6**, 1195–1211.
- 182 T. Wolf, T. Steinbach and F. R. Wurm, *Macromolecules*, 2015, **48**, 3853–3863.
- 183 S. Mihara, K. Yamaguchi and M. Kobayashi, *Langmuir*, 2019, **35**, 1172–1180.
- 184 C.-C. Su, M. He, C. Peebles, L. Zeng, A. Tornheim, C. Liao, L. Zhang, J. Wang, Y. Wang and Z. Zhang, *ACS Appl. Mater. Interfaces*, 2017, **9**, 30686–30695.
- 185 G. Manolikakes, N.-W. Liu and S. Liang, *Synthesis*, 2016, 1939–1973.
- 186 S.-T. Fu, S.-L. Liao, J. Nie and Z.-B. Zhou, *J. Fluor. Chem.*, 2013, **147**, 56–64.
- 187 C.-C. Su, M. He, J. Shi, R. Amine, Z. Yu, L. Cheng, J. Guo and K. Amine, *Energy Environ. Sci.*, 2017, **10**, 900–904.
- 188 M. Ganesan and P. Nagaraj, *Org. Chem. Front.*, 2020, **7**, 3792–3814.
- 189 D. Lin, Y. Liu and Y. Cui, *Nat. Nanotechnol.*, 2017, **12**, 194–206.
- 190 M. Bolloli, F. Alloin, J. Kalhoff, D. Bresser, S. Passerini, P. Judeinstein, J.-C. Leprêtre and J.-Y. Sanchez, *Electrochim. Acta*, 2015, **161**, 159–170.
- 191 R. Payne and I. E. Theodorou, *J. Phys. Chem.*, 1972, **76**, 2892–2900.

- 192 P. Shi, S. Fang, D. Luo, L. Yang and S.-I. Hirano, *J. Electrochem. Soc.*, 2017, **164**, A1991–A1999.
- 193 M. Ue, Y. Sasaki, Y. Tanaka and M. Morita, Nonaqueous Electrolytes with Advances in Solvents, in *Electrolytes for Lithium and Lithium-Ion Batteries*, Chapter 2 Part of the Modern Aspects of Electrochemistry Book Series, Springer, New York, NY, pp. 93–165, 2014.
- 194 M. He, C.-C. Su, C. Peebles and Z. Zhang, *J. Electrochem. Soc.*, 2021, **168**, 010505.
- 195 X. Q. Zhang, X. Chen, X. B. Cheng, B. Q. Li, X. Shen, C. Yan, J. Q. Huang and Q. Zhang, *Angew. Chem., Int. Ed.*, 2018, **57**, 5301–5305.
- 196 J. Shen, H. Chen, L. Yu, D. Huang and Z. Luo, *J. Electroanal. Chem.*, 2019, **834**, 1–7.
- 197 A. Gupta and A. Manthiram, *Adv. Energy Mater.*, 2020, **10**, 2001972.
- 198 Z. Wang, Z. Sun, Y. Shi, F. Qi, X. Gao, H. Yang, H.-M. Cheng and F. Li, *Adv. Energy Mater.*, 2021, **11**, 2100935.
- 199 M. Ue, M. Takeda, M. Takehara and S. Mori, *J. Electrochem. Soc.*, 1997, **144**, 2684–2688.
- 200 Y. Matsuda, T. Nakajima, Y. Ohzawa, M. Koh, A. Yamauchi, M. Kagawa and H. Aoyama, *J. Fluorine Chem.*, 2011, **132**, 1174–1181.
- 201 Density functional theory (DFT) calculations were performed using Gaussian 09 software package. The geometry optimizations and electronic structure computations were carried out at B3LYP level with 6-311G(d).
- 202 N. Nanbu, K. Takimoto, M. Takehara, M. Ue and Y. Sasaki, *Electrochem. Commun.*, 2008, **10**, 783–786.
- 203 J. Yang, Q. Liu, K. Z. Pupek, T. L. Dzwiniel, N. L. Dietz Rago, J. Cao, N. Dandu, L. Curtiss, K. Liu, C. Liao and Z. Zhang, *ACS Energy Lett.*, 2021, **6**, 371–378.
- 204 M. Inaba, Y. Kawatake, A. Funabiki, S.-K. Jeong, T. Abe and Z. Ogumi, *Electrochim. Acta*, 1999, **45**, 99–105.
- 205 J. Yun, L. Zhang, Q. Qu, H. Liu, X. Zhang, M. Shen and H. Zheng, *Electrochim. Acta*, 2015, **167**, 151–159.
- 206 J. Arai, H. Katayama and H. Akahoshi, *J. Electrochem. Soc.*, 2002, **149**, A217–A226.
- 207 C.-C. Su, M. He, R. Amine, Z. Chen, R. Sahore, N. Dietz Rago and K. Amine, *Energy Storage Mater.*, 2019, **17**, 284–292.
- 208 E. R. Logan and J. R. Dahn, *Trends Chem.*, 2020, **2**, 354–366.
- 209 D. Guyomard and J. M. Tarascon, *J. Electrochem. Soc.*, 1993, **140**, 3071–3081.
- 210 N. Nambu, T. Nachi, M. Takehara, M. Ue and Y. Sasaki, *Electrochemistry*, 2012, **80**, 771–773.
- 211 N. Tsukimori, N. Nanbu, M. Takehara, M. Ue and Y. Sasaki, *Chem. Lett.*, 2008, **37**, 368–369.
- 212 K. Matsumoto, K. Inoue, K. Nakahara, R. Yuge, T. Noguchi and K. Utsugi, *J. Power Sources*, 2013, **231**, 234–238.
- 213 Y. Sasaki, M. Takehara, S. Watanabe, N. Nanbu and M. Ue, *J. Fluorine Chem.*, 2004, **125**, 1205–1209.
- 214 Y. Sasaki, M. Takehara, S. Watanabe, M. Oshima, N. Nanbu and M. Ue, *Solid State Ionics*, 2006, **177**, 299–303.
- 215 M. C. Smart, B. V. Ratnakumar, K. B. Chin and L. D. Whitcanack, *J. Electrochem. Soc.*, 2010, **157**, A1361–A1374.
- 216 M. C. Smart, B. L. Lucht, S. Dalavi, F. C. Krause and B. V. Ratnakumar, *J. Electrochem. Soc.*, 2012, **159**, A739–A751.
- 217 W. Lu, K. Xie, Y. Pan, Z.-X. Chen and C.-M. Zheng, *J. Fluorine Chem.*, 2013, **156**, 136–143.
- 218 T. Nakajima, K.-i Dan and M. Koh, *J. Fluorine Chem.*, 1998, **87**, 221–227.
- 219 N. Nambu and Y. Sasaki, *Open J. Met.*, 2015, **5**, 1–9.
- 220 K. Sato, L. Zhao, S. Okada and J.-I. Yamaki, *J. Power Sources*, 2011, **196**, 5617–5622.
- 221 Y. Yang, P. Li, N. Wang, Z. Fang, C. Wang, X. Dong and Y. Xia, *Chem. Commun.*, 2020, **56**, 9640–9643.
- 222 N. Nambu, Y. Matsushita, M. Takehara and Y. Sasaki, *Electrochemistry*, 2016, **84**, 776–778.
- 223 M. Cuisinier, P.-E. Cabelguen, B. D. Adams, A. Garsuch, M. Balasubramanian and L. F. Nazar, *Energy Environ. Sci.*, 2014, **7**, 2697–2705.
- 224 S. Li, W. Zhao, Z. Zhou, X. Cui, Z. Shang, H. Liu and D. Zhang, *ACS Appl. Mater. Interfaces*, 2014, **6**, 4920–4926.
- 225 A. Abouimrane, I. Belharouak and K. Amine, *Electrochem. Commun.*, 2009, **11**, 1073–1076.
- 226 K. Xu and C. A. Angell, *J. Electrochem. Soc.*, 1998, **145**, L70–L72.
- 227 J. Demeaux, E. De Vito, M. Le Digabel, H. Galiano, B. Claude-Montigny and D. Lemordant, *Phys. Chem. Chem. Phys.*, 2014, **16**, 5201–5212.
- 228 T. Zhang, W. Porcher and E. Paillard, *J. Power Sources*, 2018, **395**, 212–220.
- 229 K. Xu and C. A. Angell, *J. Electrochem. Soc.*, 2002, **149**, A920–A926.
- 230 S.-Y. Lee, K. Ueno and C. A. Angell, *J. Phys. Chem. C*, 2012, **116**, 23915–23920.
- 231 P. Jankowski, N. Lindahl, J. Weidow, W. Wieczorek and P. Johansson, *ACS Appl. Energy Mater.*, 2018, **1**, 2582–2591.
- 232 H. M. Jung, S.-H. Park, J. Jeon, Y. Choi, S. Yoon, J.-J. Cho, S. Oh, S. Kang, Y.-K. Han and H. Lee, *J. Mater. Chem. A*, 2013, **1**, 11975–11981.
- 233 R. Gond, W. van Ekeren, R. Mogensen, A. J. Naylor and R. Younesi, *Mater. Horiz.*, 2021, **8**, 2913–2928.
- 234 K. Xu, M. S. Ding, S. Zhang, J. L. Allen and T. R. Jow, *J. Electrochem. Soc.*, 2002, **149**, A622–A626.
- 235 J. Arai, *J. Electrochem. Soc.*, 2003, **150**, A219–A228.
- 236 K. Xu, S. Zhang, J. L. Allen and T. R. Jow, *J. Electrochem. Soc.*, 2002, **149**, A1079–A1082.
- 237 P. Murmann, X. Mönnighoff, N. von Aspern, P. Janssen, N. Kalinovich, M. Shevchuk, O. Kazakova, G.-V. Röschenthaler, I. Cekic-Laskovic and M. Winter, *J. Electrochem. Soc.*, 2016, **163**, A751–A757.
- 238 P. Murmann, N. von Aspern, P. Janssen, N. Kalinovich, M. Shevchuk, G.-V. Röschenthaler, M. Winter and I. Cekic-Laskovic, *J. Electrochem. Soc.*, 2018, **165**, A1935–A1942.
- 239 N. von Aspern, S. Röser, B. R. Rad, P. Murmann, B. Streipert, X. Mönnighoff, S. D. Tillmann, M. Shevchuk, O. Stubbmann-Kazakova, G.-V. Röschenthaler, S. Nowak, M. Winter and I. Cekic-Laskovic, *J. Fluorine Chem.*, 2017, **198**, 24–33.

- 240 H. Ota, A. Kominato, W.-J. Chun, E. Yasukawa and S. Kasuya, *J. Power Sources*, 2003, **119–121**, 393–398.
- 241 D. Gao, J. B. Xu, M. Lin, Q. Xu, C. F. Ma and H. F. Xiang, *RSC Adv.*, 2015, **5**, 17566–17571.
- 242 S. Zhang, A. Li, J. Zou, L. Y. Lin and K. L. Wooley, *ACS Macro Lett.*, 2012, **1**, 328–333.
- 243 J. Zhao, X. Zhang, Y. Liang, Z. Han, S. Liu, W. Chu and H. Yu, *ACS Energy Lett.*, 2021, **6**, 2552–2564.
- 244 K. Kim, H. Ma, S. Park and N.-S. Choi, *ACS Energy Lett.*, 2020, **5**, 1537–1553.
- 245 S. S. Zhang, K. Xu and T. R. Jow, *J. Power Sources*, 2003, **113**, 166–172.
- 246 M. He, C.-C. Su, C. Peebles, Z. Feng, J. G. Connell, C. Liao, Y. Wang, I. A. Shkrob and Z. Zhang, *ACS Appl. Mater. Interfaces*, 2016, **8**, 11450–11458.
- 247 J. Wang, F. Lin, H. Jia, J. Yang, C. W. Monroe and Y. NuLi, *Angew. Chem., Int. Ed.*, 2014, **53**, 10099–10104.
- 248 N. von Aspern, D. Diddens, T. Kobayashi, M. Börner, O. Stubbmann-Kazakova, V. Kozel, G.-V. Röschenthaler, J. Smiatek, M. Winter and I. Cekic-Laskovic, *ACS Appl. Mater. Interfaces*, 2019, **11**, 16605–16618.
- 249 Y. Abu-Lebdeh and I. Davidson, *J. Electrochem. Soc.*, 2009, **156**, A60–A65.
- 250 A. N. Kirshnamoorthy, K. Oldiges, M. Winter, A. Heuer, I. Cekic-Laskovic, C. Holm and J. Smiatek, *Phys. Chem. Chem. Phys.*, 2018, **20**, 25701–25715.
- 251 S. H. Lee, J.-Y. Hwang, S.-J. Park, G.-T. Park and Y.-K. Sun, *Adv. Funct. Mater.*, 2019, **29**, 1902496.
- 252 Q. Zhang, K. Liu, F. Ding, W. Li, X. Liu and J. Zhang, *Electrochim. Acta*, 2019, **298**, 818–826.
- 253 Y.-S. Kim, T.-H. Kim, H. Lee and H.-K. Song, *Energy Environ. Sci.*, 2011, **4**, 4038–4045.
- 254 Y. Abu-Lebdeh and I. Davidson, *J. Power Sources*, 2009, **189**, 576–579.
- 255 M. Ue, K. Ida and S. Mori, *J. Electrochem. Soc.*, 1994, **141**, 2989–2996.
- 256 G.-Y. Kim and J. R. Dahn, *J. Electrochem. Soc.*, 2015, **162**, A437–A447.
- 257 D. H. C. Wong, J. L. Thelen, Y. Fu, D. Devaux, A. A. Pandya, V. S. Battaglia, N. P. Balsara and J. M. DeSimone, *Proc. Natl. Acad. Sci. U. S. A.*, 2014, **111**, 3327–3331.
- 258 L. Wu, Z. Song, L. Liu, X. Guo, L. Kong, H. Zhan, Y. Zhou and Z. Li, *J. Power Sources*, 2009, **188**, 570–573.
- 259 B. Flamme, J. Świątowska, M. Haddad, P. Phansavath, V. Ratovelomanana-Vidal and A. Chagnes, *J. Electrochem. Soc.*, 2020, **167**, 070508.
- 260 X. Ren, S. Chen, H. Lee, D. Mei, M. H. Engelhard, S. D. Burton, W. Zhao, J. Zheng, Q. Li, M. S. Ding, M. Schroeder, J. Alvarado, K. Xu, Y. S. Meng, J. Liu, J.-G. Zhang and W. Xu, *Chem*, 2018, **4**, 1877–1892.
- 261 J. Wang, Y. Yamada, K. Sodeyama, E. Watanabe, K. Takada, Y. Tateyama and A. Yamada, *Nat. Energy*, 2018, **3**, 22–29.
- 262 K. R. Olson, D. H. C. Wong, M. Chintapalli, K. Timachova, R. Janusziewicz, W. F. M. Daniel, S. Mecham, S. Sheiko, N. P. Balsara and J. M. DeSimone, *Polymer*, 2016, **100**, 126–133.
- 263 M. Chintapalli, K. Timachova, K. R. Olson, S. J. Mecham, D. Devaux, J. M. DeSimone and N. P. Balsara, *Macromolecules*, 2016, **49**, 3508–3515.
- 264 K. Timachova, M. Chintapalli, K. R. Olson, S. J. Mecham, J. M. DeSimone and N. P. Balsara, *Soft Matter*, 2017, **13**, 5389–5396.
- 265 D. B. Shah, K. R. Olson, A. Karny, S. J. Mecham, J. M. DeSimone and N. P. Balsara, *J. Electrochem. Soc.*, 2017, **164**, A3511–A3517.
- 266 C. V. Amanchukwu, Z. Yu, X. Kong, J. Qin, Y. Cui and Z. Bao, *J. Am. Chem. Soc.*, 2020, **142**, 7393–7403.
- 267 H. Wang, Z. Yu, X. Kong, W. Huang, Z. Zhang, D. G. Mackanic, X. Huang, J. Qin, Z. Bao and Y. Cui, *Adv. Mater.*, 2021, **33**, 2008619.
- 268 E. Niecke, H. Thamm and O. Glemser, *Z. Naturforsch. B*, 1971, **26**, 366–367.
- 269 L. Xia, Y. Xia and Z. Liu, *J. Power Sources*, 2015, **278**, 190–196.
- 270 Y. Ji, P. Zhang, M. Lin, W. Zhao, Z. Zhang, Y. Zhao and Y. Yang, *J. Power Sources*, 2017, **359**, 391–399.
- 271 X. Li, W. Li, L. Chen, Y. Lu, Y. Su, L. Bao, J. Wang, R. Chen, S. Chen and F. Wu, *J. Power Sources*, 2018, **378**, 707–716.
- 272 J. Liu, X. Song, L. Zhou, S. Wang, W. Song, W. Liu, H. Long, L. Zhou, H. Wu, C. Feng and Z. Guo, *Nano Energy*, 2018, **46**, 404–414.
- 273 H. Li, Z. Wen, D. Wu, W. Ji, Z. He, F. Wang, Y. Yang, P. Zhang and J. Zhao, *ACS Appl. Mater. Interfaces*, 2021, **13**, 57142–57152.
- 274 T. Dagger, C. Lürenbaum, F. M. Schappacher and M. Winter, *J. Power Sources*, 2017, **342**, 266–272.
- 275 J. Feng, X. Gao, L. Ci and S. Xiong, *RSC Adv.*, 2016, **6**, 7224–7228.
- 276 Y. Gu, S. Fang, L. Yang and S.-I. Hirano, *J. Mater. Chem. A*, 2021, **9**, 15363–15372.
- 277 T. Shiga, C.-a Okuda, Y. Kato and H. Kondo, *J. Phys. Chem. C*, 2018, **122**, 9738–9745.
- 278 M. Schmidt, P. Sartori and N. Ignat'ev, *Eur. Patent*, 1088814, 2001.
- 279 A. Shyamsunder, W. Beichel, P. Klose, Q. Pang, H. Scherer, A. Hoffmann, G. K. Murphy, I. Krossing and L. F. Nazar, *Angew. Chem., Int. Ed.*, 2017, **56**, 6192–6197.
- 280 S. Feng, M. Huang, J. R. Lamb, W. Zhang, R. Tatara, Y. Zhang, Y. G. Zhu, C. F. Perkinson, J. A. Johnson and Y. Shao-Horn, *Chem*, 2019, **5**, 2630–2641.
- 281 W. Xue, M. Huang, Y. Li, Y. G. Zhu, R. Gao, X. Xiao, W. Zhang, S. Li, G. Xu, Y. Yu, P. Li, J. Lopez, D. Yu, Y. Dong, W. Fan, Z. Shi, R. Xiong, C.-J. Sun, I. Hwang, W.-K. Lee, Y. Shao-Horn, J. A. Johnson and J. Li, *Nat. Energy*, 2021, **6**, 495–505.
- 282 W. Xue, R. Gao, Z. Shi, X. Xiao, W. Zhang, Y. Zhang, Y. G. Zhu, I. Waluyo, Y. Li, M. R. Hill, Z. Zhu, S. Li, O. Kuznetsov, Y. Zhang, W.-K. Lee, A. Hunt, A. Harutyunyan, Y. Shao-Horn, J. A. Johnson and J. Li, *Energy Environ. Sci.*, 2021, **14**, 6030–6040.
- 283 L. Suo, W. Xue, M. Gobet, S. G. Greenbaum, C. Wang, Y. Chen, W. Yang, Y. Li and J. Li, *Proc. Natl. Acad. Sci. U. S. A.*, 2018, **115**, 1156–1161.

- 284 D. Lu, Y. Shao, T. Lozano, W. D. Bennett, G. L. Graff, B. Polzin, J. Zhang, M. H. Engelhard, N. T. Saenz, W. A. Henderson, P. Bhattacharya, J. Liu and J. Xiao, *Adv. Energy Mater.*, 2015, **5**, 1400993.
- 285 X. Fan, X. Ji, L. Chen, J. Chen, T. Deng, F. Han, J. Yue, N. Piao, R. Wang, X. Zhou, X. Xiao, L. Chen and C. Wang, *Nat. Energy*, 2019, **4**, 882–890.
- 286 A. C. Thenuwara, P. P. Shetty, N. Kondekar, S. E. Sandoval, K. Cavallaro, R. May, C.-T. Yang, L. E. Marbella, Y. Qi and M. T. McDowell, *ACS Energy Lett.*, 2020, **5**, 2411–2420.
- 287 J. Holoubek, Y. Yin, M. Li, M. Yu, Y. S. Meng, P. Liu and Z. Chen, *Angew. Chem., Int. Ed.*, 2019, **58**, 18892–18897.
- 288 S. Chen, J. Zheng, L. Yu, X. Ren, M. H. Engelhard, C. Niu, H. Lee, W. Xu, J. Xiao, J. Liu and J.-G. Zhang, *Joule*, 2018, **2**, 1548–1558.
- 289 S. Chen, Z. Wang, H. Zhao, H. Qiao, H. Luan and L. Chen, *J. Power Sources*, 2009, **187**, 229–232.
- 290 M. J. Zachman, Z. Tu, S. Choudhury, L. A. Archer and L. F. Kourkoutis, *Nature*, 2018, **560**, 345–349.
- 291 Y. Li, Y. Li, A. Pei, K. Yan, Y. Sun, C.-L. Wu, L.-M. Joubert, R. Chin, A. L. Koh, Y. Yu, J. Perrino, B. Butz, S. Chu and Y. Cui, *Science*, 2017, **358**, 506–510.
- 292 X. Liu, Z. Yu, E. Sarnello, K. Qian, S. Seifert, R. E. Winans, L. Cheng and T. Li, *Energy Mater. Adv.*, 2021, **2021**, 7368420.
- 293 Y. S. Meng, V. Srinivasan and K. Xu, *Science*, 2022, **378**, eabq3750.
- 294 D. Liu, Z. Shadike, R. Lin, K. Qian, H. Li, K. Li, S. Wang, Q. Yu, M. Liu, S. Ganapathy, X. Qin, Q. H. Yang, M. Wagemaker, F. Kang, X. Q. Yang and B. Li, *Adv. Mater.*, 2019, **31**, e1806620.
- 295 Q. Cheng, L. Wei, Z. Liu, N. Ni, Z. Sang, B. Zhu, W. Xu, M. Chen, Y. Miao, L. Q. Chen, W. Min and Y. Yang, *Nat. Commun.*, 2018, **9**, 2942.
- 296 A. Van der Ven, Z. Deng, S. Banerjee and S. P. Ong, *Chem. Rev.*, 2020, **120**, 6977–7019.
- 297 N. Yao, X. Chen, Z.-H. Fu and Q. Zhang, *Chem. Rev.*, 2022, **122**, 10970–11021.
- 298 V. Tshitoyan, J. Dagdelen, L. Weston, A. Dunn, Z. Rong, O. Kononova, K. A. Persson, G. Ceder and A. Jain, *Nature*, 2019, **571**, 95–98.
- 299 Y. Zhang, X. He, Z. Chen, Q. Bai, A. M. Nolan, C. A. Roberts, D. Banerjee, T. Matsunaga, Y. Mo and C. Ling, *Nat. Commun.*, 2019, **10**, 5260.
- 300 A. Hajibabaei and K. S. Kim, *J. Phys. Chem. Lett.*, 2021, **12**, 8115–8120.
- 301 Z. Ahmad, T. Xie, C. Maheshwari, J. C. Grossman and V. Viswanathan, *ACS Cent. Sci.*, 2018, **4**, 996–1006.